HEAT TRANSFER AND HYBRID NANOFLUIDS FLOW THROUGH THE CHANNEL WITH NOVEL HYBRID RIBS

2023
MASTER THESIS
MECHANICAL ENGINEERING

Wisam Abdulhussein Hasan AL-HUSSEIN

Thesis Advisors
Assist. Prof. Dr. Enes KILINÇ
Assist. Prof. Dr. Hussein TOGUN

HEAT TRANSFER AND HYBRID NANOFLUIDS FLOW THROUGH THE CHANNEL WITH NOVEL HYBRID RIBS

Wisam Abdulhussein Hasan AL-HUSSEIN

Thesis Advisors

Assist. Prof.Dr. Enes KILINÇ

Assist. Prof. Dr. Hussein TOGUN

T.C.

Karabük University

Institute of Graduate Programs

Department of Mechanical Engineering

Prepared as

Master Thesis

KARABUK

September 2023

I certify that in my opinion the thesis submitted by Wisam Abdulhussein Hasan AL-HUSSEIN titled " HEAT TRANSFER AND HYBRİD NANOFLUİDS FLOW THROUGH CHANNEL WITH NOVEL HYBRIDS RIBS" is fully adequate in scope and quality as a thesis for the degree of Master of Science.

Assist. Prof. Dr. Enes KILINÇ .....

Thesis Advisor, Department of Mechanical Engineering

This thesis is accepted by the examining committee with a unanimous vote in the Department of Mechanical Engineering as a Master of Science.01/09/2023

Examining Committee Members (Institutions)	Signature
Chairman : Prof. Dr. Mehmet ÖZKAYMAK (KBU)	.....
Member : Assist. Prof. Dr. Enes KILINÇ (KBU)	.....
Member : Assist. Prof. Dr. Fatih UYSAL (SUBU)	.....
Member : Assist. Prof. Dr. Hussein TOGUN (UTQ)	.....
Member : Assoc. Prof. Dr. Selçuk SELİMLİ (KBU)	.....

The degree of Master of Science by the thesis submitted is approved by the Administrative Board of the Institute of Graduate Programs, Karabük University.

Assoc. Prof. Dr. Zeynep ÖZCAN .....

Director of the Institute of Graduate Programs

"I declare that all the information within this thesis has been gathered and presented by academic regulations and ethical principles, and I have, accordingto the requirements of these regulations and principles, cited all those which do not originate in this work as well."

Wisam Abdulhussein Hasan AL-HUSSEIN

ABSTRACT

M. Sc. Thesis

HEAT TRANSFER AND HYBRID NANOFLUIDS FLOW THROUGH THE CHANNEL WITH NOVEL HYBRID RIBS

Wisam Abdulhussein Hasan AL-HUSSEIN

Karabuk University
Institute of Graduate Programs
The Department of Mechanical Engineering

Thesis Advisor:
Assist. Prof. Dr. Enes KILINC
Assist. Prof. Dr. Hussein TOGUN
September 2023, 81 pages

This thesis can be seen as a numerical study of the two-dimensional hybrid (0.5% Al_2o_3, 0.5% TiO_2) nanofluid flow and heat transfer within a ribbed pipe of different rib configurations, including rectangular, triangular, semi-circular, and hybrid rib arrangements. The diameter of the pipe is 15 mm, and the length is 1000 mm. Four Reynold number values, Re = 10000, 20000, 30000, and 40000, are determined in the study, and a constant heat flux at 5000 $W/m^{2.}$ Six cases are applied on the pipe walls. Six different designs with different ribs heights (h = 0.075 and 1.5 mm) and different pitch distances (p = 15, 30, and 60 mm) are included in the simulation to investigate the effect of rib parameters on the thermal and flow fields. The study is carried out by applying the turbulent kinetic energy – -dissipation (k – ε) model using ANSYS FLUENT software.

The results show that increasing the Reynolds number causes a considerable increase in both heat transfer coefficient and pressure drops for all rib arrangements. Also, decreasing the pitch distance and/or increasing the height ratio increases the heat transfer rates and pressure losses. The study concludes that the rectangle ribs arrangement provides the best characteristics in terms of heat transfer coefficient values and overall thermal performance factor. The semi-circular ribs also presented high values of thermal performance factor due to the lowest pressure drops reported in this type of ribs. On the other hand, the triangle ribs have examined the largest pressure drops and consequently have the lowest thermal performance. The hybrid ribs arrangement results are consistent with the single ribs data.

Keywords **:** Numerical study, nanofluid, ribbed pipe, heat transfer coefficient, pressure drop, thermal performance.

Science Code : 91412

ÖZET

Yüksek Lisans Tezi

YENİ HİBRİT KANATÇIKLAR İLE KANAL İÇİNDE ISI TRANSFERİ VE HİBRİT NANOAKIŞKAN AKIŞI

Wisam Abdulhussein Hasan AL-HUSSEIN

Karabük Üniversitesi
Lisansüstü Eğitim Enstitüsü
Makina Mühendisliği Anabilim Dalı

Tez Danışmanları:
Dr. Öğr. Üyesi Enes KILINC
Dr. Öğr. Üyesi Hussein TOGUN
Eylül 2023, 81 sayfa

Bu çalışmada, dikdörtgen, üçgen, yarı dairesel ve hibrit kanatçık düzenlemeleri dahil olmak üzere farklı kanatçık konfigürasyonlarına sahip kanatçıklı bir boru içindeki iki boyutlu hibrit (%0,5 Al_2O_3, %0,5 TiO_2) nanoakışkan akışı ve ısı transferi sayısal olarak incelenmiştir. İncelenen borunun çapı 15 mm ve uzunluğu 1000 mm'dir. Çalışmada Re = 10,000, 20,000, 30,000 ve 40,000 olmak üzere dört farklı Reynold sayısı değeri ve 5000 W/m^2'de sabit bir ısı akısı belirlenmiştir. Boru duvarlarına altı farklı durum uygulanmıştır. Farklı kanatçık yüksekliklerine (h = 0,075 ve 1,5 mm) ve farklı kanatçıklar arası mesafeye (p = 15, 30 ve 60 mm) sahip altı farklı tasarım, kanatçık parametrelerinin ısıl ve akış alanları üzerindeki etkisini araştırmak için simülasyona dahil edilmiştir. Çalışma, ANSYS Fluent yazılımı kullanılarak türbülanslı kinetik enerji - dağılım (k - ε) modeli uygulanarak gerçekleştirilmiştir.

Sonuçlar, Reynolds sayısının artırılmasının tüm kanatçık durumları için hem ısı transfer katsayısında hem de basınç düşüşlerinde önemli bir artışa neden olduğunu göstermektedir. Ayrıca, kanatçıklar arası mesafesinin azaltılması ve/veya yükseklik oranının artırılması ısı transfer oranlarını ve basınç kayıplarını artırmaktadır. Çalışmada, ısı transfer katsayısı değerleri ve genel ısıl performans faktörü açısından dikdörtgen kanatçık düzenlemesinin en iyi özellikleri sağladığı sonucuna varılmıştır. Yarı dairesel kanatçıklar da bu tip kanatçıklarda rapor edilen en düşük basınç düşüşleri nedeniyle yüksek termal performans faktörü değerleri sunmuştur. Öte yandan, üçgen kanatçıklar en büyük basınç düşüşlerini incelemiş ve sonuç olarak en düşük termal performansa sahip olmuştur. Hibrit kanatçık düzenlemesi sonuçları tek kanatçık verileriyle tutarlıdır.

Anahtar Sözcükler : Sayısal çalışma, nanofluid, nervürlü boru, ısı transfer katsayısı, basınç düşüşü, termal performans

Bilim Kodu : 91412

ACKNOWLEDGMENT

I owe thanks and praise to Allah first and foremost for this success. I would like to express my special thanks to my thesis supervisor, Assist. Prof. Dr. Enes KILINÇ and Assist. Prof. Dr. Hussein Togun. I also thank the Head of the Department of Mechanical Engineering, Prof. Dr. Kamil Arslan, and his staff for the help they provided me.

My thanks go to my family, brothers and sisters, and my father, especially to my mother's soul. May God have mercy on her. I thank my dear wife who took responsibility for me and what she gave me. My gratitude is extended to my children as they always pray for me.

I want to thank all my friends for standing with me in accomplishing my study.

Lastly, I would like to thank all my supporters.

I dedicate this thesis to my beloved country, Iraq. And to the beautiful Turkey, which embraced this scientific experience and contributed to providing all possibilities for graduating in this distinguished way.

CONTENTS

Page

Page

Page

LIST OF FIGURES

Page

Page

Page

Page

LIST OF TABLES

Page

ABBREVIATIONS AND SYMBOLS INDEX

ABBREVIATIONS

CFD	Computational Fluid Dynamic
CVD	Chemical Vapor Deposition
RANS	Reynolds Averaged Navier-Stokes
SST	Shear Stress Transport
RST	Reynolds Stress Transport
FV	Finite Volume
FMWCNT	Functionalized Multi-Walled Carbon NanoTube
EG	Ethylene Glycol
RNG	Re-Normalization Group
PDE	Partial Differential Equations
BDS	Backward Difference Scheme
SIMPLE	Semi-Implicit Method for Pressure Linked Equation

SYMBOLS

D (d), Dh	[m]	Diameter, Hydraulic Diameter
P	[m]	Pitch distance
e, h	[m]	Rib height
w	[m]	Rib width
k	[J/kg] = [m^2/s^2]	turbulent kinetic energy
ε	[m^2/s^3]	turbulent energy dissipation
ω	[s^{-1}]	The specific dissipation
ε	[m^2/s^3]	turbulent energy dissipation
ω	[s^{-1}]	The specific dissipation

Re	-	Reynolds Number
Nu	-	Nusselt Number
f	-	friction factor
h	[W/m^2.K]	convective heat transfer coefficient
P, ΔP	[Pa]	Pressure, Pressure drop
k	[W/m.K]	Thermal conductivity
U, V, W	[m/s]	velocity component
x,y,z	[m]	Cartesian coordinate
ρ	[kg/m^3]	Density
T	[K]	Temperature
Pr	-	Prandtl number
μ	[Pa.s]	Dynamic viscosity
$Iu^{'}$, $T^{'}$	[m/s], [K]	fluctuation velocity, temperature
Wν_t	[m^2/s]	turbulent kinetic viscosity
σ_t	-	Turbulent Prandtl number
P_k	[m^2/s^3]	Production term
t	[s]	time
$C_\mu, C_{\varepsilon 1}, C_{\varepsilon 2}, \sigma_\varepsilon$	-	Constants
ϕ	-	Nanoparticle volume fraction
C	[J/kg.K]	Specific heat
q	[W/m^2]	Heat flux
L	[m]	Length

PART 1

INTRODUCTION AND RESEARCH BACKGROUND

1.1. GENERAL BACKGROUND

Many engineering problems involve using fluid to transport heat through channels of different cross-sections. Some examples are cooling systems in vehicles, buildings, and many industrial processes. For many years, enhancing heat transfer has always been a challenging matter for engineers and researchers, particularly for applications of large heat transfer generation. To improve the thermal performance of the application, many attempts have been made, including examining different channel shapes and utilizing various working fluids. About modifying the channel shape, using ribs and fins of different configurations in the channel has been one of the most active methods for improving thermal performance efficiency. On the other hand, regarding the working fluid, because, water, oil, and other conventional fluids have limited thermal transport properties, engineers had to look for alternatives to attain high heat transfer rates. One of the most important solutions was to add thermally conductive solids into these conventional fluids. This new generation of heat carrier fluid is simply known now as nanofluid.

Convective heat transfer processes are highly involved in several industrial systems. Maximizing the heat transfer rates and minimizing the required input power have been the main concerns of engineers and researchers. Different strategies have been examined to enhance the heat transfer rates, including applying vibration to the surfaces of heat transfer, using improved heat transfer surfaces, and utilizing heat transfer fluids of enhanced thermophysical properties. It has been stated that using ribbed heat transfer surfaces can cause a significant increase in the rates of heat transfer [1]. Furthermore, many researchers have reported that adding solid nanoparticles of

high thermal conductivity can remarkably increase the thermal conductivity of the base fluid, and hence significantly enhance the heat transfer rates [2].

1.2. NANOTECHNOLOGY AND NANOFLUIDS

The thermal conductivity of the heat transfer fluid has an important role in determining the efficiency of the heat transfer process. Despite the huge efforts put toward enhancing heat transfer from conventional fluids, only minimal success has been reported. This was because conventional fluids have low thermal conductivity. It is well known that solid metals have much higher thermal conductivity compared to liquid. Hence, fluids with solid metallic particles suspended in them are expected to have improved heat transfer properties compared to conventional fluids without adding [3]. Researchers have conducted extensive studies on the hydraulic and thermal behaviours of these very small solid particles suspended in liquids to identify how the thermal efficiency of the process could be improved. Although the heat transfer rates have considerably increased, some drawbacks associated with using these particles have been reported, such as increasing pressure drop, and hence, further research is still required to obtain an optimal performance [4].

Nanotechnology is a field of science that uses, controls, and manipulates materials on atomic or even subatomic scale to produce new materials with enhanced properties. Recently, this technology has verified promising improvements in various sectors, particularly medicine and energy [5]. Nanomaterials refer to those which have a length scale ranging between 1 to 100 nm. At this length scale, materials start to show unique features that may affect their overall behaviour. A nanometre (nm) is an extremely small length unit equal to 10^{-9} m. Figure 1.1 represents a comparison between nano and micro scales for some components [6]. Utilizing and developing nanotechnology and its applications are nowadays at the core of the researcher's and scientists' interest.

The high-speed growth of nanotechnology applications has led to the development of a new generation of fluids called nanofluids. The Nanofluid is a liquid consisting of a base liquid with nanoparticles suspended in it. The idea of suspending nanoparticles in

a base conventional liquid to enhance its thermal properties was first proposed by a research team at the Argonne National Laboratory in Illinois in 1995 [7,8]. It was found that adding solid nanoparticles to a base fluid can considerably increase the heat transfer rates. This has been attributed to the low thermal conductivity of the base fluid, and the high thermal conductivity of the suspended nanoparticles [8]. Table 1.1 displays the thermal conductivity of the various metallic, non-metallic solids, and base fluids commonly used in nanofluids [9]. Nanofluids are currently found in many engineering applications, including industrial and domestic cooling systems, electronic cooling components, solar energy absorption systems, energy storage systems and so on.

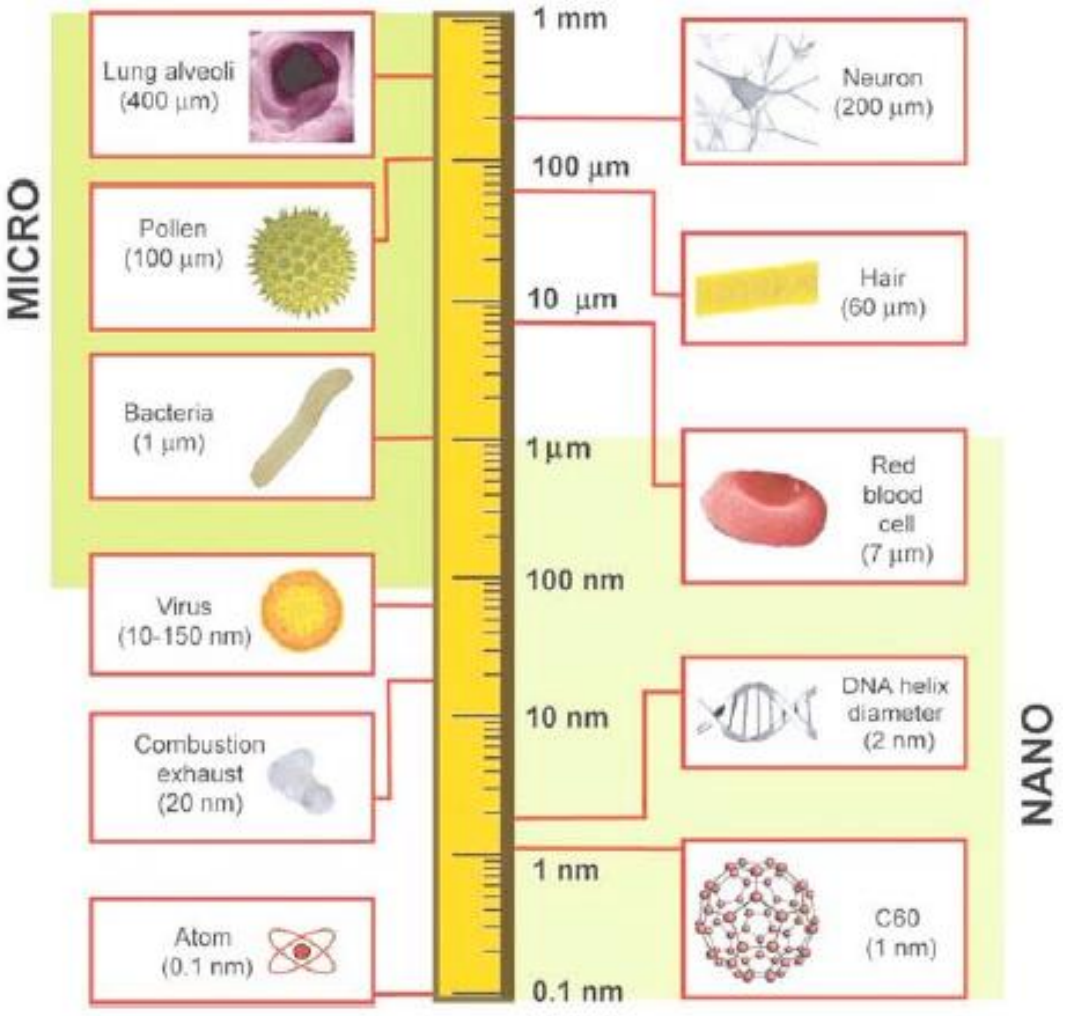

Figure 1.1. Comparison between micro components and nanomaterials [6].

Table 1.1. Thermal conductivity for some common nanoparticles and base fluid [9].

	Material	**Thermal conductivity W/m.K**
Metallic solids	Cu	401
	Al	237
	Ag	428
	Au	318
	Fe	835
Non-metallic solids	Al_2O_3	40
	CuO	67.5
	Si	148
	SiC	270
	CNTs	3000
Base fluids	H_2O	0.613
	Ethylene Glycol	0.253
	Engine Oil	0.145

The most commonly used nanoparticles are metals or metal oxides, such as those listed in Table 1.1, which have high thermal conductivity. However, due to the high cost of metallic nanoparticles, metal oxide nanoparticles, such as Al_2O_3 and TiO_2, which are used in the current study, are usually utilized in research and industry. They are still having a thermal conductivity that is higher than that of the common base fluid. Recent literature has shown that these nanoparticles not only improve the thermal conductivity of the base fluid but also enhance the convective heat transfer coefficient. Nevertheless, the studies have also indicated that using nanoparticles would increase the pressure drop and, as a result, the pumping power due to their relatively high viscosity [10].

In traditional fluids, the suspended particles are usually of micrometre scale. Nanoparticles have several advantages over micro-sized particles, which make them desirable in different engineering applications. Nanoparticles are more stable and can stay suspended in the base fluid for a longer period. Also, nanoparticles have larger surface areas than microparticles, so they can contribute more effectively toward heat transfer enhancement. In addition, nanoparticles have a higher thermal conductivity in comparison to micro-scaled particles [11].

It is worth mentioning that in some cases, using nanofluids could decrease the heat transfer rather than enhance it. This is particularly true in natural convection heat transfer studies, where increasing the concentration of the nanoparticles has caused a decrease in Nusselt number values and, hence, the heat transfer rates due to the negative effect of the dynamic viscosity and inertia forces [12, 13]. Fortunately, no such effect has been claimed for forced convection heat transfer cases, the subject of the current study.

1.2.1. Manufacturing of Nanoparticles and Nanofluid

There are several ways to produce nanoparticles that are used in nanofluid, and they can be divided into two main groups: physical and chemical methods. The physical techniques typically encompass methods such as the mechanical grinding process and the inert-gas-condensation procedures. The chemical techniques, on the other hand, encompass chemical processes, such as Chemical Vapor Deposition (CVD), chemical precipitation, spray pyrolysis, thermal spraying, and micro-emulsions. The procedures that are specifically involved in producing metal nanoparticles comprise physical and chemical synthesis processes, including mechanical grinding, inter-gas- -condensation, thermal spray, spray pyrolysis, and chemical precipitation [14].

Nanoparticles are usually manufactured and formed as a powder for most nanomaterials. The nanofluids are then produced by dispersing the nanoparticle in the powder form into a base host liquid. Different base liquids, organic or aqueous, and different nanomaterial powders are selected based on the specific application of the nanofluid [14].

To prepare nanofluids, there are two typical methods: a one-step approach and a two-step approach [15]. In the two-step procedure, the most widely used method for preparing nanofluids, the dry powder of nanoparticles is firstly produced by chemical or physical processes, and then the nanoparticle powder is scattered within the base liquid. The two-step procedure is considered an economical procedure for mass production of nanofluids, particularly when using an inert-gas-condensation procedure

to produce the nanoparticles [16]. However, the two-step method has an important disadvantage, which is the problem of nanoparticle accumulation. Because of the attraction forces, the nanoparticles tend to build up very fast before they achieve the dispersion processes within the base fluid successfully [14]. Some suggestions have been introduced to overcome this problem and achieve a stable nanofluid, including applying some physical methods such as stirring and ultrasonication or adding a small amount of a stabilizing agent to the mixture.

On the other hand, in the one-step procedure, the nanoparticles are prepared and scattered within the base fluid only in one process. This procedure can be used to avoid the nanoparticle spread problem and hence can help in producing stable nanofluids. As an example of using the one-step technique in producing a nanofluid, Estman et al. could produce uniform, not agglomerating, Cu/ethylene glycol nanofluid. They produced Cu nanoparticles from the vapour phase straight into the ethylene glycol base fluid [17]. However, because of the high cost and long time required to produce nanofluids using the one-step technique, it is only used for research work [14].

1.2.2. Hybrid Nanofluid

As already mentioned, the nanofluid is a base fluid in which nanoparticles are suspended. When more than one type of different nanoparticles is suspended in the base fluid, it is then called a hybrid nanofluid. This new type of nanofluids has been developed by researchers and scientists to further improve the thermal performance of the cooling media to meet the continuously increased requirements. Most of the relevant studies have confirmed that hybrid nanofluids have larger thermal conductivity compared to mono nanofluids. Nevertheless, there are still some studies that reported opposite results [18,19]. It was concluded that the thermal conductivity of the nanofluid is dependent on the base fluid and also on the size and shape of the nanoparticles. Both nanoparticle concentration and temperature had a positive impact on the thermal conductivity of the nanofluids, providing that there were upper limits for concentration and temperature not to be exceeded [19].

Hybrid nanofluids are like mono nanofluids and can be prepared in two ways, either the one-step method or the two-step method. Although the two-step method is more common due to the low cost of preparation and the ease of manufacture, there is again the problem of stability that arises from this preparation method. Using more than one type of nanoparticles, such as in a hybrid nanofluid, may lead to more nanoparticle agglomeration and, thus, less stability. However, ultrasonication for a specific time with applying some additions was found to be sufficient to achieve a hybrid nanofluid of good stability [20].

1.3. COOLING RIBS

The heat transfer rates through channels can be considerably enhanced by providing the inner surfaces with a rib turbulator. The ribs-roughened channels are widely used in many engineering applications. The ribs increase the internal surface area and the production of turbulent kinetic energy by periodically disturbing the boundary layer and main flow, increasing the convective heat transfer rates [21]. However, the areas in front of and behind the ribs, which cover a sizable part of the channel walls, represent low heat transfer regions. As can be seen from Figure 1.2 these stagnation zones are characterized by recirculating currents, and as a result, these regions have low heat transfer rates and high pressure losses. The reattachment area in the distance between the two following ribs has the maximum heat transfer rates [22].

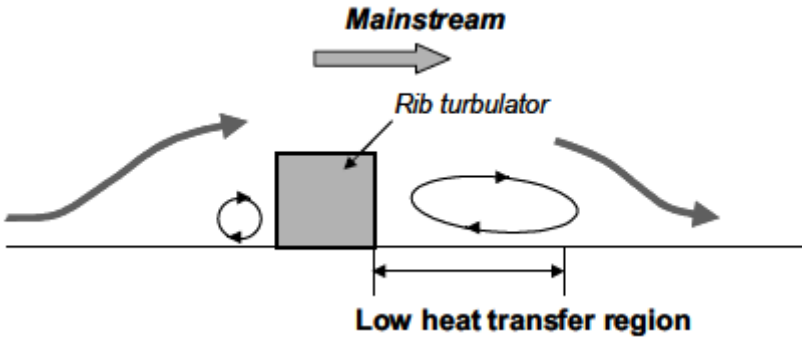

Figure 1.2. Flow recirculation around a rib [22].

Several factors affect the heat transfer from ribbed surfaces, including rib shape, rib height, attack angle, and pitch distance. The shape of the ribs, their sizes, as well as

the way they are distributed along the cooling channels may vary according to the application. It is essential to optimize the rib parameters to attain the maximum possible heat transfer rates and the minimum drag [23].

The distance between the adjacent ribs plays a vital role in determining the characteristics of the flow over rib roughness [24]. Figure 1.3 shows that depending on the rib spacing, the flow might be skimming, un-reattached, or attached flow. The recognized flow pattern directly affects the heat transfer rates and pressure losses. In addition to the rib spacing, the rib height is also an important factor and has substantial and direct consequences on the flow over the roughness. The rib's height should not exceed a specific ratio of the channel height to attain the essential flow category [24, 25].

Furthermore, the Reynolds number, the cooling fluid, and the rib shape and number are also important factors that influence the flow behaviour and the thermal performance of the ribbed channels. Generally, sharp-edge rib shapes cause greater heat transfer augmentation than round rib shapes, but the results are reversed about the pressure drops [23].

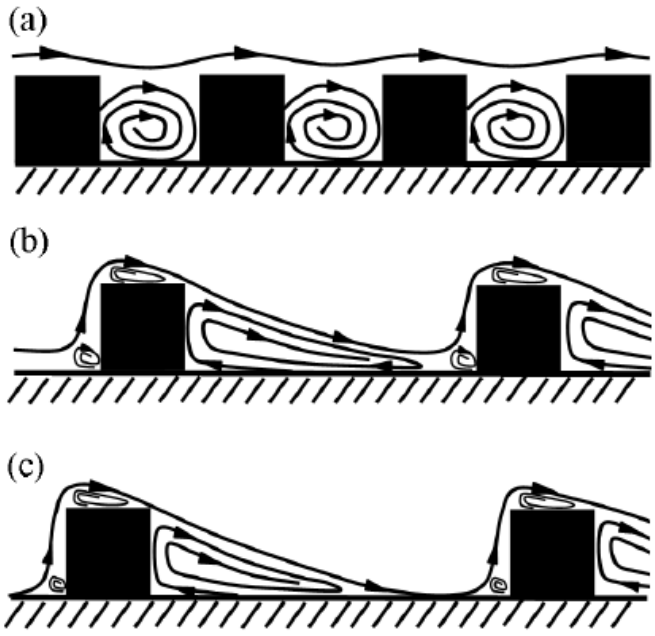

Figure 1.3. Flow regimes over rod roughness: (a) Skimming flow; (b) Un-reattached flow; (c) Reattached flow [25].

Despite numerous studies that have considered heat transfer in rough surfaces (some of them will be reviewed in Chapter Two), detailed flow physics is still under the scope of research interest. Most of the available experimental measurement instruments have demonstrated to be not accurate enough for rough surfaces, because of the high turbulence intensities there. Computational Fluid Dynamic (CFD) studies have become more popular and an attractive choice in analysing different engineering problems, especially with the continuous advancement in computational resources.

1.4. RESEARCH PROBLEM

Enhancing heat transfer rates is a desirable goal for many engineering applications. To achieve this objective, different procedures could be followed, including using mono or hybrid nanofluids instead of the conventional fluids as a heat carrier, and/or using ribs-roughened geometries instead of plain-walled ones. Reference research has shown that both procedures can result in a significant increase in heat transfer rates, and numerous studies are available in the literature concerning the enhancement of convective heat transfer rates and pressure losses. Nevertheless, these studies have examined enhancing heat transfer of single or hybrid nanofluids flowing in a channel with regular ribs. None of them have looked into employing hybrid nanofluids in a channel with unique hybrid ribs. The idea of this study is to carry out a numerical investigation of hybrid nanofluid flow and heat transfer within an innovative hybrid ribbed channel.

1.5. RESEARCH OBJECTIVES

This research includes a two-dimensional CFD simulation of a hybrid nanofluid (0.5% Al_2O_3 - 0.5% TiO_2)/water heat flow through a hybrid ribbed pipe of different configurations using the ANSYS FLUENT package. The primary purposes of this research are:

- Determining the effect of Reynolds number on local and average heat transfer and pressure drop along the channel. Four different Reynolds number values, namely 10000, 20000, 30000, and 40000, are considered in the study.
- Determining the effect of the rib shapes on the heat transfer and pressure drop enhancement. Three different shapes of the ribs, including rectangular, triangular, and semi-circular, with single and hybrid arrangements, are considered in the study.
- Determining the effect of ribs parameters: the pitch distance and step height on the flow and heat characteristics. Six different designs of the rib parameters are considered in the study.

1.6. THESIS OUTLINES

In Chapter Two, the relevant literature from different resources, whichever experimental or numerical investigations, regarding the heat transfer and pressure drop enhancement as well as the thermal and flow characteristics of nanofluids, will be presented and discussed. Because this study is numerical, the main focus will be directed to simulation research.

Chapter Three describes the methodology followed in the research to obtain the required results. The averaged Navier Stokes equations together with the selected turbulence model equations, are first presented. The ribbed channel designs are modelled, the computational domains are meshed, the boundary conditions are introduced, and the numerical settings are defined. A validation case is first carried out for better confidence in the numerical results, and the obtained results are compared to a reference experiment study before moving on to the main numerical cases.

The detailed simulation results for the different studied cases are demonstrated and discussed in Chapter Four. The local and average convective heat transfer coefficients and pressure drops are determined and presented for all considered designs. The effect of Reynolds number, rib shapes and parameters are discussed in detail in this chapter.

Although the thermal performance factor is calculated for all configurations, the best arrangement is determined.

Finally, in Chapter Five, the complete results will be briefly summarized and the most important findings will be presented. Also, this chapter includes some suggestions for future researchers.

PART 2

LITERATURE REVIEW

2.1. PRELIMINARY REMARKS

For many years, the topic of raising the thermal performance of cooling processes has been the subject of numerous studies. There has always been an increasing demand to achieve high heat transfer rates in different engineering applications. Many attempts have been made either to find a working fluid of enhanced thermal properties or to modify the design of the cooling channel to increase the heat transfer rates. Introducing nanofluids has contributed to enhancing heat transfer to some extent, and also the channel geometry has had a significant impact on heat transfer enhancement. A huge number of publications are available in the literature regarding nanofluid technology or cooling ribs. However, in this chapter, the focus will be only on the studies concerning the convective heat transfer and pressure drop of nanofluid flow through ribbed channels of different geometries and configurations. Although the current work is a numerical investigation, the most relevant experimental studies will also be presented and discussed. The experimental data is essential for the validation of numerical results and can provide a more complete understanding of the research problem. However, the previous numerical studies are of particular interest here, and therefore, they will be discussed in more detail.

2.2. PREVIOUS WORKS

Maurer et al. [26] carried out a numerical and experimental study to evaluate the heat transfer and pressure loss of V-shaped ribs within a rectangular channel at various Reynolds numbers. Different rib parameters were examined, including e/Dh = 0.0625 and 0.02, and P/e = 10, where e, Dh, and P refer to rib height, channel hydraulic diameter, and pitch distance, respectively. Three-dimensional RANS equations

together with the energy equation and k- ε turbulence model, were solved using FLUENTTM software. The obtained experimental and numerical results were heat transfer and friction factors. The V-rib influenced down-washing vortex flow and considerably increased heat transfer in the downstream zone, according to the researcher's findings. The rib height-to-width ratio has a significant impact on heat transmission and flow resistance. Reducing the rib height caused a slight drop in heat transfer level but, at the same time, caused a remarkable reduction in pressure losses. The results showed that the optimal thermal performance could be attained by using ribs at a small scale.

Manca et al. [27] carried out a two-dimensional numerical study aiming at investigating the flow behaviour and the heat transfer performance of a turbulent nanofluid through a ribbed channel whose length and height were 250 mm and 10 mm, respectively, and subjected to constant wall heat flux at 20,000 W/m2. The nanofluid was Al2O3/water of different nanoparticle volume fractions in the range from 0% to 4%. The ribs had triangle and square shapes with different height and pitch distance parameters. The governing RANS equations with SST k- ω turbulent model are solved using Fluent code, and then the Nusselt number and friction factors were obtained for Reynolds number values from 20,000 to 60,000. The results demonstrated that both Nusselt numbers and friction factors increased with increasing Reynolds number, and also by increasing the nanoparticles concentrations. The best heat transfer results were found for a pitch-to-height ratio equal to 8 for the square ribs and equal to 10 for the rectangular ribs. On the other hand, the worst pressure drop data was reported at a pitch-to-height ratio equal to 10 for both rectangle and square-shaped ribs.

Elwakeel et al. [28] used the traditional k- ω, Shear Stress Transport (SST), and Reynolds Stress Transport (RST) turbulence models to simulate the turbulent heat transfer and fluid flow in a channel with various rib forms, including square ribs, triangular ribs, and trapezoidal ribs with constant parameters. They used the ANSYS CFX program in the simulation and obtained detailed flow and heat transfer data for the steam and steam/mist (6% mass fraction) flows. The results indicated that when compared to the other cases and relevant measurements, the SST turbulence model had

the best data agreement. Furthermore, it was concluded that the mist injection had a positive impact on the heat transfer and performance factor, with trapezoidal ribs having the highest heat transfer coefficient. The worst thermal performance was reported for the triangle-shaped ribs.

Togun et al. [29] used a FORTRAN programming code and Finite Volume (FV) method to solve the governing equation of the heat transfer and nanofluid flow over a backward-facing step in laminar and turbulent conditions. For turbulence modelling, the SST k- ω model was used. The simulation included studying the effect of the concentration of the nanoparticle (Cu) within the base fluid (water) on the Nusselt number and pressure drop at a wide range of Reynolds number values. The results showed that the heat transfer rate was improved by introducing the backward-facing step and also by using the nanofluid. The recirculation current generated by the step resulted in a significant increase in Nusselt number values. The Nusselt numbers were further enhanced by increasing the nanoparticle concentrations in both laminar and turbulent conditions. The researchers concluded that the maximum improvements in the heat transfer rates corresponded to a volume fraction of 4%, and reached 36% and 26% for laminar and turbulent conditions, respectively.

In close research, Safaei et al. [30] carried out a numerical study with similar objectives, but by using different types and concentrations of nanoparticles and also by using different step designs in turbulent flow conditions. The nanofluid in this investigation was a water/functionalized multi-walled carbon nanotube (FMWCNT) with volume fractions ranging between 0% to 0.25%, and the step was forward-facing. The simulation was performed using a developed FORTRAN code and finite volume algorithm with the SST SST k- ω turbulence model. The results confirmed that the developed mathematical model could predict the real flow behaviour correctly, and the numerical data matched well the relevant experimental measurements. Consistent with the previous study, the results showed that the recirculation flow created by the step design caused a remarkable increase in heat transfer values. Furthermore, the results confirmed the remarkable positive effect of increasing both Reynolds number and nanoparticle concentrations on the augmentation of the heat transfer levels.

Moghadassi et al. [31] numerically modelled mono (Al2O3/water) and hybrid (Al2O3-Cu/water) nanofluids convective heat transfer in a uniformly heated horizontal pipe in laminar flow condition, Re < 2300. The dimensions of the pipe were 1000 mm in length and 10 mm in diameter. The concentration of the nanoparticles was 0.1%, and their average size was 15 nm, similar to the specifications specified in the experimental work of Suresh et al. [32], which was used to validate the numerical result. The CFD simulation results included heat transfer and pressure drop as a function of Reynolds number. The results exhibited good agreement with the experimental reference data [32]. The heat transfer rate was found to significantly increase by increasing the Reynolds number, particularly when using hybrid nanoparticles. The Nusselt number values increased by up to 13 % compared to pure water flow, and by about 5 % compared to the mono nanoparticles case. The pressure drop data was not affected that much when using nanoparticles, and the increase in friction factor of hybrid nanofluid was less than 7% compared to the pure water flow case.

Togun [33] carried out a comparative study between the heat transfer from the flow of CuO/water nanofluid in a backwards–facing step with plain walls and also with obstacles of different sizes, including 1.5 mm, 3 mm and 4.5 mm height. The flow condition was laminar, and the Reynolds numbers were in the range of 75 to 225. The effect of the nanoparticle volume fraction was also considered in the investigation, and concentrations between 1 and 4% were examined. A two-dimensional numerical simulation was conducted using a programming code based on the finite volume method for discretizing the governing equations. The results confirmed the strong impact of Reynolds number, nanoparticle concentration, and rib height on the heat transfer rates. It was shown that the heat transfer rates could be improved by up to 22% when using a properly sized obstacle compared to the plain-wall case. However, increasing the Reynolds number, nanoparticle concentrations, and obstacle height hurt pressure losses.

Abdulrazzak et al. [34] and Togun et al. [35] considered the effect of nanofluid flow separation on the heat transfer within a concentric annular pipe. The base fluid in both studies was water, but with TiO2 nanoparticles in the first study and Al2O3 in the

second study. The examined Reynolds numbers and nanoparticle volume fraction ranges were almost the same in both studies. The Reynolds number varied between 10,000 to 50,000, and the nanoparticle concentrations between 0.5 to 2%. The inner pipe in the two studies was insulated, with constant diameter and length at 25 mm and 2500 mm, respectively. The outer pipe, however, was of different geometry specifications in the two studies. Abdulrazzak et al. used an entrance part of a length of 1000 mm, a diameter of 100 mm, an exit part of a length of 1500 mm, and different diameters at 100, 80, and 60 mm. The whole outer cylinder was exposed to a constant heat flux of 6000 W/m2. On the other hand, Togun et al. used an outer insulated entrance part of length 1500 mm and different diameters 80, 60, and 50 mm, and an exit outer part of length 1000 mm and constant diameter 100 mm exposed to a uniform heat flux. The researchers carried out three-dimensional numerical simulation using ANSYS software, based on the FV method and SST k- ω model for turbulence modelling. The results also confirmed the previously reported positive impact of increasing Reynolds number nanoparticlecle concentration on heat transfer rates. Furthermore, the results revealed that sudden expansion (or sudden contraction) produced recirculation flow and consequently increased the heat transfer rates and, at the same time, the pressure dropped. The maximum heat transfer and pressure drop were reported for the castor, corresponding to the highest examined Reynolds number and the highest expansion (or contraction) ratio.

Later on, Togun et al. [36] continued the research in the same direction and carried out a numerical and experimental study to investigate the separation of turbulent nanofluid flow in concentric pipes. They kept almost the same geometry dimensions, expansion ratios, Reynolds number range, and nanoparticle volume fractions but examined more nanofluid types, including Al2O3, CuO, and TiO2. The numerical and experimental results showed a resemblance, and the results were consistent with the previous works of the research team. The enhancement of heat treatment resulting from introducing the expansion to the straight pipe reached about 37% when using pure water and further increased to about 49% when adding nanoparticles to the base water. The Al2O3 nanoparticles attained the best results among other examined nanoparticles. However, it must be mentioned that the results also showed that the pressure drop

considerably increased by using the arrangement of nanofluid and a pipe with a sudden expansion. The pressure drop increment reached up to 65% (with CuO nanoparticles) compared to pure water and straight pipe.

Khdher et al. [37] carried out an experimental and numerical investigation to obtain the pressure drop and heat transfer coefficient for nanofluid (Al2O3/water) flow within a pipe with turbulators. The pipe was 14.9 in diameter, circumferentially provided with ribs of different parameters, and exposed to a uniform heat flux. The effect of rib size and pitch distances, as well as the effect of nanoparticle concentrations, were considered for Reynolds number values between 10,000 and 40,000. The results indicated that the heat transfer coefficient could be enhanced up to 620% compared to the plain tube when using optimal rib parameters and nanoparticle concentrations. However, the friction factor could, in parallel, increase by up to 240% compared to non-ribbed pipe.

Togun [38] studied numerically the turbulent heat transfer and alumina/water nanofluid flow in a pipe with half-circle ribs. The investigation aimed to examine the effect of Reynolds number, nanofluid volume fraction, pitch ratio and step height of ribs on heat transfer. The results showed that increasing both nananoparticle's concentration from 1% to 4% and Reynolds number from 10000 to 25000 caused a considerable increase in the local heat transfer coefficient. However, it was noticed that, at the same time, these increments in Reynolds number and nanoparticle concentration resulted in increasing the pressure drorp ordered to find the effective ribs parameters on heat transfer. The researcher considered six different cases with variable rib heights and pitch distances. It was shown that decreasing the distance between ribs increased the heat transfer as a result of increasing the number of ribs. In conclusion, the greatest heat transfer coefficient was found at a step height of 5 mm, per centent Al2O3 nanofluids, and at a Reynolds number of 25000.

Sometime later, Togun et al. [39] worked on similar purposes but with different geometry and different nanoparticles. They considered heat transfer in a channel with semicircle ribs and Al2O3-Cu/water hybrid nanofluid. Different nanofluid volume

fractions (0.33, 0.75, 1, and 2%), different Reynolds numbers 10000, 15000, 20000 and 25000, and different ratios of ribs height to channel height and pitch distances were included in the 2D simulation using ANSYS Fluent. The researchers found that the best results in terms of heat transfer enhancement corresponded to a high Ra-Reynolds number and high nanofluid concentration. The recirculation zones noticed before and after the ribs positively contributed to Nusselt number values, but negatively to the tion coefficient. Again, decreasing the pitch distance and hence increasing the ribs number increased the heat transfer levels.

Al Kumait et al. [40] carried out an experimental and numerical investigation on the heat and fluid flow of TiO2/water nanofluid of nanoparticle concentrations ranging from 0 to 1%, inside a ribbed tube of length 1 m and diameter of 15 mm. A uniform heat flux at 5000 W/m2 was applied on the tube walls, and the flow was assumed to be turbulent at Reynolds number values of 5000 to 40000. The research included different configurations, longitudinal, helical, and circumferentially ribs, with three different pitch distances of 5.89, 7.86, and 11.79 meters. Results showed that a ribs configurations improved the heat transfer rates, and the enhancement was the maximum for the helical ribs at the highest Reynolds number, where it reached 2% compared to the plain tube. However, the results also showed that the swirling effect noticed in the helical ribs configuration increased the flow resistance and consequently increased the pressure drop. This behaviour was most noticeable at the smallest pitch distance considered in the study.

Alrashed et al. [41] used the FV method and carried out a two-dimensional numerical simulation of the laminar water/ FMWCNT nanofluid flow and heat transfer backwards-facing contracting channel. The channel had one wall insulated and the other exposed to a uniform heat flux. They considered the effect of Reynolds number between 1 to 150, nanoparticle 'articles weight fraction ranged from 0 to 0.25 on the thermal performance. The obtained results included Nusselt number, friction factor, pressure drop, and velocity and temperature contours. It has been noticed that the channel sections of low velocity had low heat transfer coefficients and low friction fact backwards-facing-facing step caused recirculation flow. Increasing the Reynolds

number increased the axial velocity, reduced the surface temperature, and improved the heat transfer rates. Furthermore, increasing the nanoparticle mass fraction caused a significant increase ase in the Nusselt number, with a little variation in pressure drop. The nanofluid and heat transfer in channels with forward or backward steps have been the subject of intensive investigations aiming at enhancing the heat transfer performance in this geometry. The studies were experimental and numerical, in laminar and turbulent conditions, with the use of mono and hybrid nanofluids of different concentrations, with applying various boundary conditions, and with using different geometry scales. Salman et al. [42] provided a detailed review of the research that deals with this problem. Their article presented the overall previous findings and also outlined the future progress in such research.

Ekiciler and Çetinkaya [43] compared the thermal performance and flow behaviour of mono and hybrid nanofluids within a ribbed duct. The mono and hybrid nanofluids were Al2O3/water and Al2O3- Cu/water, respectively, with a nanoparticle volume fraction of 1%. The duct length was 250 mm and its height was 10 mm, having walls exposed to a constant heat flux at 20,000 W/m2. Three different rib shapes, including square, ellipse, and triangle, with dimensions of height 1 mm, width 2 mm, and the distance between two adjacent ribs 20 mm. The researchers used the SYS Fluent program and carried out a two-dimensional numerical study to analyse the heat transfer and the turbulent nanofluid flow through the ribbed duct. The obtained data included Nusselt number and friction coefficient at Reynolds number values ranging from 20,000 to 60,000. The results confirmed the Reynolds number, nanofluid type, and throbs shape all had significant effects on both heat transfer and flow data. The best heat transfer rates were reported for the hybrid nanofluid and triangle-shaped ribs at the highest Reynolds number, where the Nusselt number increased by about 32% compared to the plane duct case. This increment was only 18% for the same conditions but with the use of a mono nanofluid. However, using the hybrid nanofluid, on the other hand, caused an increase in the friction factor due to the higher viscosity compared to the mono nanofluid.

In another study, Ekiciler [44] carried out a two-dimensional numerical investigation to examine the effect of different nanofluids, including pure Ethylene Glycol (EG), TiO2/EG, Cu/EG, and TiO2-Cu/EG, on the heat transfer and fluid flow within a duct provided with a triangle-shaped turbulator. The duct was 0.1 m in length and 0.01 m in height, with a bottom wall exposed to a uniform heat flux of 500 W/m2 and an adiabatic upper wall. The triangle rib was placed on the active bottom wall, and its position and dimensions took different values during the simulation. The flow was considered to be turbulent at Reynolds number values between 50,000 and 100,000, and the RNG k-ε model was used for turbulence modelling. The simulation was carried out using the ANSYS FLUENT package, and the Nusselt number and friction factor values were obtained at different nanoparticle concentrations and different rib parameters. The results confirmed that increasing Reynolds number and nanoparticle volume fractions caused an increase in heat transfer rates but, at the same increases, in pressure drop. Furthermore, the rib parameters also had a significant impact on the heat transfer performance, particularly the rib height. The highest increment in heat transfer performance was reached up to 33.44% compared to plain duct the ith pure, lithe uid flow, and it was reported for the novel hybrid nanofluid with a nanoparticle's concentration equal to 4%, and with a rib parameter defined as ri height-to-duct height-ratio = 0.3, rib width-to-duct height-ratio = 1.5, and rib distance-to-duct height-ratio = 5.

Kumar and Sarkar [45] numerically analysed the thermal and hydraulic behaviours of different hybrid nanofluids within mini-channel heat sink having ribs of different shapes, including rectangular, semi-circular, trapezoid, and triangular ribs. The examined hybrid nanofluids were Al2O3 – TiO2/DI water and Al2O3 – Cu/DI water, with a constant volume fraction of 0.1%. A two-dimensional simulation was carried out using Ansys Fluent software, and the Nusselt number, friction factor, heat transfer coefficient, pressure drop, and thermal performance factor results were obtained. The results showed that all ribbed channel configurations achieved a thermal performance evaluation criterion larger than 1. The best heat transfer enhancement, interpreted by the est heat transfer coefficient and Nusselt number, was recorded for semi-circular ribs and Al2O3 – Cu hybrid nanoparticles. Also, the semi-circular ribs had the

minimum resistance, and hence attained the minimum pressure drop and friction factor. As a result, the semi-circular channel with both hybrid nanofluid types accomplished the highest thermal performance factor, particularly with increasing Reynolds number values.

Finally, Togun et al. [46] used an innovative hybrid ribs arrangement, including triangle, cross, L-shape, and trapezoidal ribs, in a forward-facing contracting heated channel to investigate the effect on heat transfer rate and pressure drop magnitude. The flow was assumed to be turbulent (Re = 10000, 20000, 30000 and 40000), and the ribs dimensions were selected 1 cm by 1 cm with a distance between two adjacent ribs at 11 cm. ConConsistent relevant studies, the results confirmed that increasing Reynthe old number increased both the heat transfer coefficient and pressure drop. The results also showed that using a hybrid arrangement was generally superior to using a single shape rib in terms of heat transfer enhancement, while having a negative impact on pressure drop. However, each shape of ra ibs had a different impact on heat and fluid flow behaviour. A maximum pressure drop was noticetriangle-shapedngle shape the ib, due to the complete pattern which was reported for this type. The study recommended examining the effect of using a throw within the same or didn't toiletry but keeping hybrid ribs arrangement in the tested channel is the objective of the current study.

2.3. SUMMARY OF LITERATURE REVIEW

The most important and relevant previous experimental and numerical studies, with a main focus on numerical works, have been reviewed and analysed in this chapter. The reviewed studies included considering the effect of nanoparticle type (mono or hybrid) and concentration, the rib shape and parameters, the boundary conditions, the flow conditions and The Reynolds number on heat and flow behaviour. Detailed results, such as dimensionless Nusselt number and friction coefficient, convective heat transfer coefficient and pressure drop, and also the thermal performance efficiency, have been obtained.

Most, if not all, the presented studies confirmed that both heat transfer rates and pressure drops increase with increasing Reynolds number and nanoparticle concentrations. In general, the ribs, regardless of their shapes and parameters also have a significant impact on heat transfer and pressure data. The level of heat transfer and pressure drop increment depends on the geometry shape of the ribs parameters and nanofluid type.

In fact, to the author's knowledge, all the previous investigations have considered single or hybrid nanofluids flowing in a channel with regular ribs. None of them has examined the effect of utilizing a hybrid nanofluid in a channel with unique hybrid ribs. The present study aims to provide detailed thermal and flow data for a hybrid nanofluid flow within a pipe provided with regular and hybrid rib arrangements.

PART 3

RESEARCH METHODOLOGY

3.1. COMPUTATIONAL FLUID DYNAMICS (CFD)

Computational Fluid Dynamics (CFD) is a branch of mechanics that is concerned with the analysis of heat and fluid flow problems using computers. With advanced specifications, powerful computers enable CFD programs to find numerical solutions to very complicated flow problems relevant to a wide range of engineering applications, which are impossible to solve analytically. Furthermore, CFD techniques can produce detailed results, which are very hard to obtain experimentally, especially when the experiment is costly or practically impossible to carry out [47].

The CFD methodology depends on solving the flow governing equations, which are usually Partial Differential Equations (PDE), by first converting them to algebraic equations, and then solving the resulting system of equations using one of the numerical methods. The computational domain is divided into a group of cells, and the flow parameters, such as velocity, pressure, and temperature, are stored at the centre or corners of each cell of the grid. This step is known as meshing. The governing differential equations are then approximated to a set of algebraic equations that connect the values of the parameters stored at the adjacent nodes. This process is called discretization. There are three different discretization methods: finite difference, finite element, and finite volume. Most commercial CFD packages, including ANSYS Fluent which is used in the current study, use the finite volume method in the discretization process. Finally, the discretized equations are solved using one of the numerical solution techniques, usually in an iterative procedure [48].

The finite volume method (FV), which is widely used in CFD codes, depends on dividing the computational domain into a group of control volumes of different sizes

and shapes. The transport differential equations are then integrated into each control volume, and, as a result, a set of algebraic equations linking the unknown parameters of the adjacent nodes are obtained. The main advantages of this method are the conservation property is guaranteed and that it can use unstructured meshes [47].

3.2. GOVERNING EQUATIONS

The majority of the commercial CFD software, including ANSYS Fluent used in the present study, use the Reynolds Averaged Naiver Stocks (RANS) equations, along with an appropriate turbulent model. For steady state, three dimensional, incompressible, turbulent flow, RANS equations are given in tensor form as [49]:

$$\frac{\partial(\rho U_i)}{\partial x_i} = 0 \tag{3.1}$$

$$\frac{\partial(\rho U_i U_j)}{\partial x_j} = -\frac{\partial P}{\partial x_i} + \frac{\partial}{\partial x_j}\left[\mu\left(\frac{\partial U_i}{\partial x_j} + \frac{\partial U_j}{\partial x_i}\right) - \rho\overline{u_i' u_j'}\right] \tag{3.2}$$

For flows involving heat transfer, the energy equation must also be solved. It is given in the following transport equation:

$$equal\,\frac{\partial(\rho U_j T)}{\partial x_j} = \frac{\partial}{\partial x_j}\left(\frac{\mu}{Pr}\frac{\partial T}{\partial x_j} - \rho\overline{u_j' T'}\right) \tag{3.3}$$

It is well known that the system of equations that describe turbulent heat and fluid flow, equations 1-3, are not closed, and hence, a turbulent model must be used to approximate Reynolds stresses ($\overline{u_i' u_j'}$) and turbulent heat flux ($\overline{u_j' T'}$); the prime symbol denotes the fluctuation part of the quantity.

3.3. TURBULENCE MODELLING

The Reynolds stresses and turbulent heat flux can be approximated using turbulent viscosity models, which relate these unknown terms to the turbulent viscosity according to the equations [50]:

$$\overline{u_i' u_j'} = (2/3)k\delta_{ij} - \nu_t\left(\frac{\partial U_i}{\partial x_j} + \frac{\partial U_j}{\partial x_i}\right) \quad (3.4)$$

$$\overline{u_i' T'} = -(\nu_t/\sigma_t)\frac{\partial T}{\partial x_i} \quad (3.5)$$

The turbulent viscosity is defined by the equation:

$$\nu_t = C_\mu\, k^2/\varepsilon \quad (3.6)$$

The values of the constants are: $C_\mu = 0.09$ and $\sigma_t = 0.9$.

The turbulent kinetic energy – -dissipation ($k - \varepsilon$) model is considered one of the most widely used turbulent viscosity models, and it is used in the current study, based on the literature recommendations. This model solves two transport equations: one for the turbulent kinetic energy k and one for the rate of its dissipation ε, of the form:

$$\frac{Dk}{Dt} = P_k - \varepsilon + \frac{\partial}{\partial x_j}\left[(\upsilon + \upsilon_t/\sigma_k)\frac{\partial k}{\partial x_j}\right] \quad (3.7)$$

$$\frac{D\varepsilon}{Dt} = C_{\varepsilon 1}\frac{\varepsilon}{k}P_k - C_{\varepsilon 2}\frac{\varepsilon^2}{k} + \frac{\partial}{\partial x_j}\left[(\upsilon + \upsilon_t/\sigma_\varepsilon)\frac{\partial \varepsilon}{\partial x_j}\right] \quad (3.8)$$

The term P_k represents the kinetic energy generation rate, and it is given by the expression: $P_k = -\overline{u_i' u_j'}\,\partial U_i/\partial x_j$. The model constants are taken to be: $C_{\varepsilon 1} = 1.44$, $C_{\varepsilon 2} = 1.92$, $\sigma_k = 1$, and $\sigma_\varepsilon = 1.3$. All other symbols in the above equations 1-8 have its usual meanings.

3.4. NANOFLUID THERMOPHYSICAL PROPERTIES

To determine the thermophysical properties of the nanofluid, single or hybrid, the equations which are available in the relevant literature can be used. The density (ρ_{nf}),

specific heat (C_{nf}), viscosity (μ_{nf}), and thermal conductivity (k_{nf}) of a monotype nanofluid are obtained from the following equation [43]:

$$\rho_{nf} = \phi\rho_p + (1-\phi)\rho_f \tag{3.9}$$

$$C_{nf} = \frac{\phi(\rho C)_p + (1-\phi)(\rho C)_f}{\rho_{nf}} \tag{3.10}$$

$$\mu_{nf} = \mu_f[123\phi^2 + 7.3\phi + 1] \tag{3.11}$$

$$k_{nf} = k_f\left[\frac{(k_p + 2k_f) - 2\phi(k_f - k_p)}{(k_p + 2k_f) + \phi(k_f - k_p)}\right] \tag{3.12}$$

Where the subscripts f and p stand for the base fluid and the nanoparticles, respectively; $phi\ denotes$ the equation the volume fraction.

For hybrid nanofluid, the same formulas are used to evaluate the thermophysical properties. However, $\rho_p, C_p, and\ phi$and phi for hybrid nanoparticles are obtained from the equations below [37]:

$$\rho_p = \frac{\rho_{p1}\phi_{p1} + \rho_{p2}\phi_{p2}}{\phi} \tag{3.13}$$

$$C_p = \frac{C_{p1}\phi_{p1} + C_{p2}\phi_{p2}}{\phi} \tag{3.14}$$

$$k_p = \frac{k_{p1}\phi_{p1} + k_{p2}\phi_{p2}}{\phi} \tag{3.15}$$

$$\phi = \phi_{p1} + \phi_{p2} \tag{3.16}$$

In the current study, hybrid nanoparticles of Al_2O_3 - TiO_2 are suspended in water as a base fluid, with a concentration of 0.5% for each composite. The physical properties of the nanofluid are listed in Table 3.1.

Table 3.1. Physical properties of (0.5% Al_2O_3 - 0.5% TiO_2) nanofluid.

Density, ρ (kg/m^3)	**1029**
Specific heat, C (J/kg.K)	4041.68
Dynamic viscosity μ (kg/m.s)	0.00107
Thermal conductivity, k (W/m.K)	0.64

3.5. REYNOLDS NUMBER, NUSSELT NUMBER, AND FRICTION FACTOR

The Reynolds number for the nanofluid flow is defined using the equation:

$$Re_{nf} = \frac{\rho_{nf} u_{nf} D}{\mu_{nf}} \tag{3.17}$$

The Nusselt number is expressed using the equation:

$$Nu_{nf} = \frac{h_{nf} D}{k_{nf}} \tag{3.18}$$

Where h_{nf} is the heat transfer coefficient, and it is evaluated from the knowledge of the wall heat flux q_w, and the temperature difference between the wall and bulk flow $(T_w - T_b)$, using the equation:

$$h_{nf} = \frac{q_w}{(T_w - T_b)} \tag{3.19}$$

The friction factor is estimated from the equation:

$$f_{nf} = \frac{\Delta P (D/L)}{\rho_{nf}\left(u_{nf}^2/2\right)} \tag{3.20}$$

Where ΔP is the pressure difference, and L is the length of the tube.

3.6. NUMERICAL SOLUTION METHODS

CFD packages include two procedures to simulate the flow: pressure-based solver and density-based solver. The first procedure was initially developed for low-speed incompressible flow, while the second one was developed for high-velocity compressible flow. However, both techniques have been expanded and reformulated to fit a wide range of flow conditions [48]. The velocity field is concluded from the momentum equations in both approaches. However, the pressure field is concluded from the state equation in the density-based procedure, while it is determined from the pressure or corrected-pressure equation, derived from the coupling between the continuity and momentum equations in the pressure-based procedure [48]. The current study uses the pressure-based procedure in solving the flow governing equation.

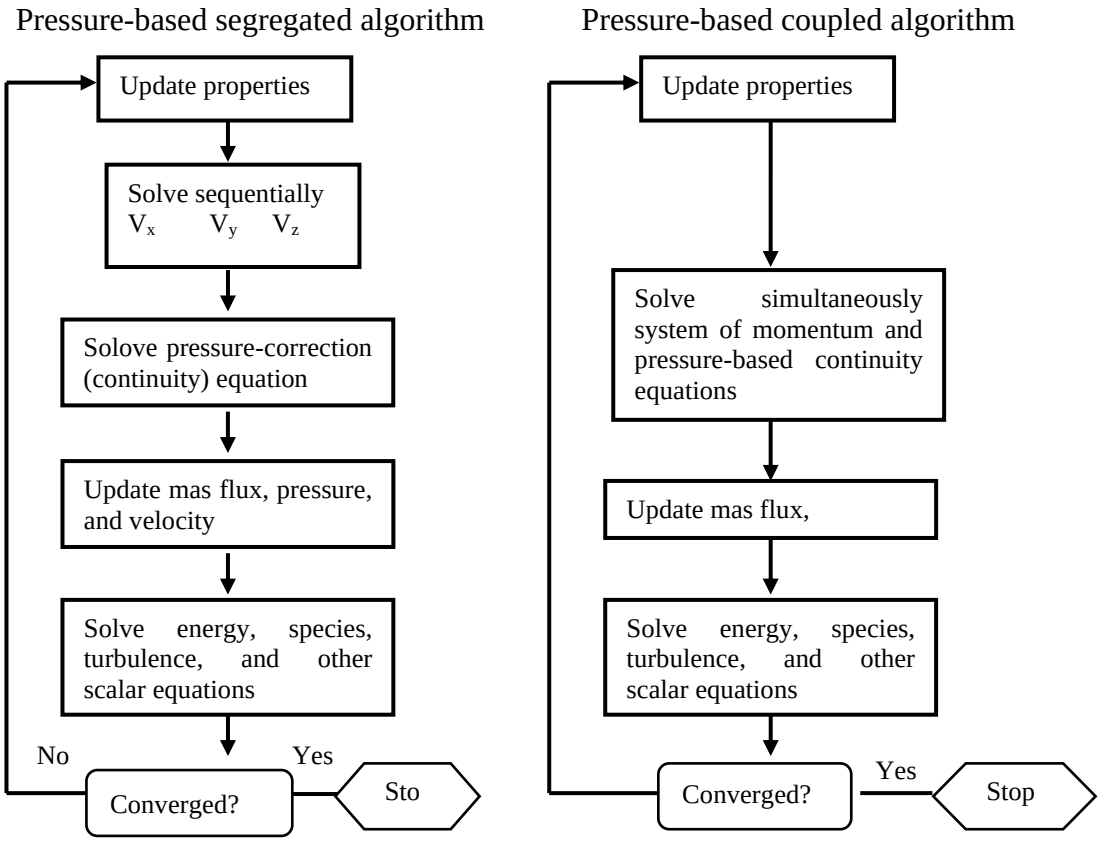

Figure 3.1. Segregated and coupled pressure-based algorithms [48].

Pressure-based solver includes two algorithms: segregated algorithm and coupled algorithm. Figure 3.1 shows the flowchart of both algorithms. In the segregated algorithm, the governing equations are solved independently one by one, while the coupled algorithm solves the whole system of equations simultaneously. Because the continuity and momentum equations in the coupled algorithm are solved at the same time, the convergence rate is improved considerably compared to the segregated algorithm. However, the memory needs are larger for the coupled algorithm [48].

3.7. CASE STUDY AND METHODOLOGY

Here in this study, a computational investigation of heat transfer and nanofluid flow through a ribbed circular channel is carried out using ANSYS Fluent software. A hybrid (0.5% Al2O3 - 0.5% TiO2)/ water nanofluid is used in the simulation. Four values of Reynolds number, 10000, 20000, 30000, and 40000 are employed for the flow. Three different rib shapes, including rectangular, triangular, and semi-circular ribs, in single and hybrid arrangements are considered in the study. The simulation includes studying the effect of (i) Reynolds numbers and (ii) pitch ratio and rib height on heat transfer coefficients and nanofluid flow pressure drops. Figure 3.2 shows the circular channel and its different rib configurations, and Table 3.2 represents the six different designs of the rib parameters considered in this study. The values in Table 3.2 are selected consistent with the relevant literature, such as Togun [38] and Togun et al. [39].

Table 3.2. Rib parameters for the studied cases.

Case	h (mm)	h/d	w (mm)	p (mm)	p/w
1	1.5	0.1	3	15	5
2	1.5	0.1	3	30	10
3	1.5	0.1	3	60	20
4	0.75	0.05	1.5	15	10
5	0.75	0.05	1.5	30	20
6	0.75	0.05	1.5	60	40

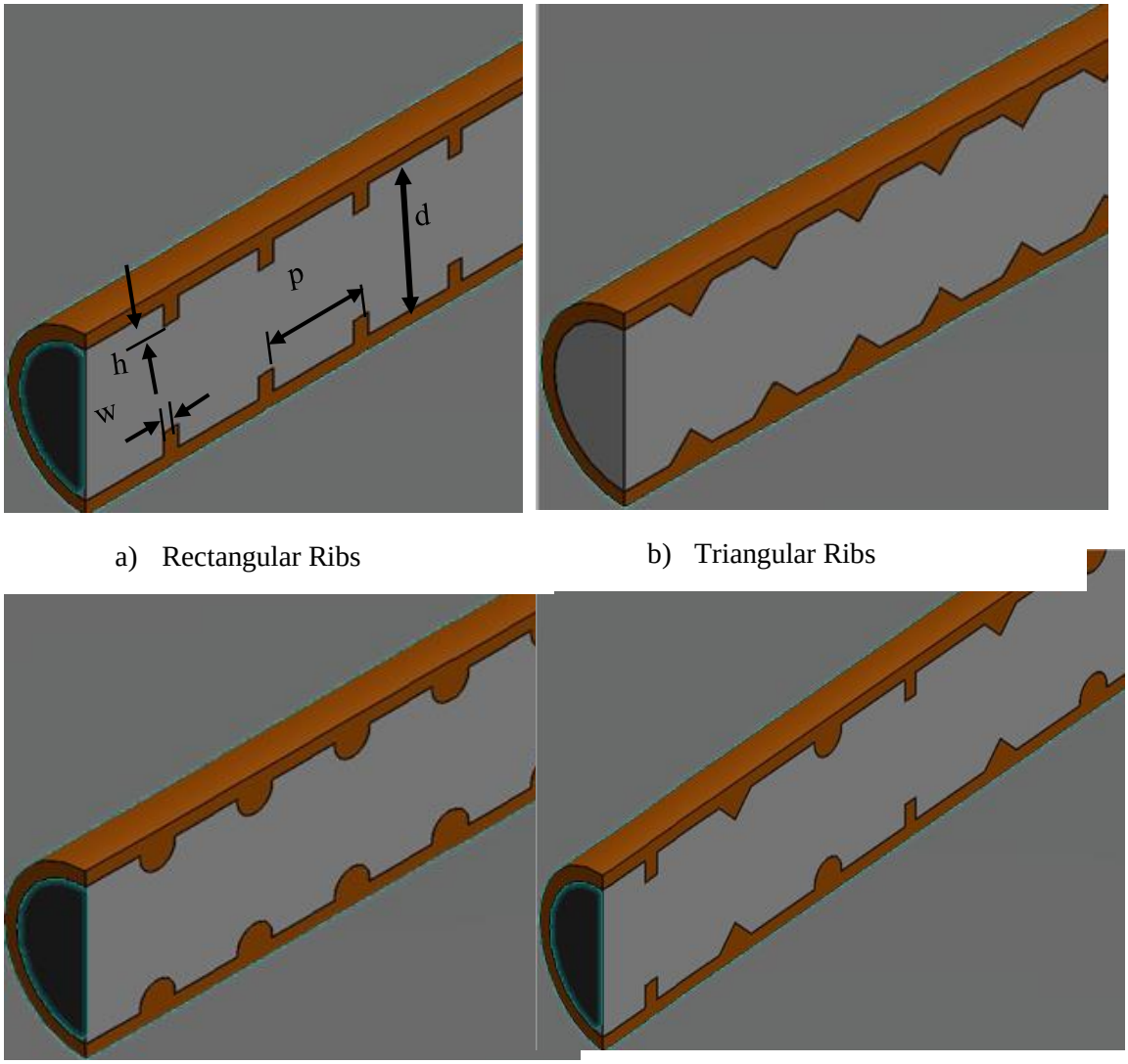

a) Rectangular Ribs

b) Triangular Ribs

c) Semi-circular Ribs

d) Hybrid Ribs

Figure 3.2. Different rib configurations.

The numerical solution using the ANSYS Fluent program follows the following steps:

3.7.1. Geometry and Computational Domain

The study geometry, which is, as mentioned above, a tube with three different types of ribs, including triangle, half-circle, and rectangle-shaped in single and hybrid configurations, is modelled using the SolidWorks program and then exported to ANSYS Fluent for simulation and analysis. Figure 3.3 shows the computational

domain of the hybrid configuration of the ribbed tube in the ANSYS program environment.

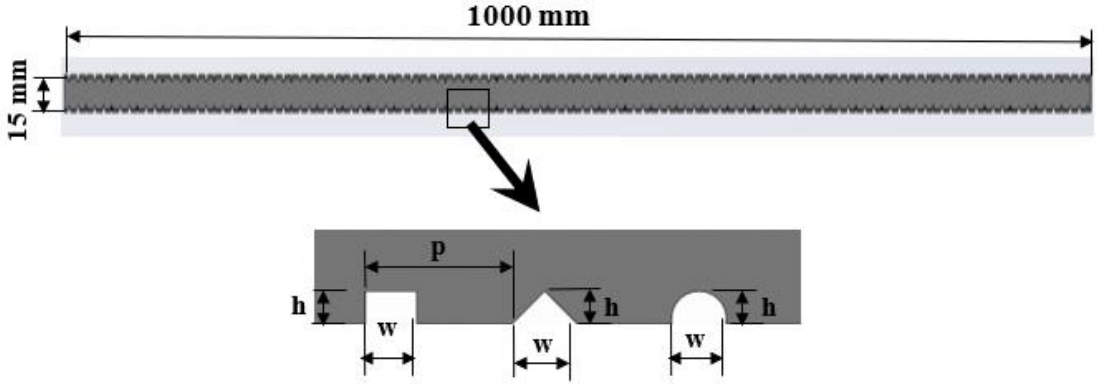

Figure 3.3. Geometrical model - the computational domain.

The tube is 15 mm in diameter and 1000 mm in length. Other dimensions are as have been listed in Table 3.2. For example, they are for one of the considered cases: the rib height (h = 3 mm), the rib width (w = 3 mm), and the pitch distance (p = 15 mm).

3.7.2. Mesh Generation and Boundary Conditions

A wide range of meshes with different structures and different element numbers are constructed using the ANSYS program. To attain accurate and economical numerical solutions, it is necessary to perform a grid independence test by examining various meshes of increasing refinements. Figure 3.4 shows the Nusselt number as a function of grid intensity for four different meshes at Reynolds number, Re = 40000. From the figure, it can be concluded that the third mesh provides an acceptable estimation of the solution and that any further mesh refinement does not affect the value of the Nusselt number too much. However, for more accurate results and because the computational resources are not expensive in the current cases, the fourth mesh details are considered in the study.

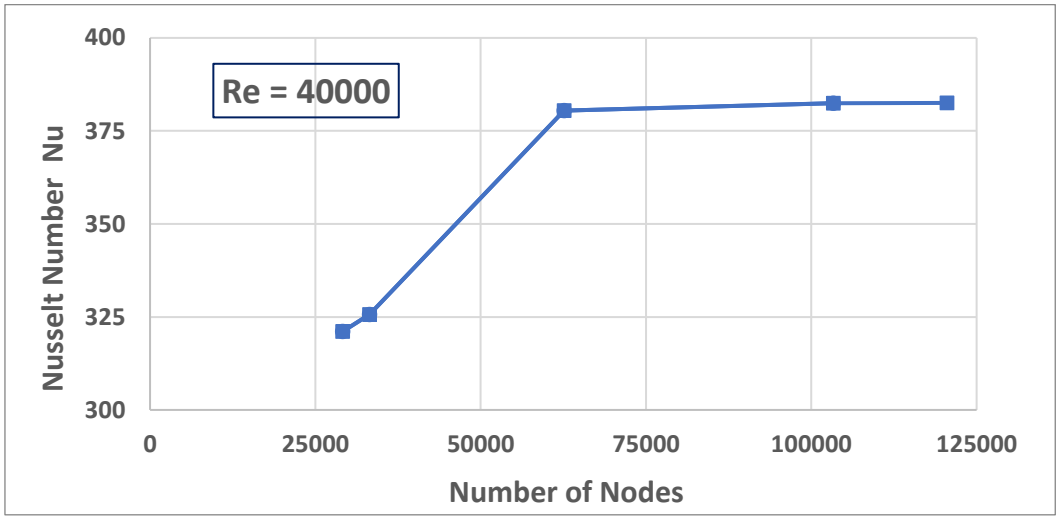

Figure 3.4. Grid independence test.

Figure 3.5 illustrates the selected mesh, a 2D unstructured mesh with quadratic elements. A face meshing with an element size of 0.4 mm, inflation with maximum layers equal to 7, and a growth rate equal to 1.2 is used to discretise the computational domain. The mesh elements and nodes total 100,192 and 103317, respectively. Table 3.3 presents the detailed specifications of the constructed mesh.

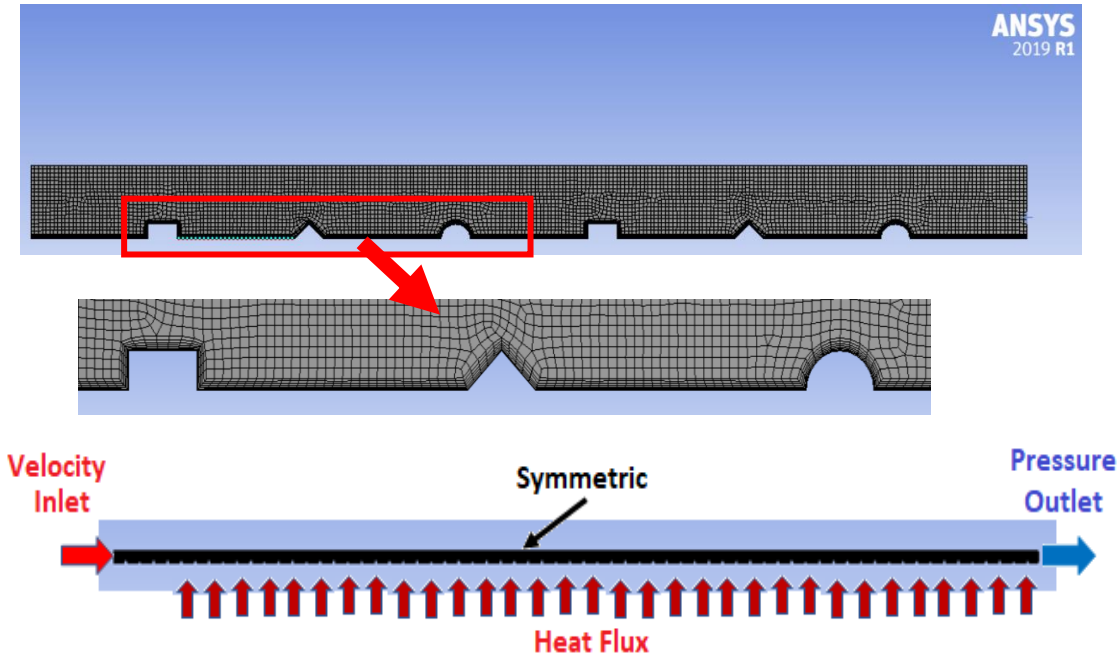

Figure 3.5. Mesh generation and boundary conditions.

Table 3.3. Mesh specifications.

Number of nodes	**103,317**
Number of elements	100,192
Element type	Quadratic

Figure 3.5 also shows the boundary conditions applied to the computational domain. The detailed values of these conditions are presented in Table 3.4.

Table 3.4. Boundary conditions.

Inlet	**Re = 10000, 20000, 30000, 40000**
Outlet	Standard pressure
Heated surface	Heat flux = 5000 W/m^2
Sym surface	Symmetric

3.7.3. Numerical Settings and Run Simulation

The nanofluid flow is assumed to be two-dimensional, steady-state, incompressible, Newtonian, and turbulent. The turbulence is modelled using the k - ε model. The governing equations are discretized using the FV – backward difference scheme. The pressure-based solver is employed. The Semi Implicit Method for Pressure Linked Equation (SIMPLE) algorithm is selected for pressure-velocity coupling. The discretized algebraic set of equations is solved using the Gauss-Zeidil iterative method. The convergence criteria for continuity, momentum, and energy equations are selected to be 10^{-3}, 10^{-6}, and 10^{-8}, respectively.

3.8. RESULTS VALIDATION

In numerical studies, it is essential to validate the obtained results as a first stage of the research. This can be done by comparing the numerical results with relevant experimental or analytical studies data. In the current study, the results validation is carried out by comparing the obtained numerical data with the experimental results of Kumait et al. [40]. The comparison includes the experimental and numerical findings for TiO_2 (1%) / water nanofluid turbulent flow within smooth and rectangle-ribbed tubes. For the plain tube case, the results are further validated by comparing them with

the well-known empirical correlation recommended by Dittus-Boelter (10,000 < Re < 5×10^6, 0.5 < Pr < 200), given by the form [51]:

$$Nu = 0.024\, Re^{0.8} Pr^{0.4} \tag{3.21}$$

Figure 3.7 and figure 3.8 demonstrate the Nusselt number results for the current study compared to those from the relevant literature data mentioned above. As can be seen from the figures, the results are almost identical, and the agreement with the reference data is excellent. The deviation in the Nusselt number values can be neglected since the relative error is very small. Hence, the numerical simulation program ANSYS Fluent, with an appropriate turbulent model, can correctly predict the thermal field of the turbulent flow of nanofluid within a ribbed tube, and one can move on to any further numerical simulation cases with real confidence.

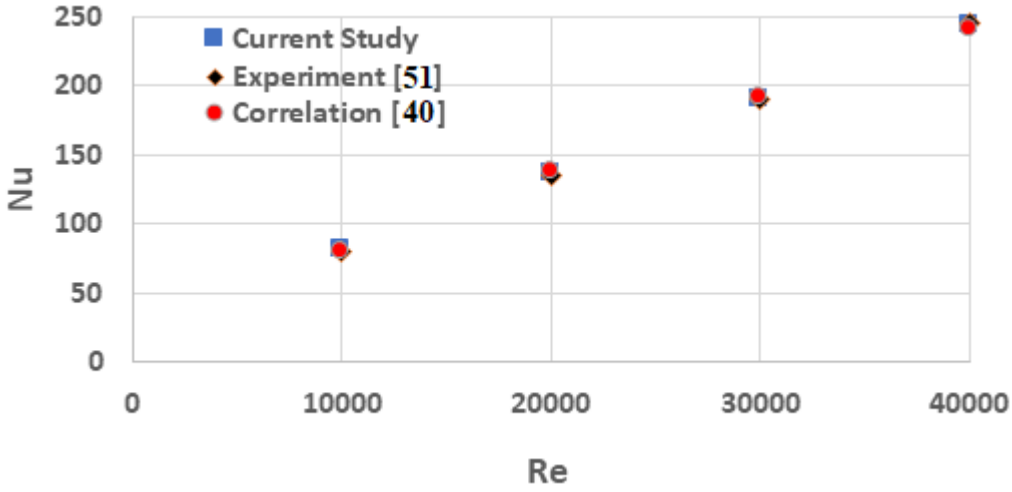

Figure 3.6. Nusselt number comparison for a smooth tube.

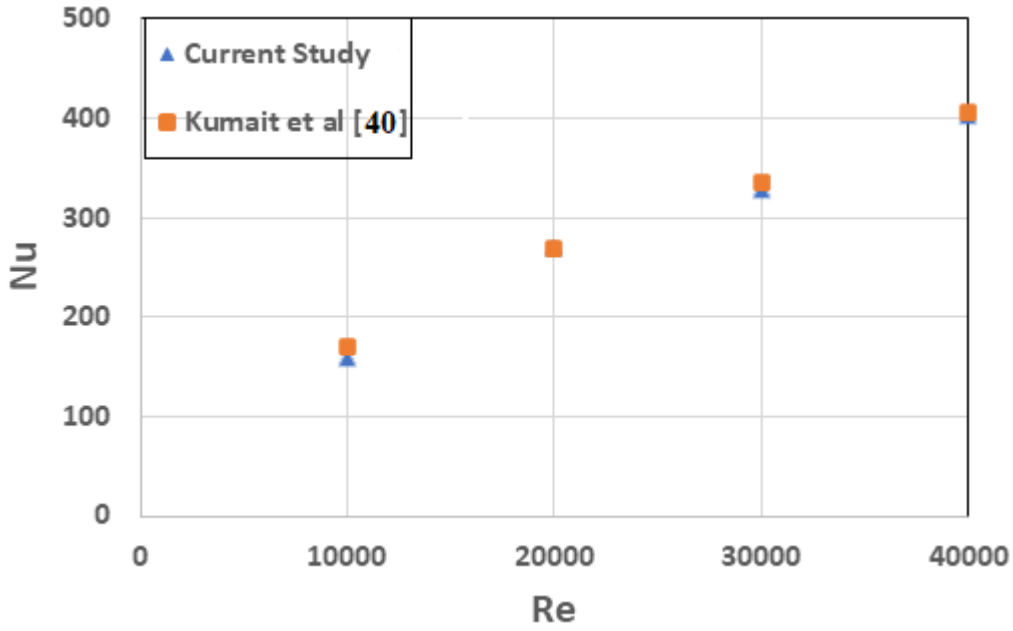

Figure 3.7. Nusselt number comparison for a ribbed tube.

PART 4

RESULTS AND DISCUSSION

This research includes a two-dimensional numerical investigation of hybrid nanofluid flow and heat transfer through a ribbed tube of different configurations. The effects of the Reynolds number, the shape of the ribs, the pitch ratio, and the step height on the heat transfer rates are determined in the study. Three different shapes of the ribs, including rectangular, triangular, and semi-circular, with single and hybrid arrangements, are considered in the study. A hybrid Al_2O_3 - TiO_2 / water nanofluids, with a total nanoparticles volume fraction of 1% (0.5% for each particle type), are considered in the simulation. The investigation is carried out for four different Reynolds numbers values, namely 10000, 20000, 30000, and 40000, and the values of convection heat transfer coefficient and pressure drop are obtained.

The main simulation is divided into four parts. Firstly, the heat flow of a hybrid (0.5% Al_2O_3 - 0.5% TiO_2) nanofluid through a circular pipe of diameter 15 mm and length 1000 mm, with rectangular ribs of different specifications, is considered for the selected values of Reynolds number. Then, the same cases are repeated but with different shapes of the ribs, specifically triangular and semi-circular. Finally, the heat flow of the hybrid nanofluids through a hybrid-ribbed tube at different Reynolds numbers is studied. The hybrid ribs arrangement is determined based on the results obtained in previous stages. To clarify the effect of introducing the different shapes and arrangements of ribs into the tube, the simulation starts by considering the heat and nanofluid flow within a plain pipe.

4.1. HEAT TRANSFER AND NANOFLUID FLOW THROUGH A PLAIN PIPE

Figure 4.1 shows the 2D geometry with the boundary conditions that are applied to the pipe. The dimensions of the pipe are as stated above: the length is L = 1m, and the

diameter is d = 15mm. A constant heat flux at q = 5000 W/m^2 is applied on the pipe walls, and different inlet velocities, corresponding to Reynolds number values 10000, 20000, 30000, and 40000, and a standard outlet pressure are selected for the study. Since the geometry is symmetric concerning the tube centreline, only half of it is considered in the simulation to save time and numerical resources.

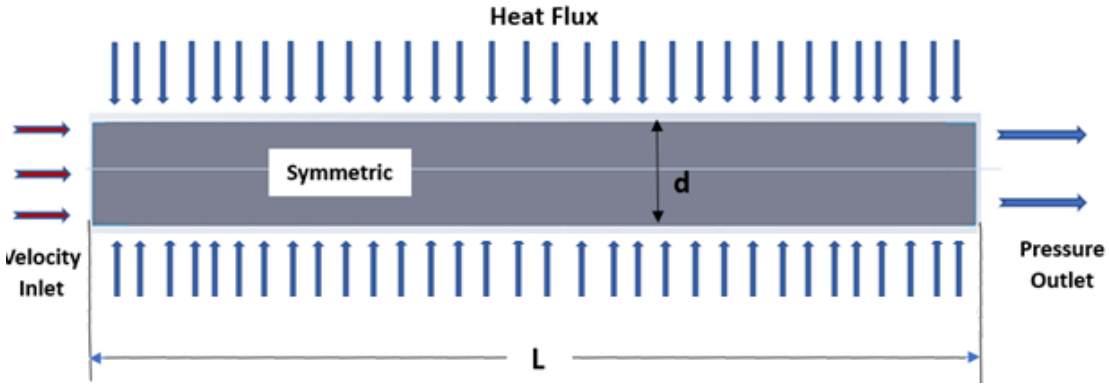

Figure 4.1. Study case geometry and boundary condition.

4.1.1. The Pressure Drop

Determining the pressure drop associated with the flow through the tube is essential in analysing any heat and fluid flow problem. The power required to pump the flow, which is of main interest in relevant engineering applications, is directly proportional to pressure drop. This is particularly true in the nanofluid flow, such as the current case, where a turbulent flow of a hybrid Al_2O_3-TiO_2/water nanofluid with a concentration of 1% (0.5% for each component) through the pipe is considered. The literature has shown that introducing nanoparticles, even at a low concentration, may cause a considerable increase in pressure drop. Figure 4.2 illustrates the pressure drop variations along the tube for different Reynolds numbers. The figure shows that for all Reynolds numbers, the pressure drop decreases almost linearly through the pipe length. The variations become sharper and more apparent as the Reynolds number increases. This is to overcome the friction caused by fluid flow against pipe walls.

Furthermore, Figure 4.3 illustrates the average pressure drop variations at different Reynolds numbers. It can be seen that the Reynolds number has a significant impact

on the pressure drops. The average pressure drop has doubled more than 10 times by increasing the Reynolds number from 10,000 to 40,000. This is because by increasing Reynolds number, the turbulence is increased and hence the fluid exerts more forces on the pipe surfaces leading to increasing the pressure drop.

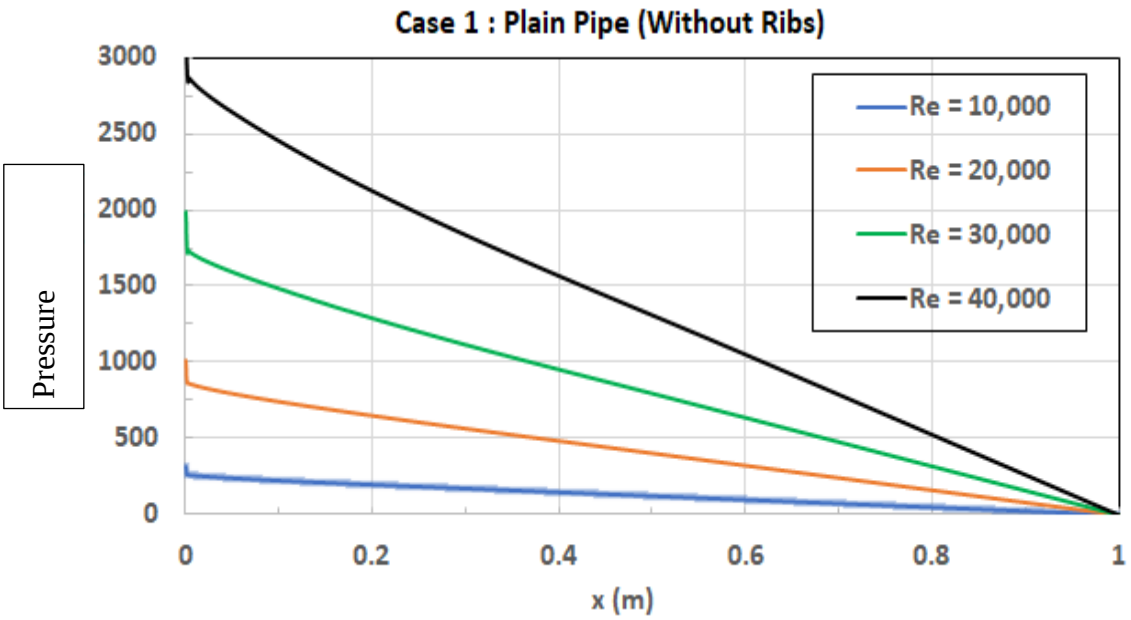

Figure 4.2. Pressure drop along a plain tube for different Reynolds numbers.

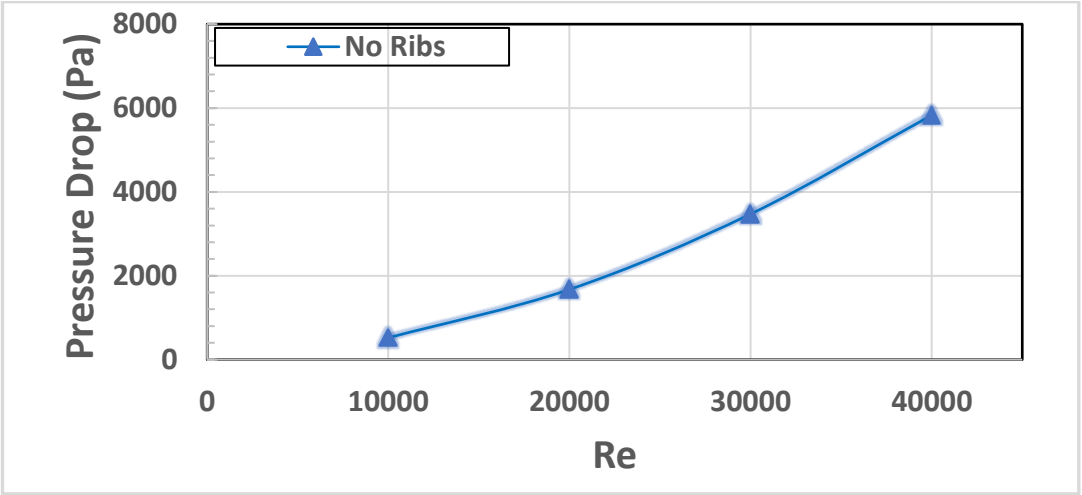

Figure 4.3. Average pressure drop at different Reynolds numbers.

4.1.2. Heat Transfer Coefficient

The variation of the heat transfer coefficient along the pipe is presented in Figure 4.4 for different Reynolds numbers. The figure demonstrates that the heat transfer coefficient has a very high value at the pipe entrance because the thickness of the thermal boundary layer is zero. The h value generally starts to decay very rapidly as the thermal boundary layer develops along the pipe walls until it reaches almost a constant magnitude when the fully developed condition is approached. The extreme variation of h at the pipe entrance is more pronounced in turbulent flow since the length of the entrance region is much smaller compared to that in the laminar flow case. It can also be shown from the figure that the heat transfer coefficient increases with increasing Reynold number due to increasing the mixing levels. This finding is more pronounced by presenting the average heat transfer coefficient variations as a function of the Reynolds number, as demonstrated in Figure 4.5.

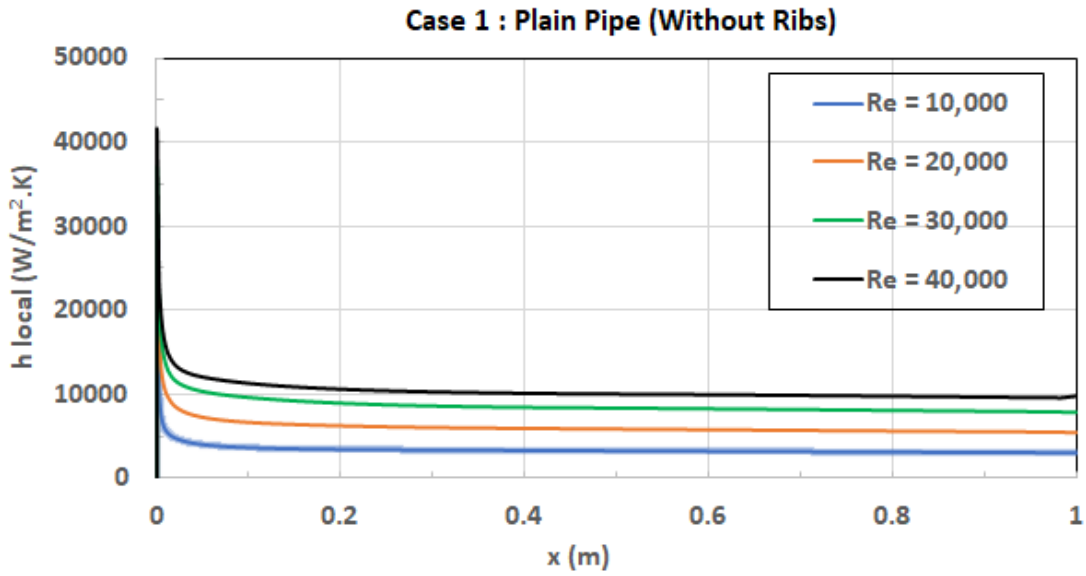

Figure 4.4. Surface heat transfer coefficient variations along the plain pipe for different Reynolds numbers.

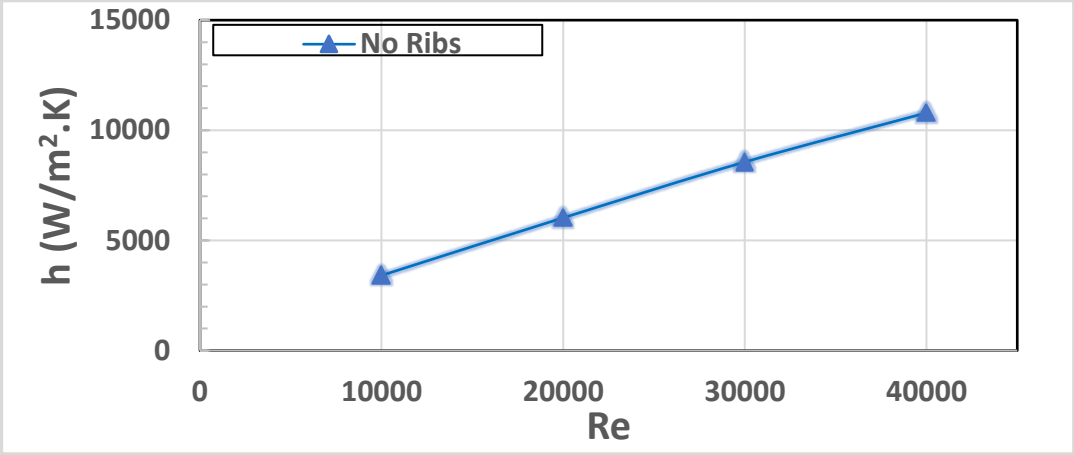

Figure 4.5. Average heat transfer coefficient variations at different Reynolds numbers.

4.2. HEAT TRANSFER AND NANOFLUID FLOW THROUGH A PIPE WITH RECTANGULAR RIBS

To enhance heat transfer rates, rectangular ribs were first added to the pipe as shown in Figure 4.6. The length and diameter of the pipe are similar to those of the plain pipe. The boundary conditions are also the same in the two cases. The rectangle-shaped rib parameters are h, w, and P, which stand for rib height, width, and pitch, respectively; different values of h, w, and P are included in the simulation.

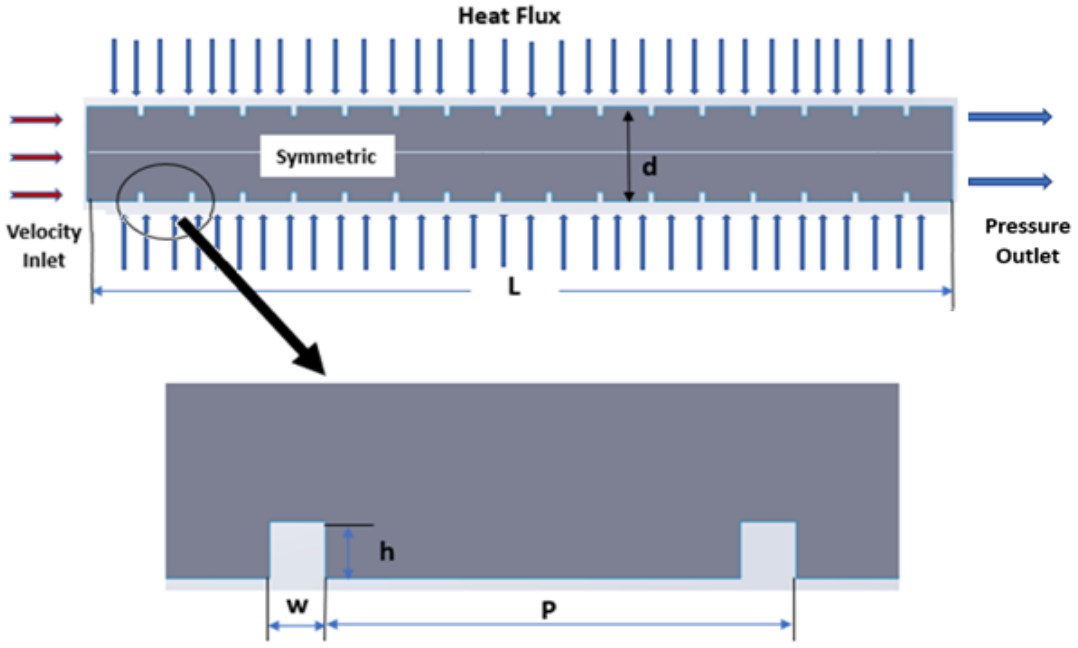

Figure 4.6. Studies case geometry and boundary conditions.

4.2.1. Effect of Reynolds Number

The hybrid nanofluid (0.5% Al2O3 - 0.5% TiO2) flow and heat transfer through the ribbed channel are studied at four different Reynold numbers to determine the impact of Reynold number on pressure drop and local heat transfer coefficient variations. The dimensions of the rectangular ribs are taken as h = 1.5 mm, w = 3 mm, and P = 15 mm. These values correspond to case 1 in Table 3.2, the case of low pitch distance and high rib height. The Reynolds numbers used in the investigation are 10000, 20000, 30000, and 40000.

Figures 4.7 and 4.8 illustrate the local pressure drop and surface heat transfer coefficient variations along the pipe at these Reynolds number values. It can be seen from the figures that increasing Reynolds number is associated with increasing both pressure drop and heat transfer coefficient. More details about the behaviour of pressure drop and convective heat transfer coefficient with Reynolds number can be obtained through the variations of the average value shown in Figures 4.9 and 4.10. The figures show that the pressure drop and heat transfer coefficient increase significantly with increasing Reynolds number. The variations become more pronounced at high Reynolds number values. For example, the pressure drop increased by about 5000 Pa when the Reynolds number increased from 1000 to 3000 and by almost 4800 Pa when the Reynolds number reached 4000. These variation behaviours can be explained as a consequence of the turbulence level and its effects on the flow and heat transfer data.

Comparing the current data of the ribbed tube to the corresponding values of the plain tube, it can be concluded that the ribs result in considerable growth in pressure drop and heat transfer coefficient values. The ribs increase the internal surface area and also the production of turbulent kinetic energy, and hence they enhance heat transfer rates. However, the areas in front of and behind the ribs represent stagnation regions with recirculating currents and have low heat transfer rates and high-pressure losses. The reattachment point in the distance between the two following ribs has the maximum heat transfer rates.

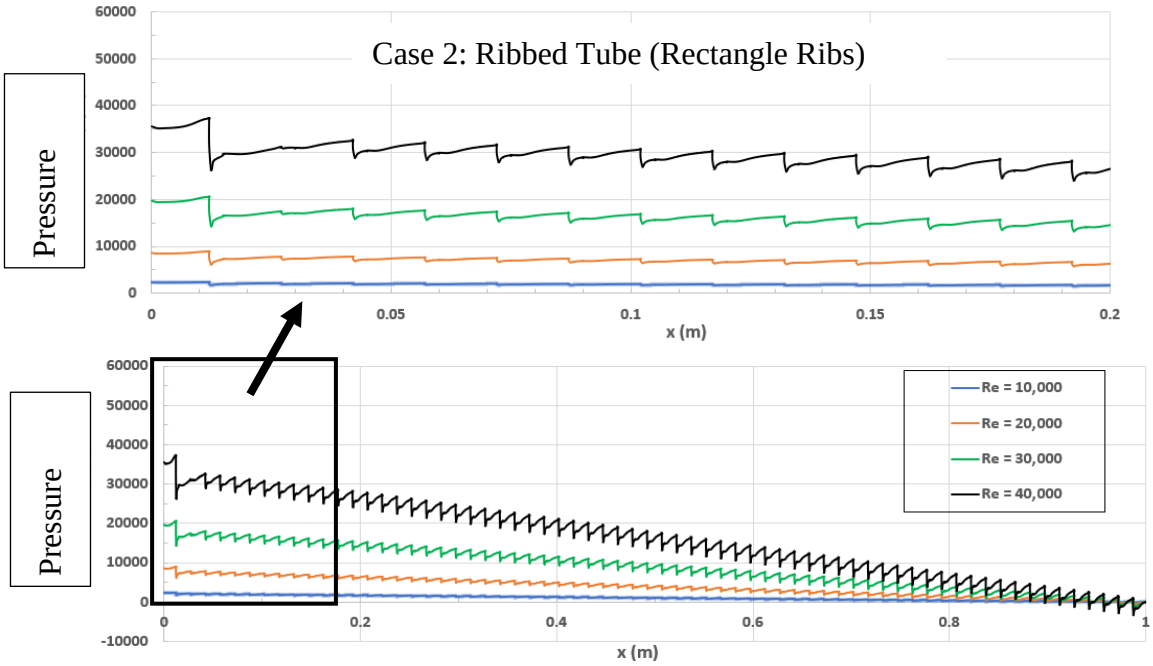

Figure 4.7. Pressure drop variations for a rectangle-shaped ribbed tube at different Reynolds numbers.

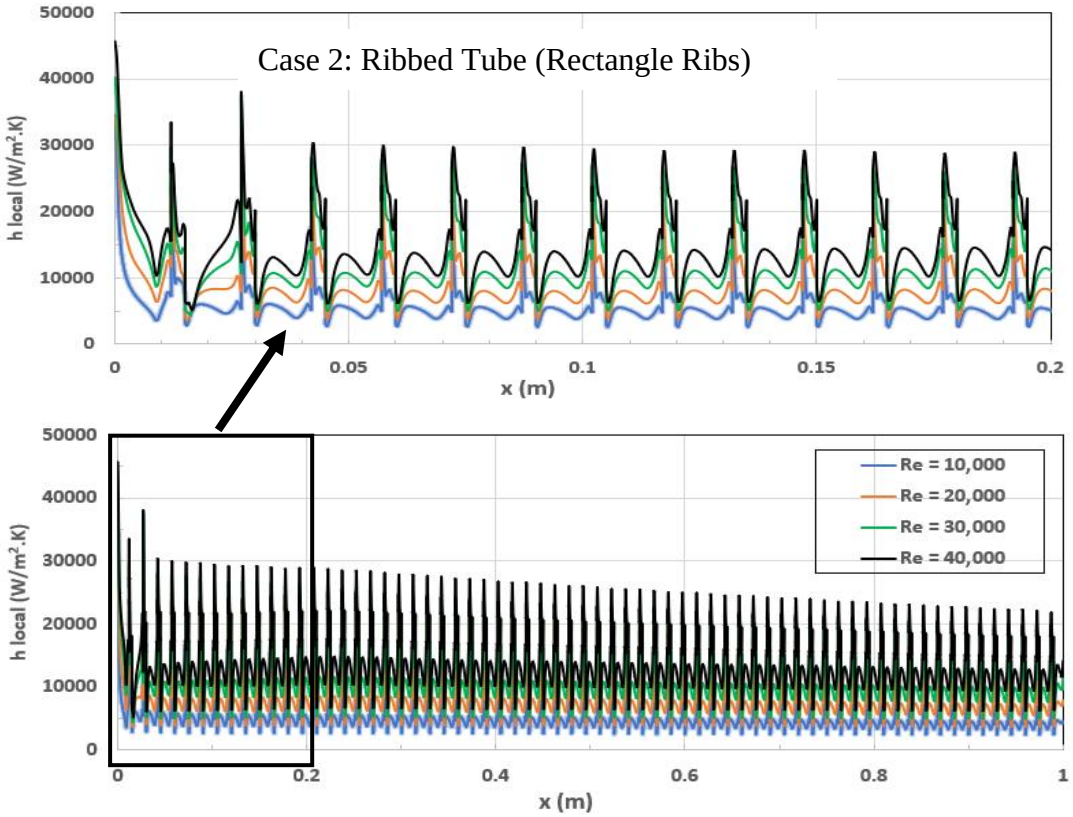

Figure 4.8. Local heat transfer coefficient variations for a rectangle-shaped ribbed tube at different Reynolds numbers.

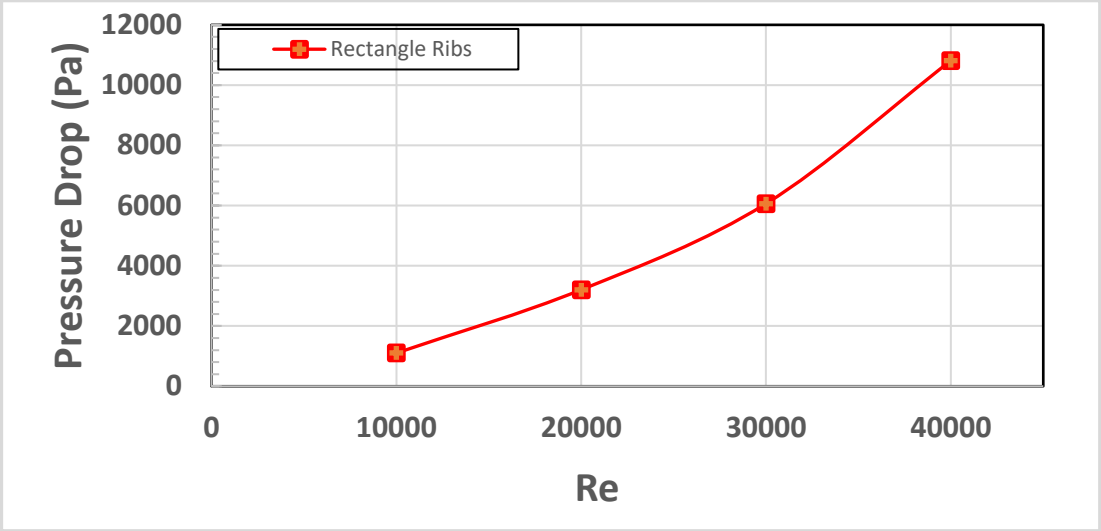

Figure 4.9. Average pressure drop variations for a rectangle-shaped ribbed tube at different Reynolds numbers.

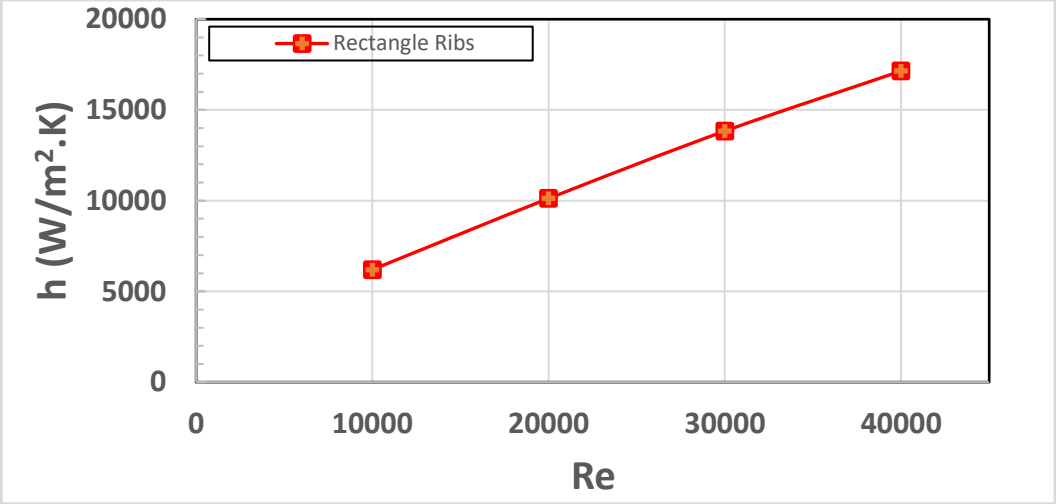

Figure 4.10. Average heat transfer coefficient variations for a rectangle-shaped ribbed tube at different Reynolds numbers.

The stagnation and recirculation regions before and after each rib can be demonstrated through the streamlined velocity contour, which is shown in Figure 4.11. Detailed views are taken at different locations along the ribbed pipe. The irrotational flow regimes can be seen in this figure. The intensive mixing caused by introducing the ribs on pipe walls can considerably increase heat transfer rates, as has already been seen in Figure 4.8. Figure 4.11 also shows velocity profiles at the entrance and fully developed regions. Useful information can also be extracted from isothermal contours shown in Figure 4.12. It is noticed that the higher temperatures are located in the areas adjacent

to the pipe walls, and in the region behind the ribs where the recirculation currents and mixing levels are maximum. This behaviour becomes more obvious downstream along the pipe as a result of developing the thermal boundary layer.

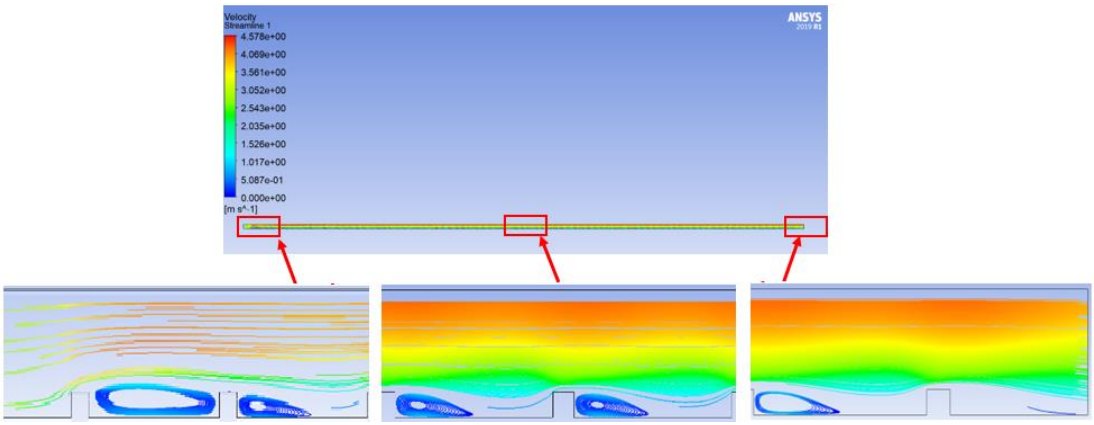

Figure 4.11. Contour of streamlined velocity at different regimes along the pipe.

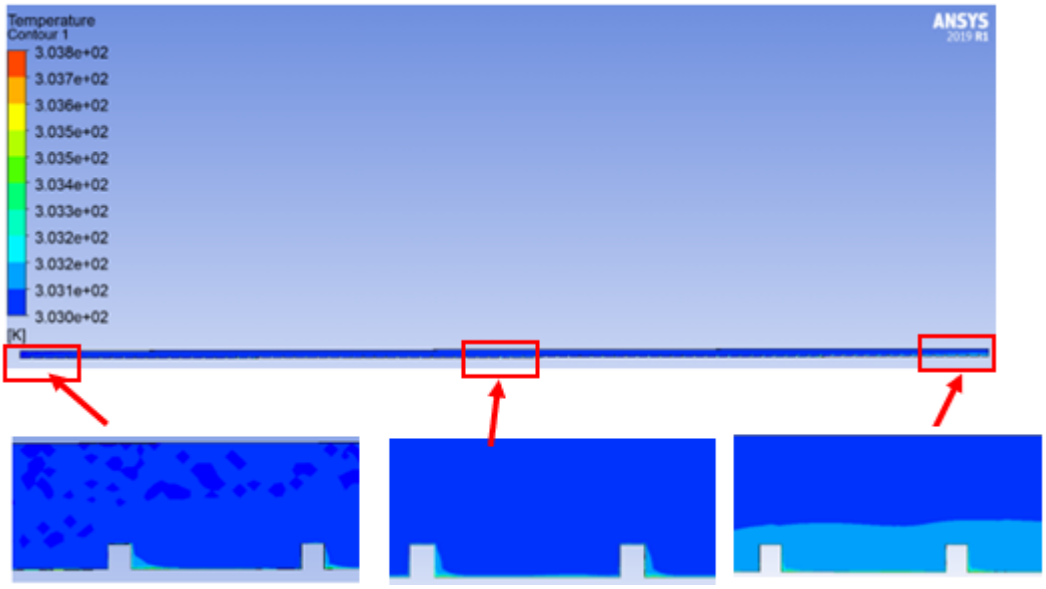

Figure 4.12. Contour of temperature at different regimes along the pipe.

4.2.2. Effect of Pitch Ratio and Ribs Height

As mentioned above, ribs work to increase turbulence intensity and, hence, heat transfer rates. However, there are inactive regions front and behind them that have low heat transfer rates. Hence, it is important to optimize the rib parameters, including the pitch-to-width ratio (p/w), and the height-to-diameter ratio (h/d), to attain the

maximum possible heat transfer rates. In this study, six different designs, as previously listed in Table 3.2, are considered to investigate these issues. The same nanofluid composition and identical boundary conditions to that previously used in this study are again employed in this section, but here, the results will be presented only at Reynolds number equal to 40000.

Figures 4.13 and 4.14 show the variation of heat transfer coefficient for pitches 15, 30, and 60 mm at ribs height-to-diameter ratios of 0.05 and 0.1, respectively. It can be noted from the figures that for both h/d ratios, the local heat transfer coefficient values considerably increase with decreasing the pitch distance. This can be attributed to the fact that by reducing the pitch distance, the number of rib turbulators are increased, and hence, the number of peaks is increased. On the other hand, decreasing the pitch distance, and, as a result, decreasing the rib numbers causes the pressure drops to increase, as shown in figures 4.15 and 4.16 for h/d = 0.05 and 0.1, respectively. The rib turbulators increase the flow interruptions and consequently increase the flow resistances.

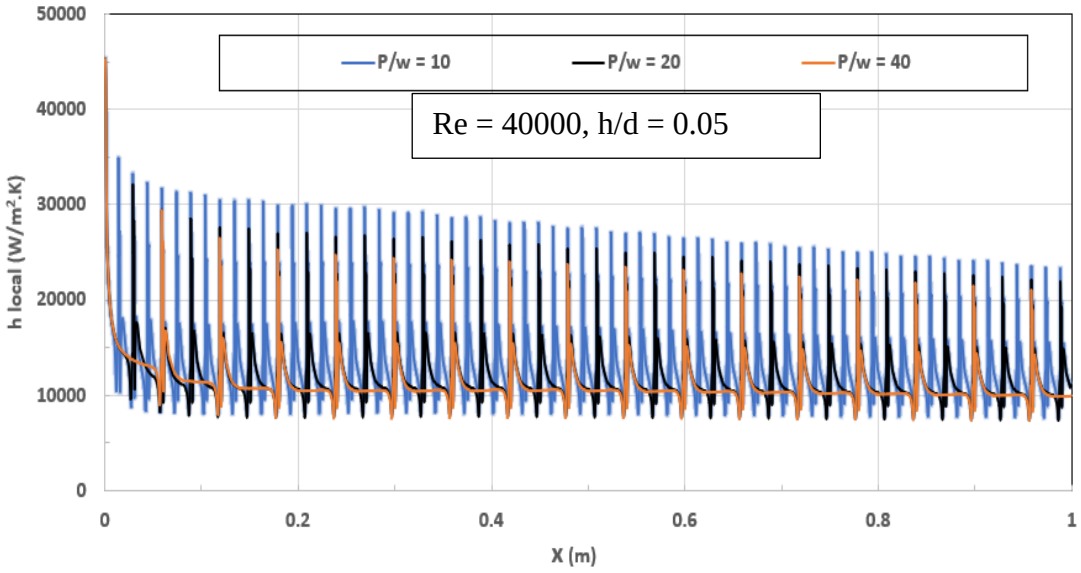

Figure 4.13. Effect of pitch ratio on local heat transfer coefficient variations for a rectangle-shaped ribbed tube.

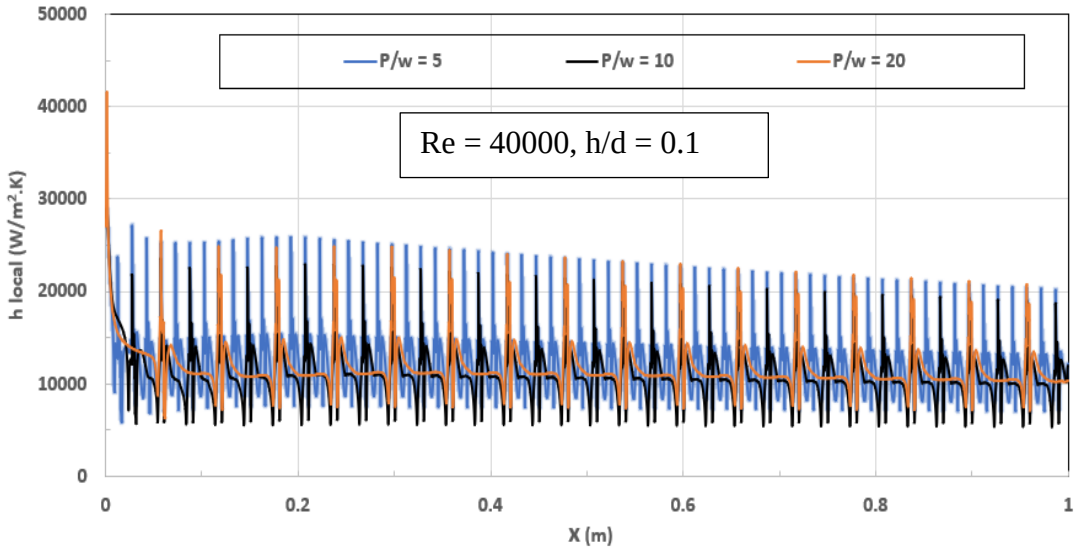

Figure 4.14. Effect of pitch ratio on local heat transfer coefficient variations for a rectangle-shaped ribbed tube.

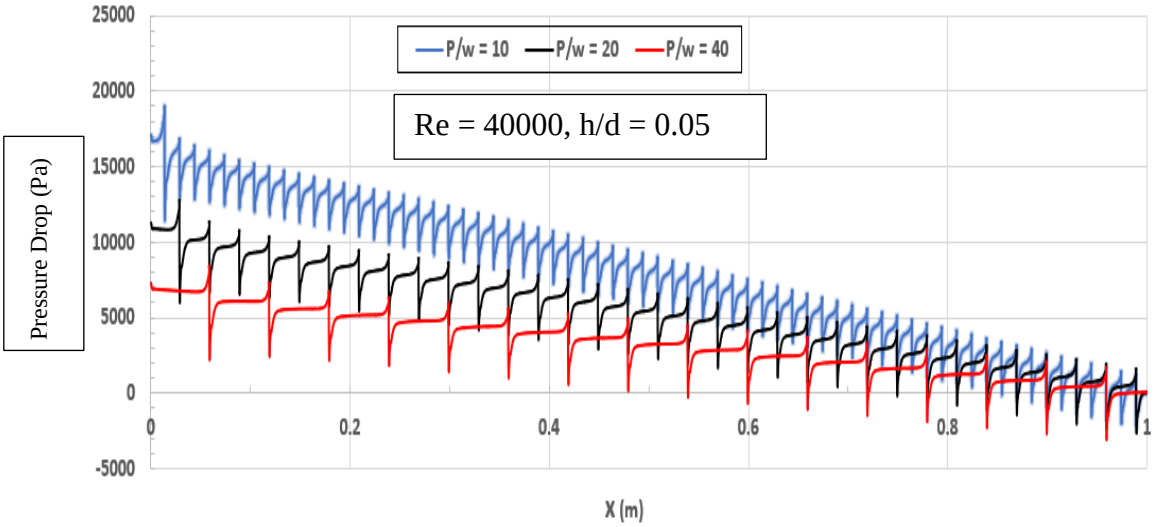

Figure 4.15. Pressure drop variations for a rectangle-shaped ribbed tube at different pitches, h/d = 0.05.

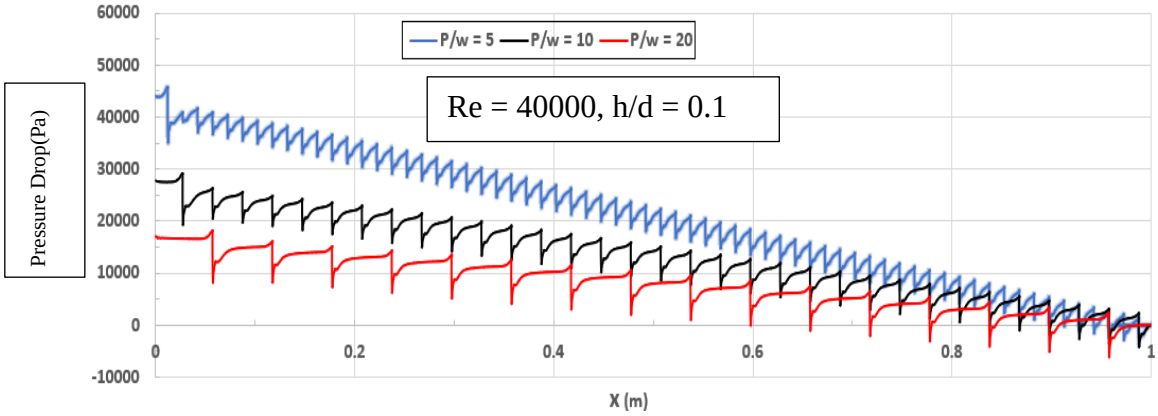

Figure 4.16. Pressure drop variations for a rectangle-shaped ribbed tube at different pitches, h/d = 0.1.

Finally, the effect of rib height on local heat transfer coefficient and pressure drops is investigated for pitch distances 15, 30, and 60 mm and Reynolds number 40000. Figures 4.17 to 4. 22 illustrate these variations along the pipe length. It can be seen from the h variations figures that the values of h increase by increasing the rib's height. This behaviour is more significant at low-pitch space values, where the number of ribs is also larger. The increase in height and number of ribs leads to increasing turbulence kinetic energy and, consequently, increasing heat transfer rates. But this, at the same time, resulted in increasing the flow resistance and friction levels. Figures 4.20-4.22 show that increasing the height of ribs, particularly at short pitch distance (large ribs number), hurts the pressure drop.

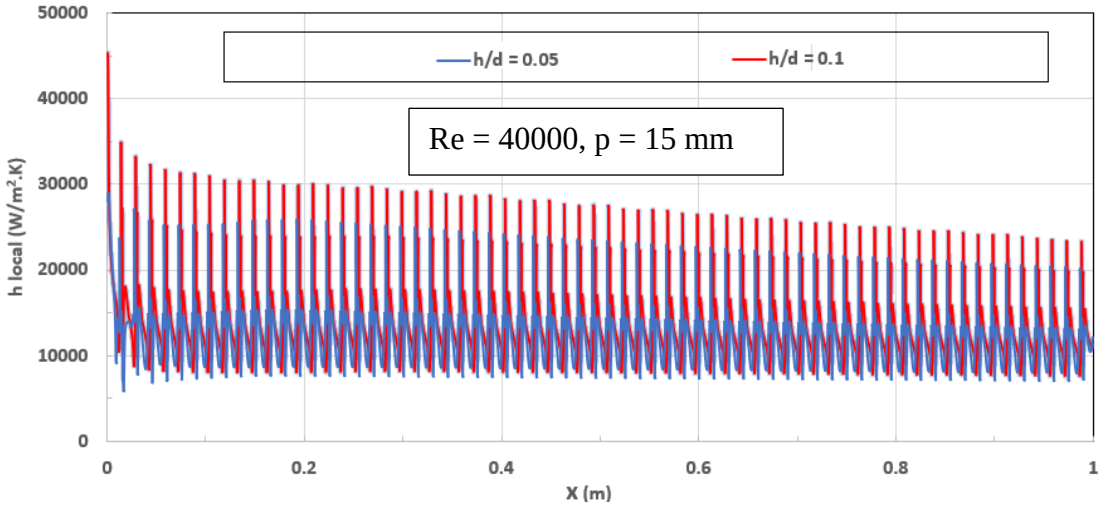

Figure 4.17. Local heat transfer coefficient variations for a rectangle-shaped ribbed tube at different height-to-diameter ratios, P = 15 mm.

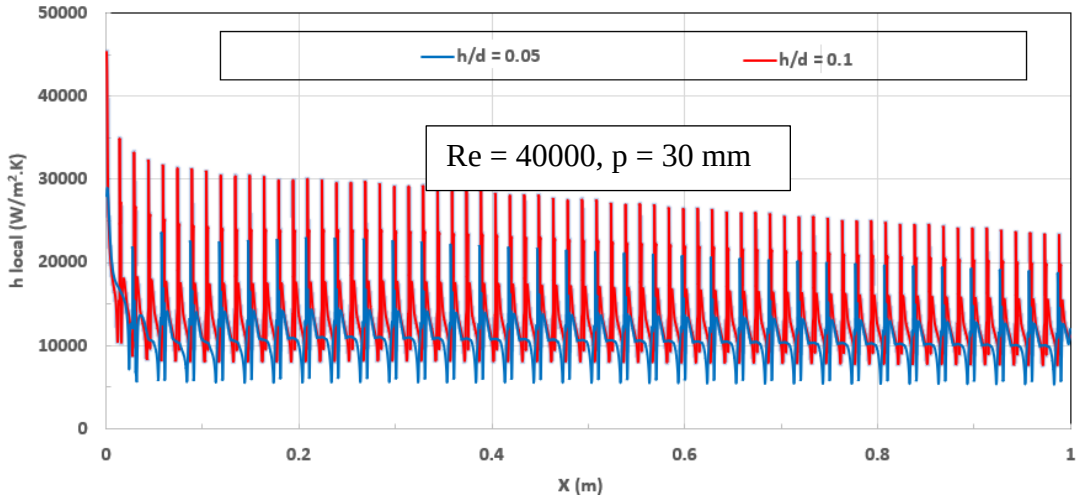

Figure 4.18. Local heat transfer coefficient variations for a rectangle-shaped ribbed tube at different height-to-diameter ratios, P = 30 mm.

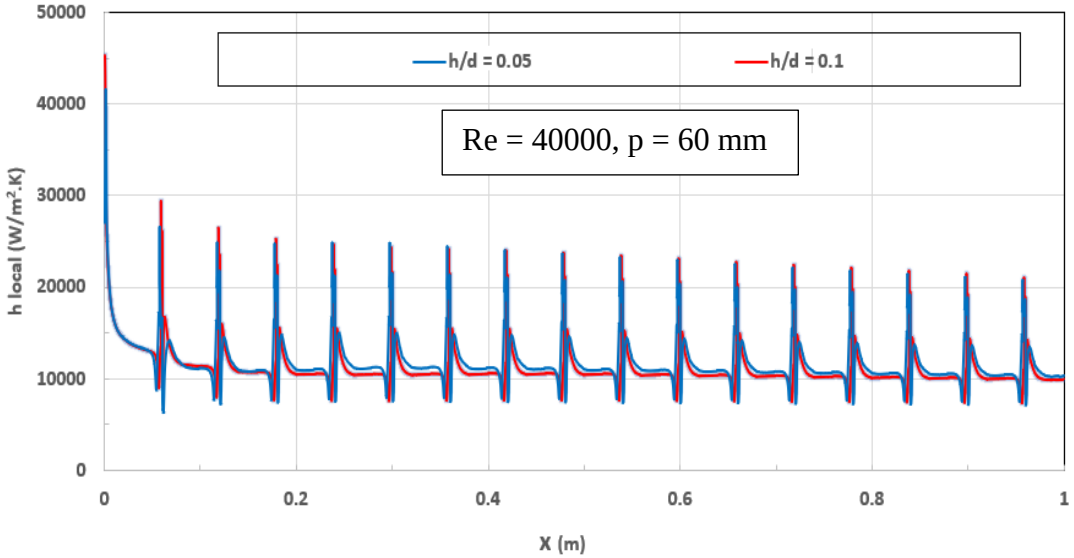

Figure 4.19. Local heat transfer coefficient variations for a rectangle-shaped ribbed tube at different height-to-diameter ratios, P = 60 mm.

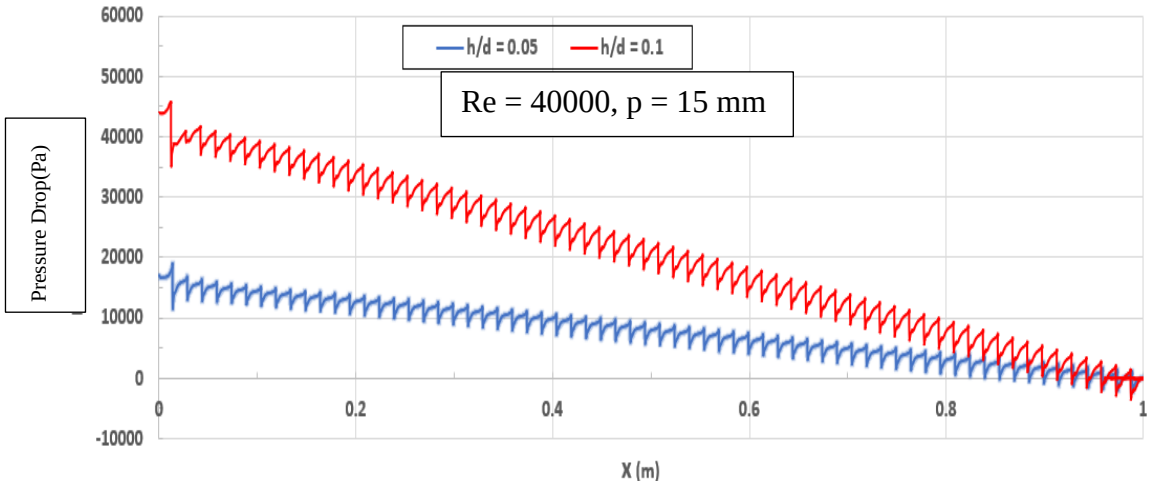

Figure 4.20. Pressure drop variations for a rectangle-shaped ribbed tube at different height-to-diameter ratios, P = 15 mm.

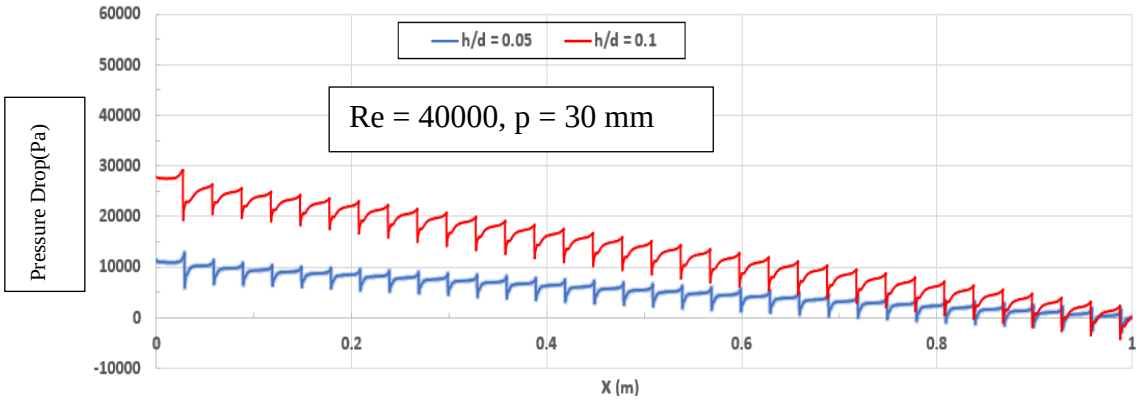

Figure 4.21. Pressure drop variations for a rectangle-shaped ribbed tube at different height-to-diameter ratios, P = 30 mm.

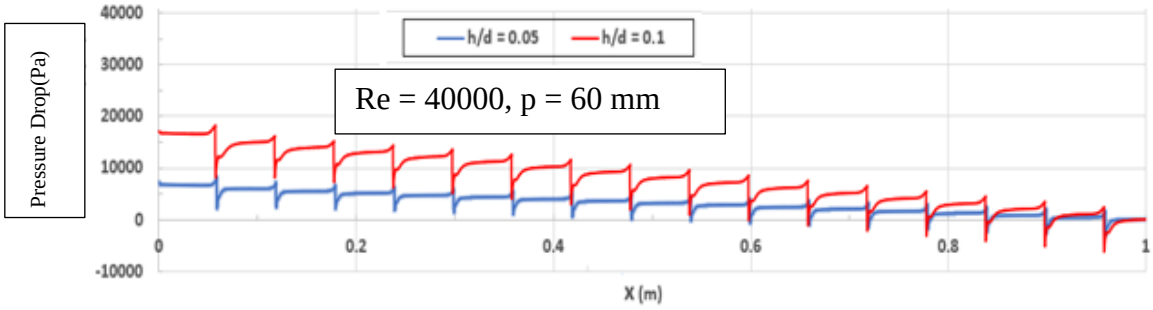

Figure 4.22. Pressure drop variations for a rectangle-shaped ribbed tube at different height-to-diameter ratios, P = 60 mm.

4.3. HEAT TRANSFER AND NANOFLUID FLOW THROUGH A PIPE WITH TRIANGLE RIBS

To investigate the effect of rib shape on heat transfer coefficient and pressure drop through the pipe, triangle-shaped ribs are used in the next step of the current research. The dimensions of the pipe, the boundary conditions, and the specifications of the nanofluid are kept constant throughout the study to compare the results with each other. Figure 4.23 represents the study case, where different rib parameters, corresponding to the values listed in Table 3.2 are considered in the analysis.

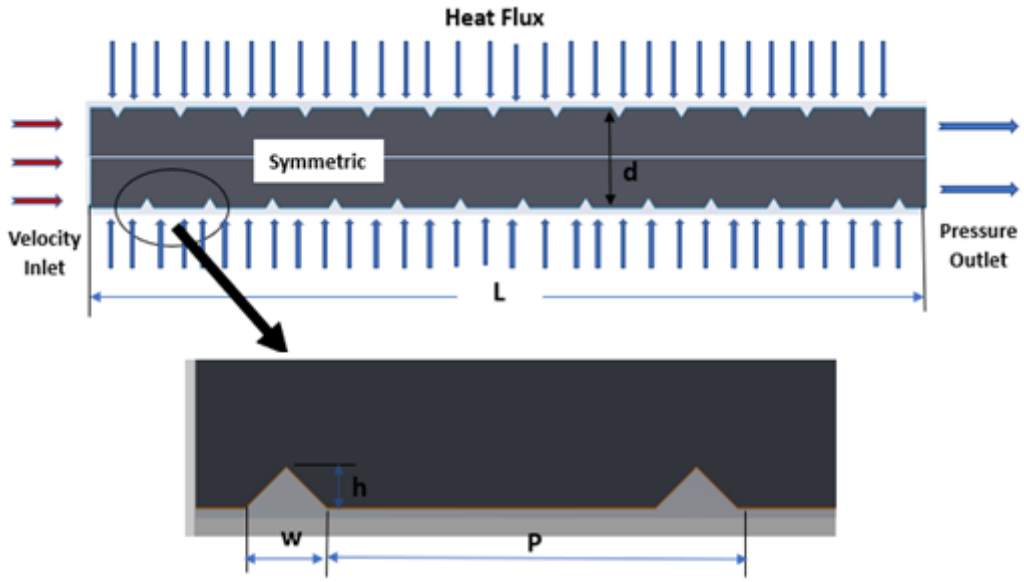

Figure 4.23. studies case geometry and boundary conditions.

4.3.1. Effect of Reynolds Number

The local pressure drop and local heat transfer coefficient variations along the ribbed pipe for various values of Reynolds numbers are demonstrated in Figures 4.24 and 4.25 respectively. The Reynolds numbers values are 10000, 20000, 30000, and 40000, as has been examined in the rectangle ribs case. The hybrid nanofluid (0.5% Al2O3 - 0.5% TiO2) is also considered in this part of the study. The dimensions of the triangle ribs are selected to be: the ribs height h = 1.5 mm (h/d = 0.1) and the pitch distance P

= 15 mm (P/W = 5). These parameters also correspond to those considered in the rectangular ribs previously investigated case.

The figures show that, as has been the case for the rectangular ribs, increasing the Reynolds number directly leads to considerable enhancement in local heat transfer coefficients as well as a large increase in pressure drop along the pipe length. However, in this case, the local heat transfer values are generally less, and the pressure drop is considerably larger than the corresponding values for the rectangular ribs case for all examined Reynolds numbers. For the highest Renolds number Re = 40000, for example, the pressure drop magnitudes in the current triangle case are higher by more than 30% compared to those in the rectangle ribs case, and the local heat transfer is a bit less, particularly in the areas around the ribs. The large increase in the pressure drop in the triangle ribs can be attributed to their sharp edges, which extremely increase the friction losses. These findings are further confirmed by the average value variations presented in Figure 4.26 and Figure 4.27 for pressure drop and convective heat transfer, respectively. Both pressure drop and heat transfer coefficient greatly increased with the Reynolds number. The convective heat transfer coefficient increased from about 5800 W/m^2K at Re = 10,000 to 16000 $W/m^2.K$ at Re = 40,000. The variations for the pressure drop were much larger, and the values doubled up to 15 times when the Renolds number from 10,000 to 40,000. These large values of the average pressure drop for the triangle ribs case are noticeable even when compared to the corresponding cases for the rectangle ribs. The maximum value in the triangle case is larger than that in the rectangle case by more than 40%. Nevertheless, the maximum average heat transfer value for triangle ribs is only 6% less than the corresponding value for the rectangle ribs. This can be attributed to the sharp edges of the triangle ribs, as has been stated above.

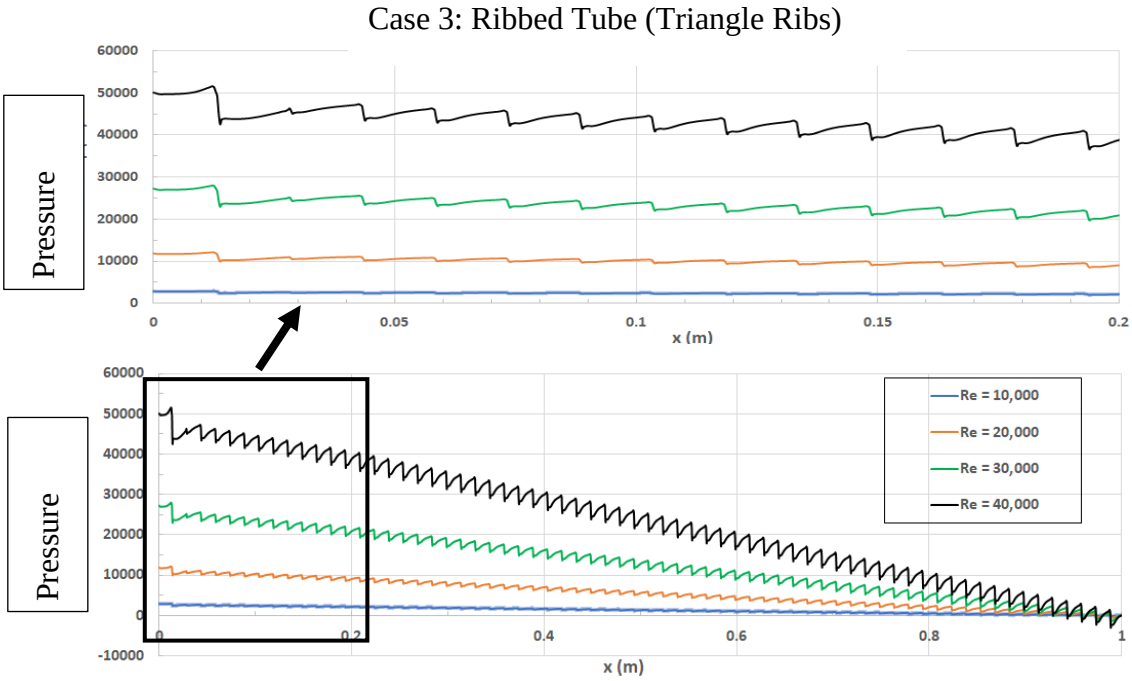

Figure 4.24. Pressure drop variations for a triangle-shaped ribbed pipe at different Reynolds numbers.

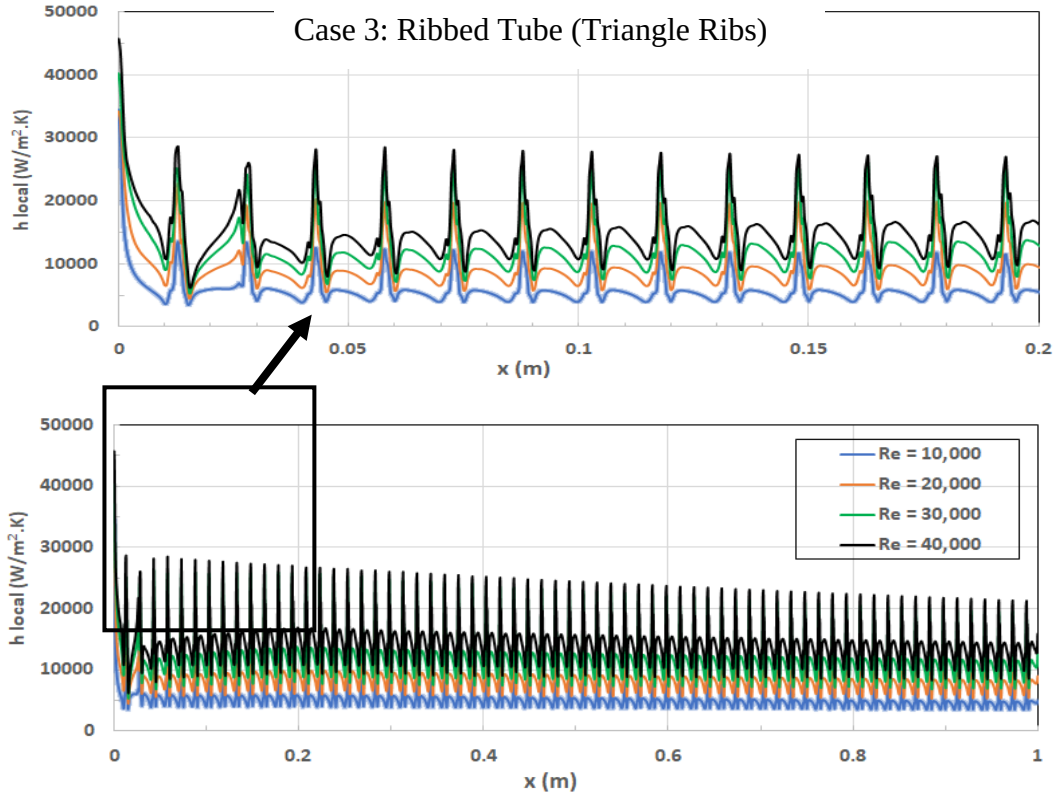

Figure 4.25. Local heat transfer coefficient variations for the triangle-shaped ribbed tube at different Reynolds numbers.

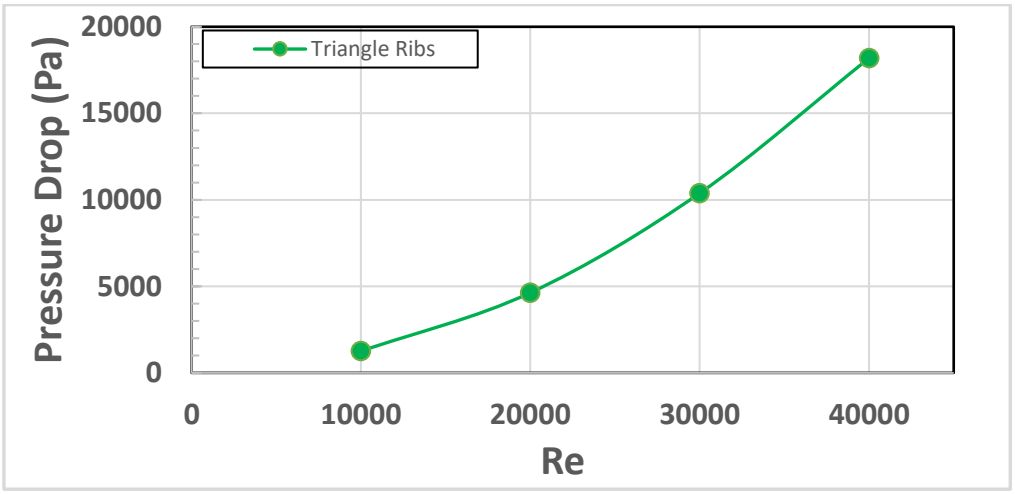

Figure 4.26. Average pressure drop variations for a triangle-shaped ribbed pipe at different Reynolds numbers.

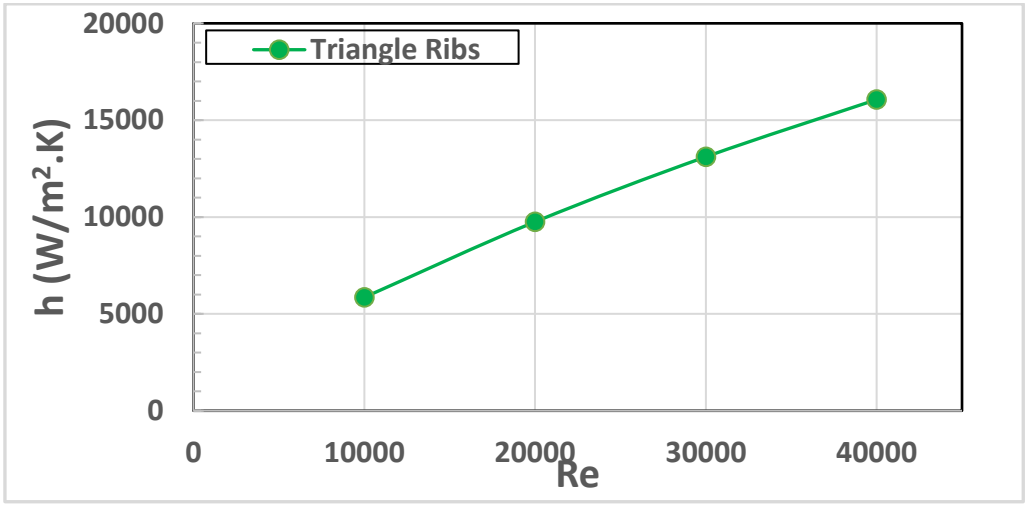

Figure 4.27. Average heat transfer coefficient variations for the triangle-shaped ribbed tube at different Reynolds numbers.

More details about the flow and temperature distributions along the ribbed pipe are given through the velocity and temperature contours shown in Figures 4.28 and 4.29. The velocity contours (Figure 4.28) demonstrate the recirculation streams and boundary separation behind the triangle ribs, which causes high-pressure drops and relatively low heat transfer rates. The following region between neighbour ribs where these separation currents reattach represents the maximum possible heat transfer rates. The almost identical velocity distribution of the fully developed turbulent region across the pipe is clear in the velocity contours in the middle and last parts of the pipe.

The temperature contours at different regions along the pipe, presented in Figure 4.29, demonstrate the high-temperature regions next to the wall and around the ribs, with a thickness increasing in the direction downstream along the pipe due to turbulence mixing there. The fully turbulent thermal boundary layer is pronounced near the pipe exit region.

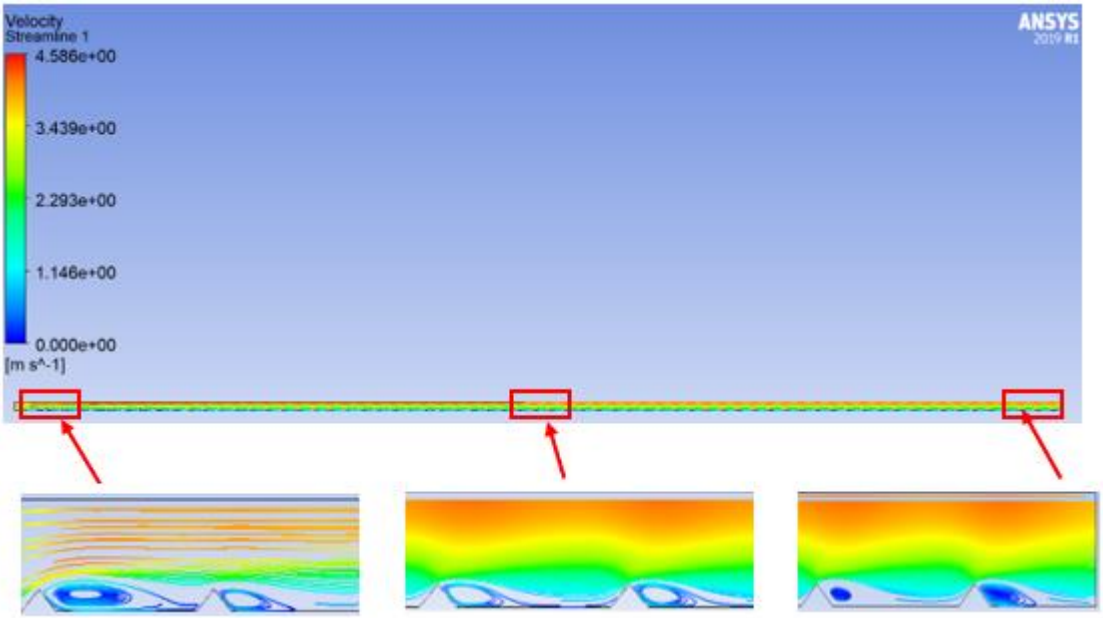

Figure 4.28. Contour of streamlined velocity at different regimes along the pipe.

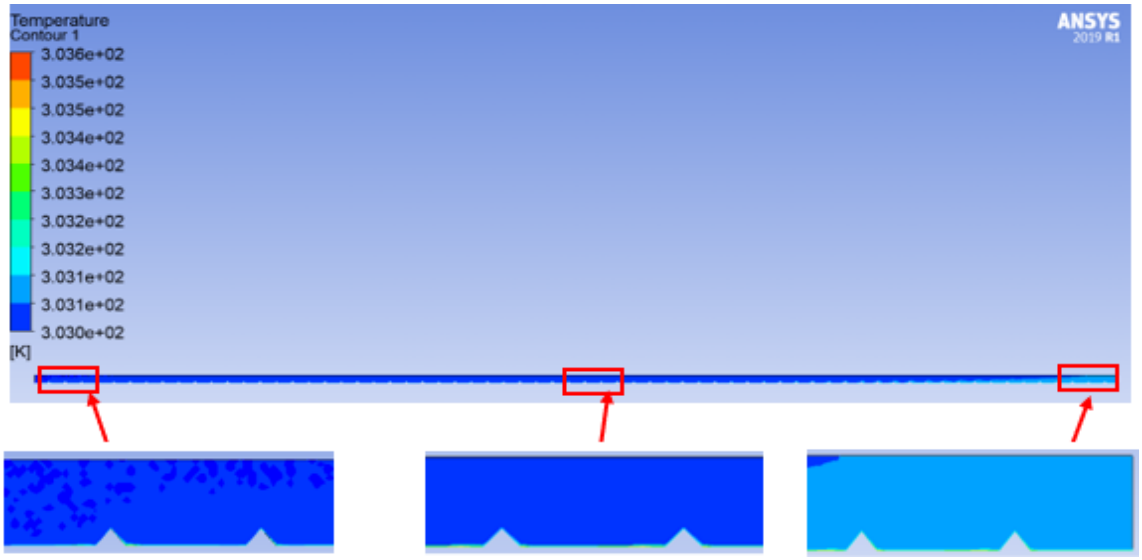

Figure 4.29. Contour of temperature at different regimes along the pipe.

4.3.2. Effect of Pitch Ratio and Ribs Height

The effect of changing the pitch distance and the rib's height on the heat transfer and pressure drop along the pipe is also considered for the triangle ribs at Reynolds number 40000. The nanofluid constitution and the boundary conditions are taken as identical to those in the rectangle ribs cases. Furthermore, the same designs as described in Table 3.2 are considered in this part. Figures 4.30 - 4.33 illustrate the local heat transfer coefficient and the pressure drop variations as a function of the pitch distance for two ribs' height-to-diameter rations, h/d = 0.05 and 0.1.

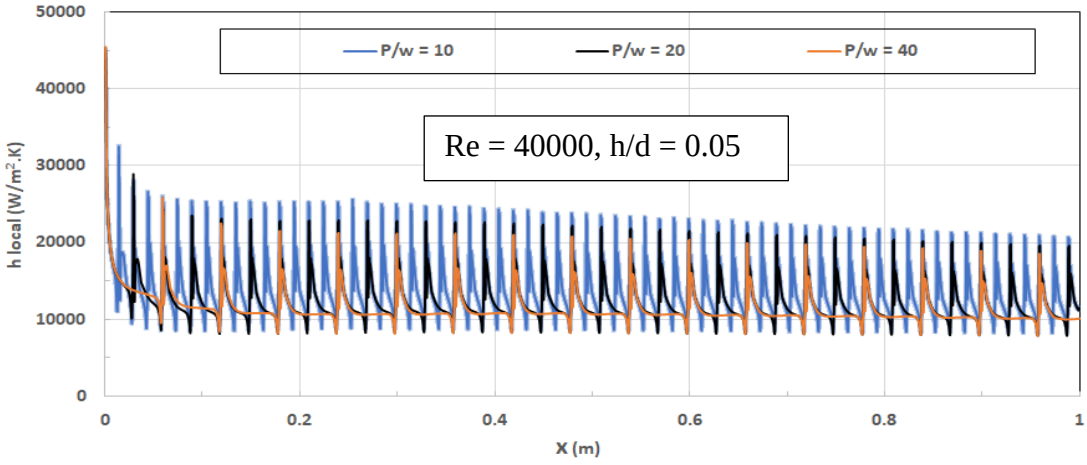

Figure 4.30. Effect of pitch ratio on local heat transfer coefficient variations for a triangle-shaped ribbed tube.

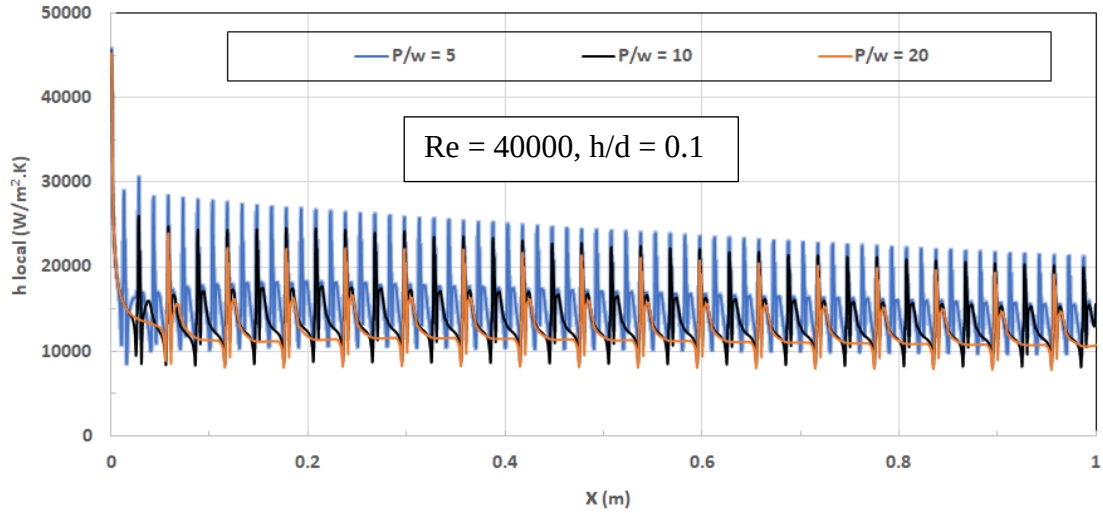

Figure 4.31. Effect of pitch ratio on local heat transfer coefficient variations for a triangle-shaped ribbed tube.

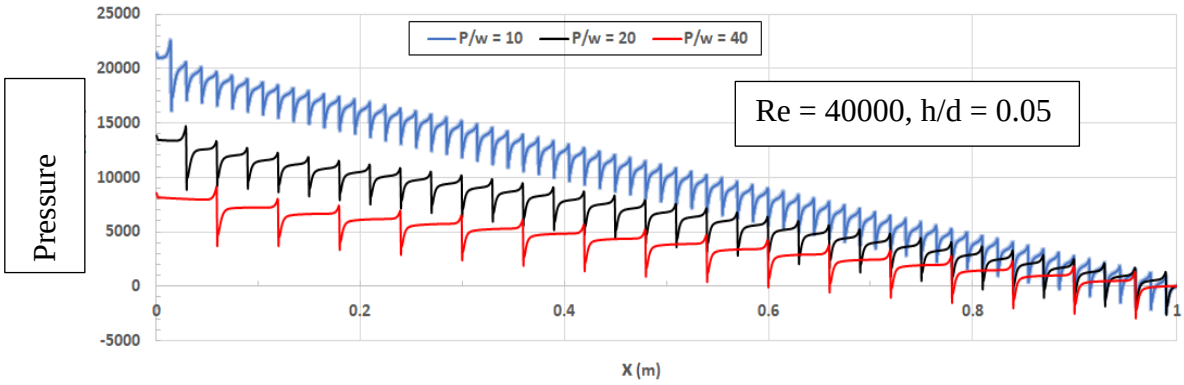

Figure 4.32. Pressure drop variations for a triangle-shaped ribbed tube at different pitches, h/d = 0.05.

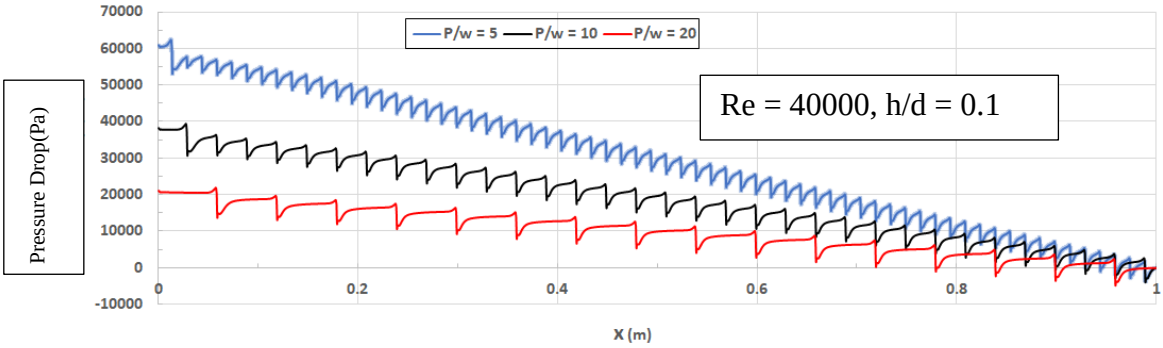

Figure 4.33. Pressure drop variations for a triangle-shaped ribbed tube at different pitches, h/d = 0.1.

The figures demonstrate similar behaviours to those noticed in the rectangular ribs cases, where decreasing the pitch distance results in increasing the local heat transfer coefficients and pressure drops considerably. In the triangle ribs case, decreasing the pitch-to-ribs width ratio by a factor of 4 almost triples the pressure drop values and increases the local heat transfer magnitudes by 25%. This can be explained, as mentioned before, by decreasing the pitch distance, leading to increasing the rib numbers, which means that higher mixing and larger friction losses will occur.

Furthermore, about the effect of the ratio of ribs' height to diameter on local heat transfer coefficients and pressure drops, figures 4.34 to 4.39 represent the results for the different investigated pitch distances, 15, 30, and 60 mm, and at Reynolds number 40000. The figures show that while the effect of h/d on the heat transfer coefficient is almost negligible, except at a small pitch distance value where the effect is relatively

more noticeable but still very limited, the effect on pressure drop is highly marked. Figure 4.28 shows that increasing the ribs' height enhances the heat transfer rates as a result of increasing the turbulence intensity. This behaviour is only clarified for the short pitch distance because, in this case, the number of ribs is large, and hence the turbulence effect is more important. On the other hand, figures 4.37 – 4.39 show that increasing the h/d ratio causes an enormous rise in pressure drop, reaching about 300% for the pitch distance p = 15 mm. This can be explained because the increase in ribs height increases the friction losses and as a result the pressure drops.

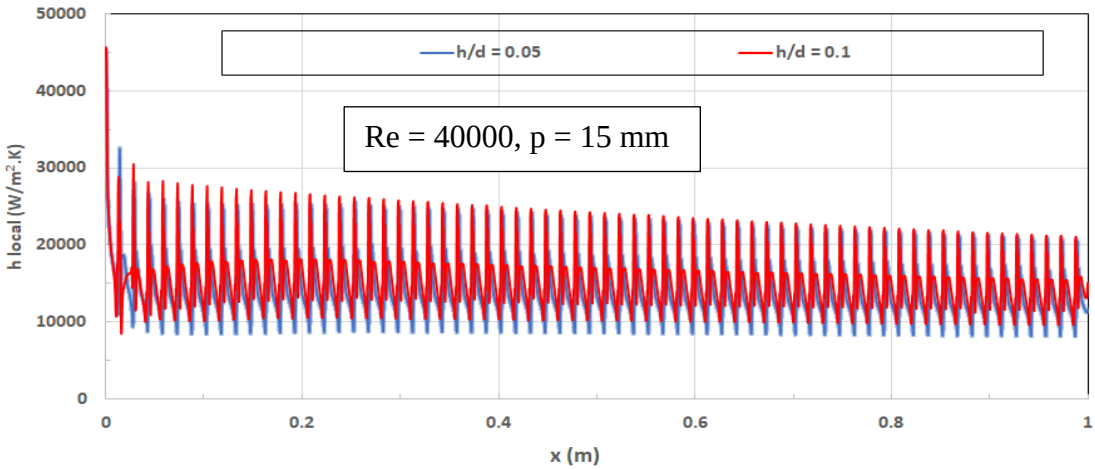

Figure 4.34. Local heat transfer coefficient variations for a triangle-shaped ribbed tube at different height-to-diameter ratios, P = 15 mm.

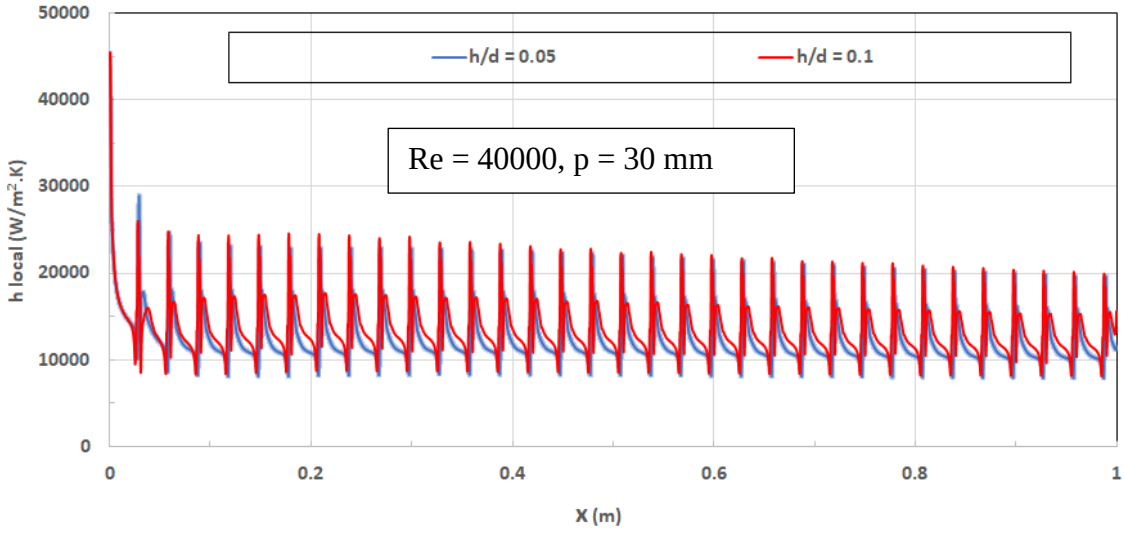

Figure 4.35. Local heat transfer coefficient variations for a triangle-shaped ribbed tube at different height-to-diameter ratios, P = 30 mm.

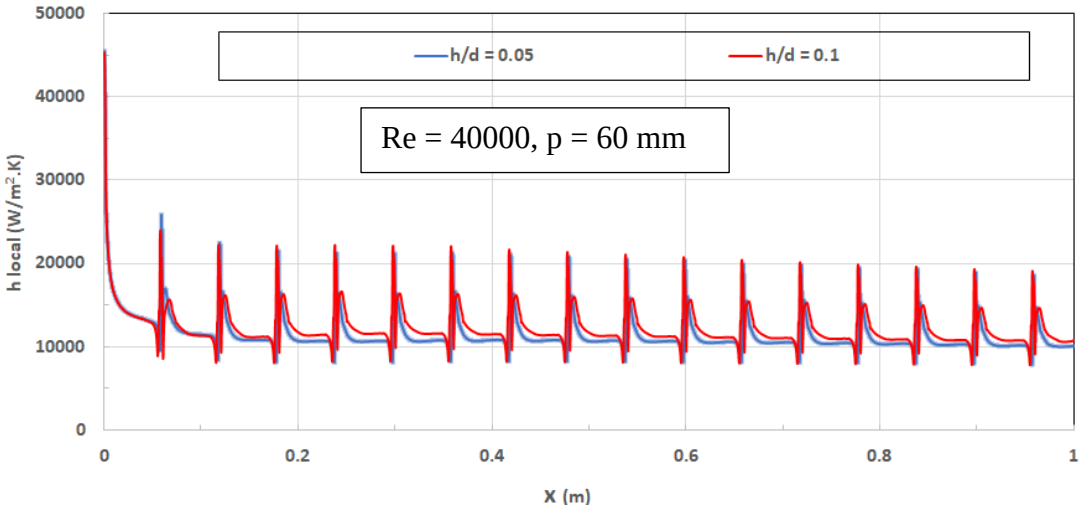

Figure 4.36. Local heat transfer coefficient variations for a triangle-shaped ribbed tube at different height-to-diameter ratios, P = 60 mm.

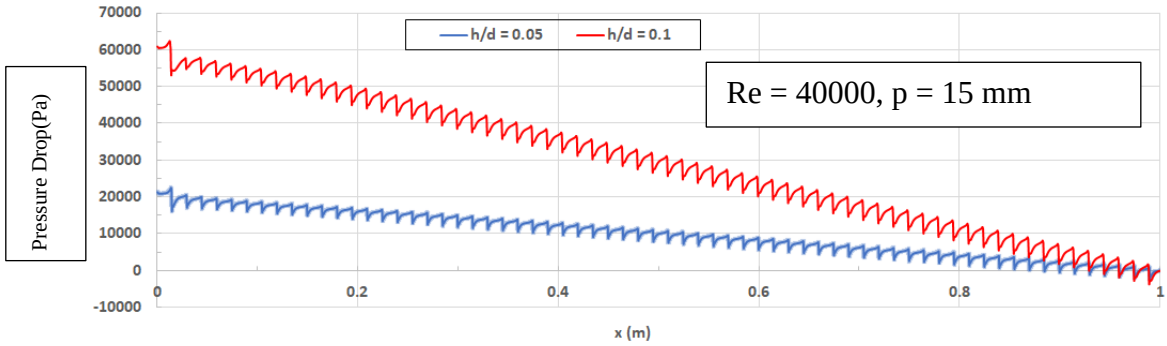

Figure 4.37. Pressure drop variations for a triangle-shaped ribbed tube at different height-to-diameter ratios, P = 15 mm.

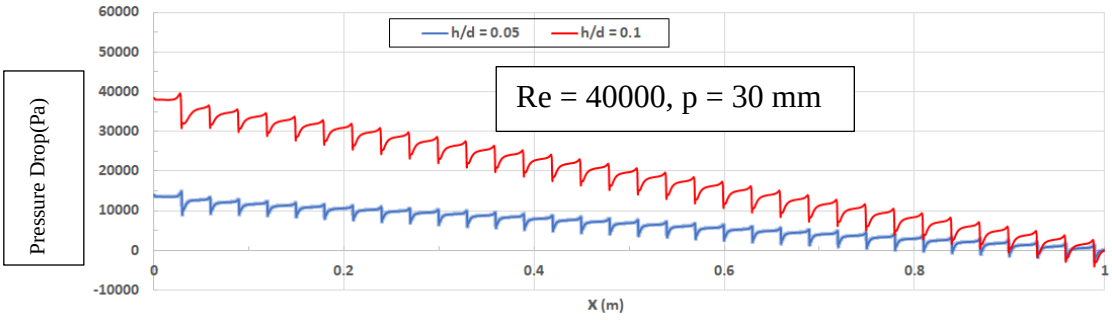

Figure 4.38. Pressure drop variations for a triangle-shaped ribbed tube at different height-to-diameter ratios, P = 30 mm.

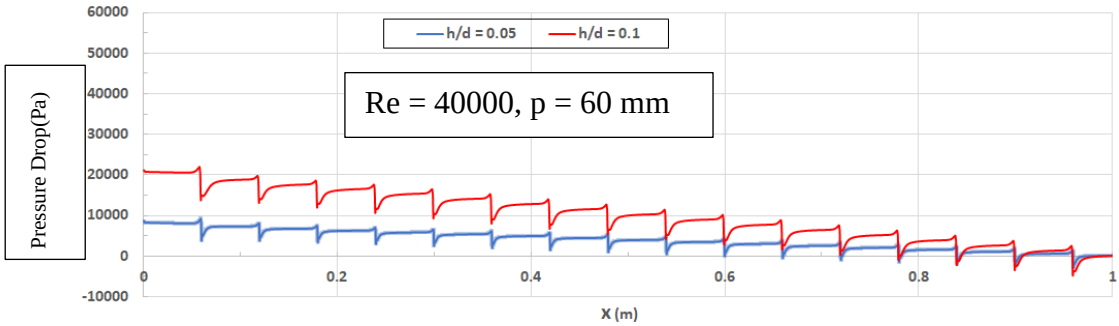

Figure 4.39. Pressure drop variations for a triangle-shaped ribbed tube at different height-to-diameter ratios, P = 60 mm.

4.4. HEAT TRANSFER AND NANOFLUID FLOW THROUGH A PIPE WITH SEMICIRCLE RIBS

The third rib shape to be considered in this research is the semicircle ribs. The heat transfer and nanofluid flow through a semicircle-shaped ribbed tube are investigated, as illustrated in Figure 4.40. Again, all the parameters of the previous cases are held the same, either the boundary conditions or the dimensions of the pipe and ribs.

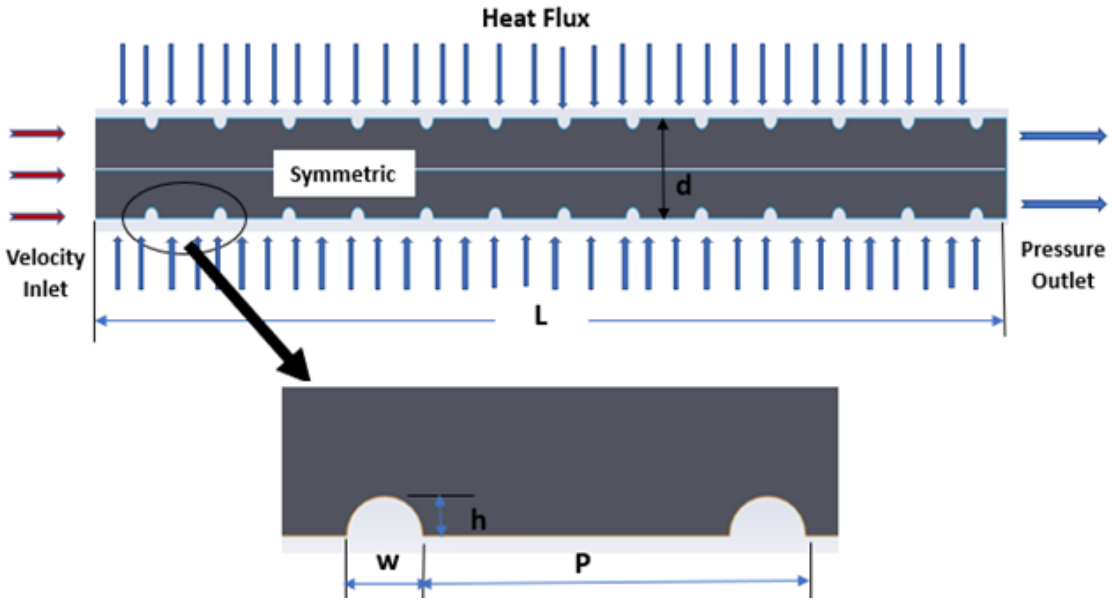

Figure 4.40. studies case geometry and boundary condition.

4.4.1. Effect of Reynolds Number

The Reynolds number impact on heat transfer and nanofluid flow through the semi-circular shaped ribbed pipe is examined and analysed. The local pressure drop and local heat transfer results for different Renolds number values, 10000, 20000, 30000, and 40000, are shown in figures 4.41 and 4.42, respectively. Also, the average values are demonstrated in Figure 4.43 and Figure 4.44. The nanofluid specifications and the rib dimensions are similar to those for the rectangular and triangle rib cases. The nanofluid is (0.5% Al2O3 - 0.5% TiO2)/water and the ribs parameters are h = 1.5 mm (h/d = 0.1) and P = 15 mm (P/W = 5).

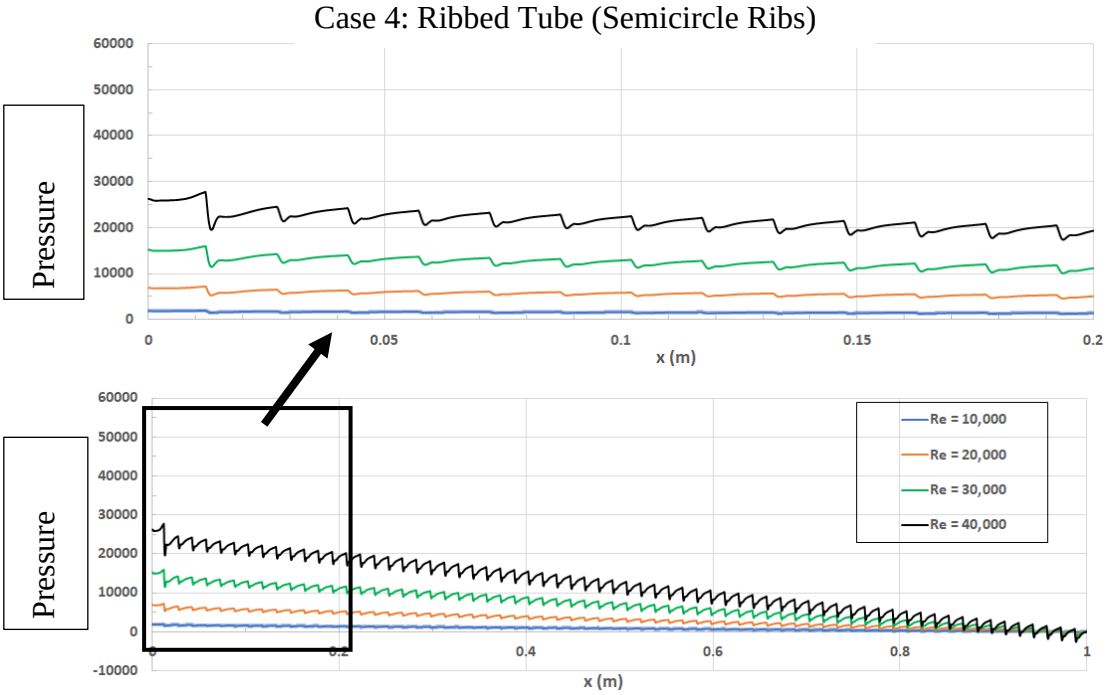

Figure 4.41. Pressure drop variations for a semicircle-shaped ribbed pipe at different Reynolds numbers.

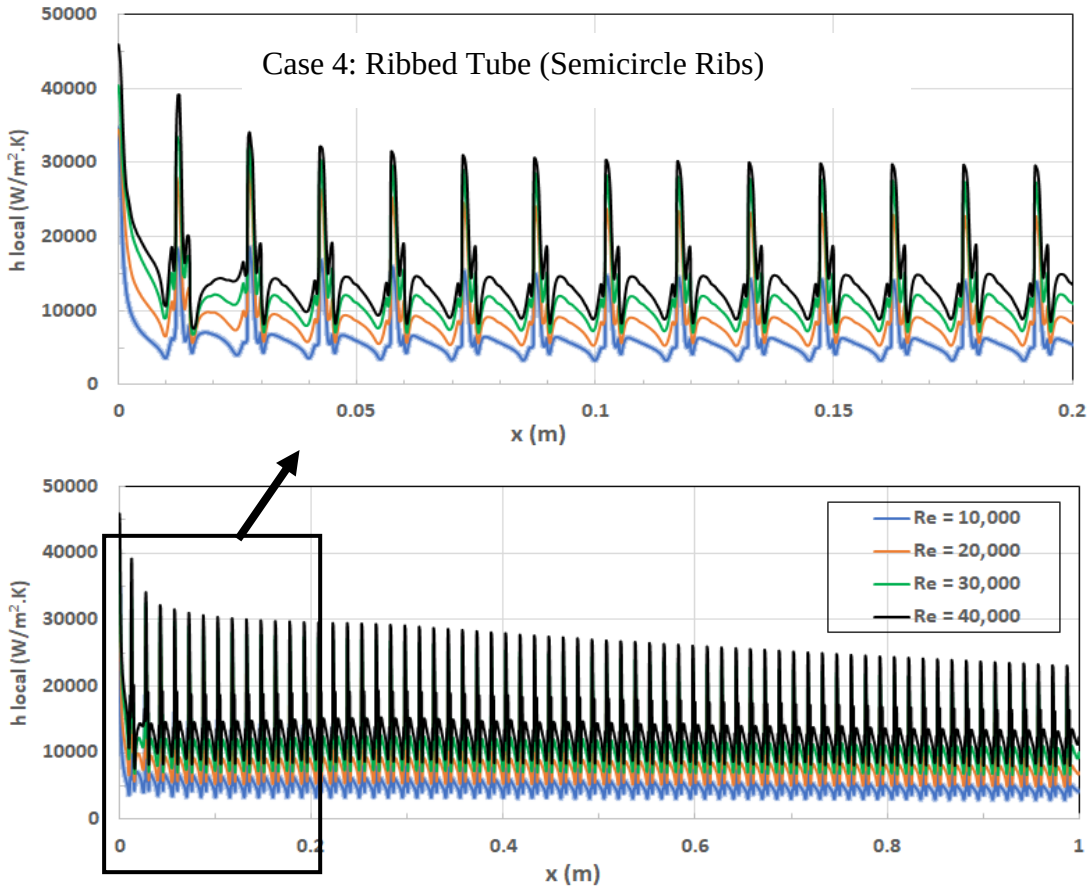

Figure 4.42. Local heat transfer coefficient variations for the semi-shaped ribbed tube at different Reynolds numbers.

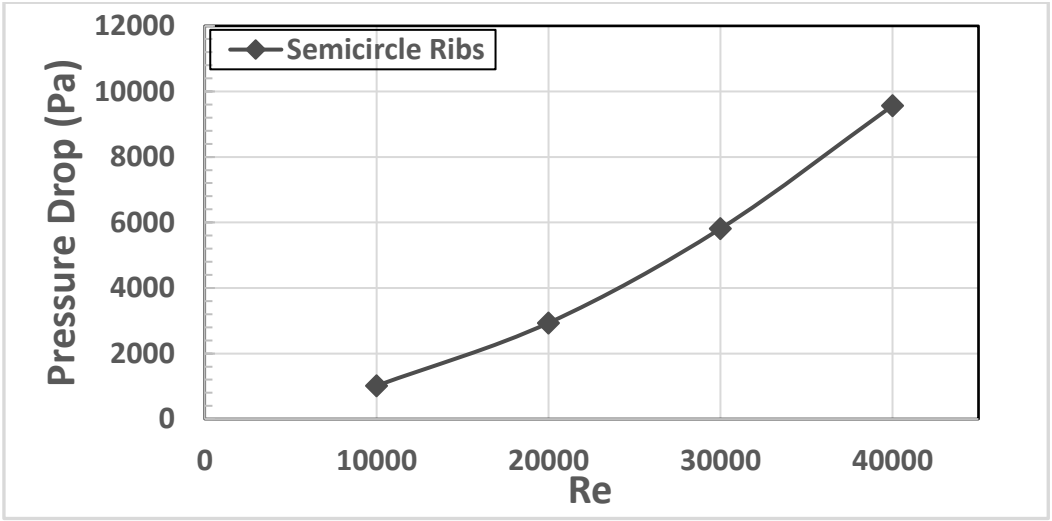

Figure 4.43. Average pressure drop variations for a semicircle-shaped ribbed pipe at different Reynolds numbers.

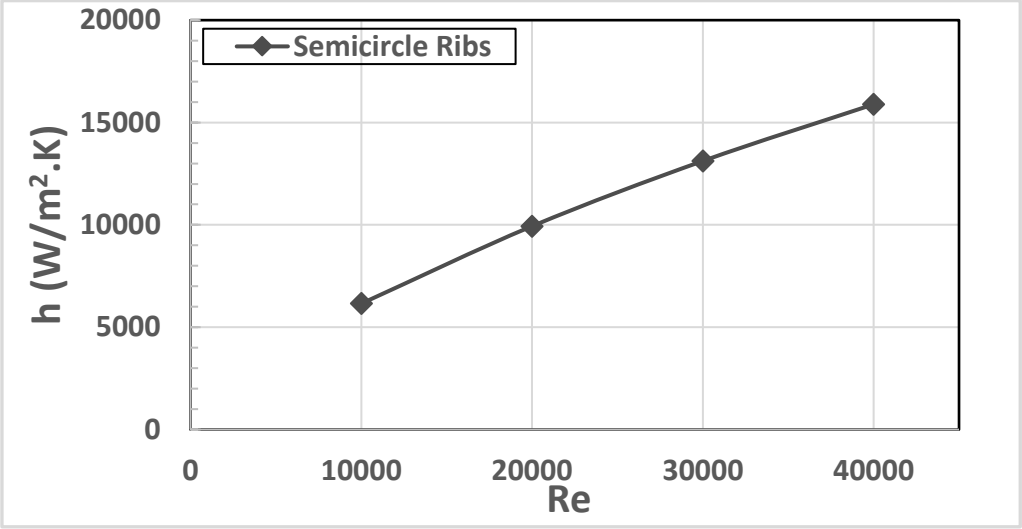

Figure 4.44. Average heat transfer coefficient variations for the semi-shaped ribbed tube at different Reynolds numbers.

As expected, the results have confirmed that high Reynolds values correspond to high heat transfer coefficients and large pressure drops in this case as well. Increasing Reynolds number enhances turbulent mixing and, as a result, increases the heat transfer rates and increases the flow resistance. However, for the semicircle ribs case, and because of the round edges, the friction losses are too much less compared to the other two previous cases for all considered Reynolds numbers. The pressure drops for the semicircle ribs are less than those of the rectangle ribs case by more than 25% and form less than half of the corresponding magnitudes of the triangle ribs. Not only pressure drop, which has been improved in the semicircle case, but the local heat transfer coefficients have also been relatively enhanced, especially at high Reynolds values. This is because the smooth turbulent flow around the semi-circular ribs reduces the separation region behind the ribs, and accelerates the flow reattachment.

The separation and reattachment phenomena are clarified by presenting the streamlined velocity contours at different locations along the pipe, including the entrance, the middle and the exit regions, as shown in Figure 4.45. The case of semicircle ribs is categorized by smooth flow around the ribs, which contributes toward attaining high heat transfer rates and low friction losses. The isothermal contours for the current case are also obtained and illustrated in Figure 4.46. The

thermal boundary layer development, as well as the temperature profile distribution along and across the pipe, are readily detectable through this figure.

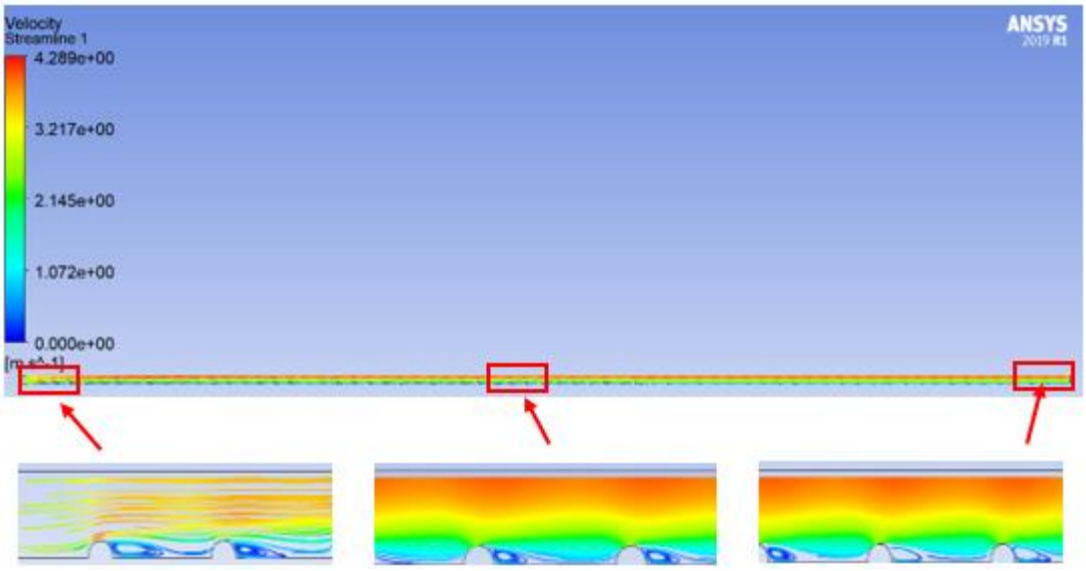

Figure 4.45. Contour of streamlined velocity at different regimes along the pipe.

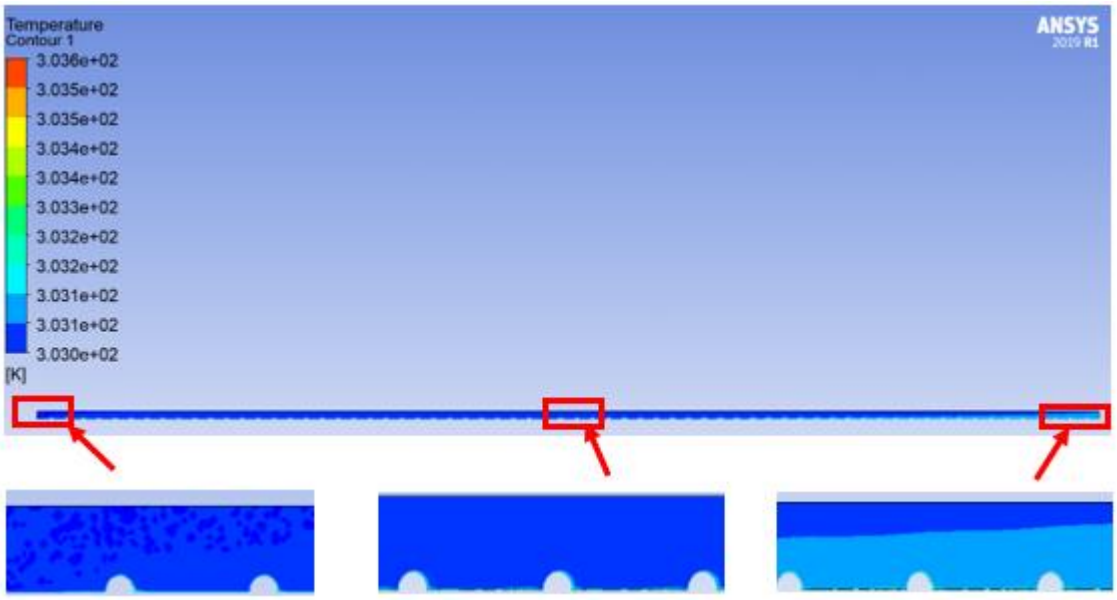

Figure 4.46. Contour of temperature at different regimes along the pipe.

4.4.2. Effect of Pitch Ratio and Ribs Height

In the semicircle ribs case, the impact of pitch ratio on heat transfer and fluid flow is almost similar to what has been reported for rectangle and triangle ribs cases. Again, decreasing the pitch distance causes an increase in both heat transfer coefficients and pressure drops for the two ribs' height-to-height-to-diameter ratios investigated, h/d = 0.05 and 0.1. These behaviours of semicircle ribs at Reynolds number equal to 40000 and for the whole designs presented in table 3.2 are demonstrated in figures 4.47 to 4.50. However, for this part, while the effect on local heat transfer is considerable for the small pitch distance p = 15 mm, it is limited for medium and large pitch distances, p = 30 and 60 mm. Moreover, the effect of pitch distances on pressure drop is more noticeable for the pitch distance p = 15, but it is still recognized for the two other pitch distances. The large ribs number in the case of a small pitch distance strongly influences the heat and nanofluid flow through the pipe.

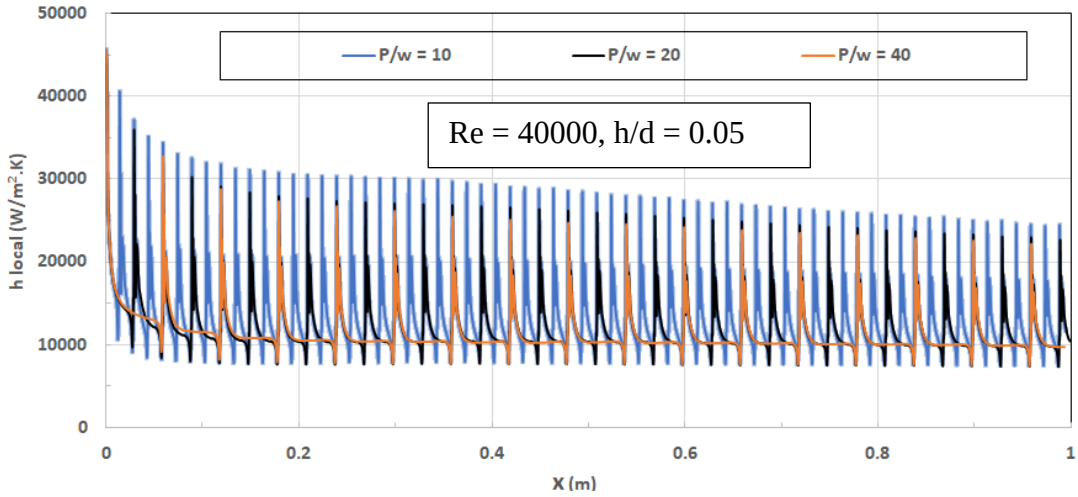

Figure 4.47. Effect of pitch ratio on local heat transfer coefficient variations for a semicircle-shaped ribbed tube.

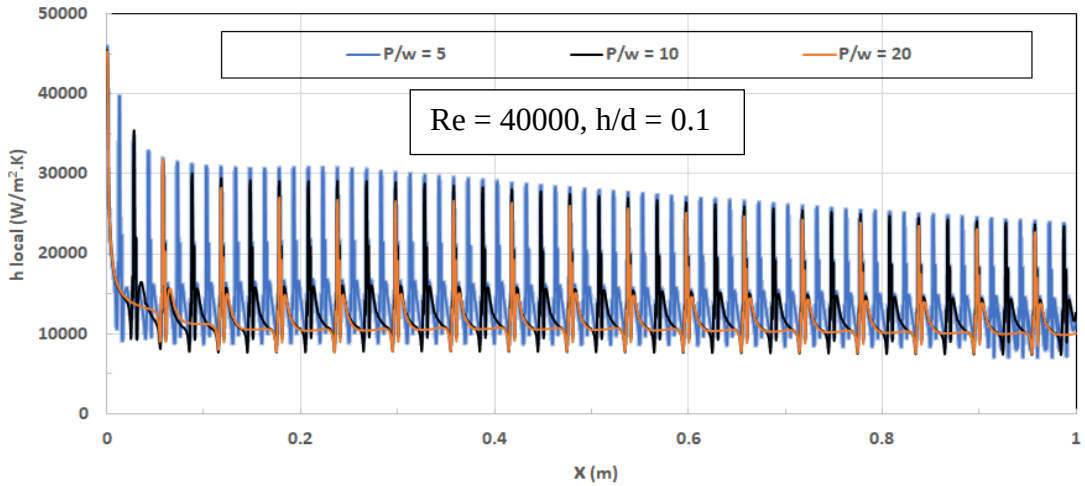

Figure 4.48. Effect of pitch ratio on local heat transfer coefficient variations for a semicircle-shaped ribbed tube.

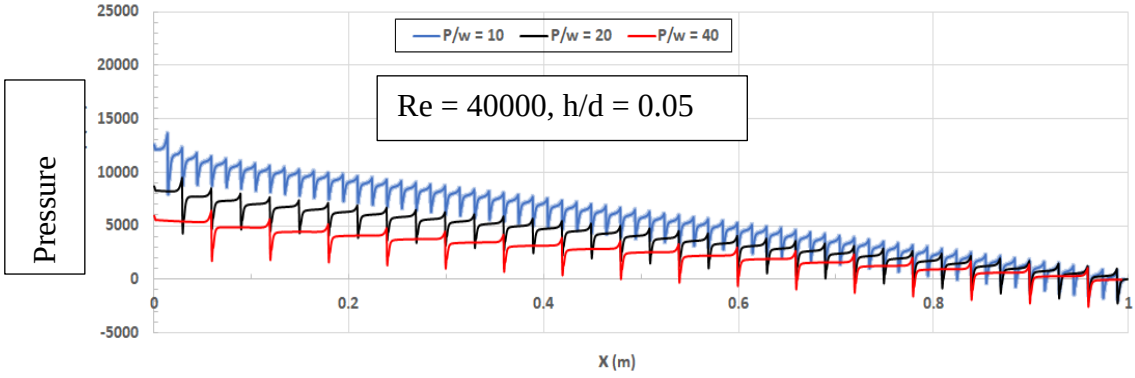

Figure 4.49. Pressure drop variations for a semicircle-shaped ribbed tube at different pitches, h/d = 0.05.

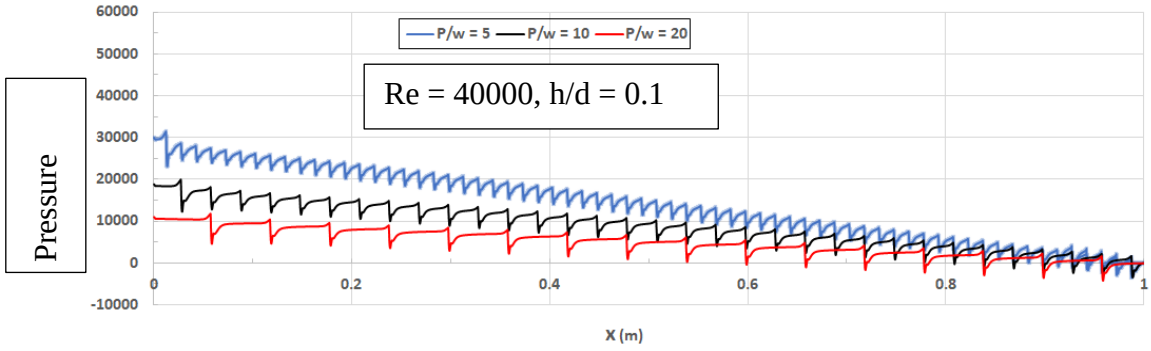

Figure 4.50. Pressure drop variations for a semicircle-shaped ribbed tube at different pitches, h/d = 0.1.

Furthermore, figures 4.51-4.56 show the effect of the ribs' height-to-diameter ratio on the local heat transfer coefficient and pressure drop variations along the pipe length. It can be seen that changing the h/d ratio from 0.05 to 0.1 does not influence the local heat transfer too much. The variations are insignificant, particularly at pitch distances p = 30 and 60 mm. The variation at p = 15 mm is relatively more obvious, but still very minor. This behaviour agrees well with the triangle ribs findings in the previous section, but the local heat transfer values for semicircle ribs are considerably higher than those for triangle ribs as mentioned before. On the other hand, the effect of the h/d ratio on pressure drops is noticeable for the three pitch distances 15, 30 and 60 mm, as shown in figures 4.54-4.56. This effect is particularly evident at the pitch distance p = 15, where increasing h/d from 0.05 to 0.1 causes the pressure drop values almost to be doubled. This is again a direct result of the magnified outcomes for the case with large ribs number, as it has been noticed for all parts of the current study.

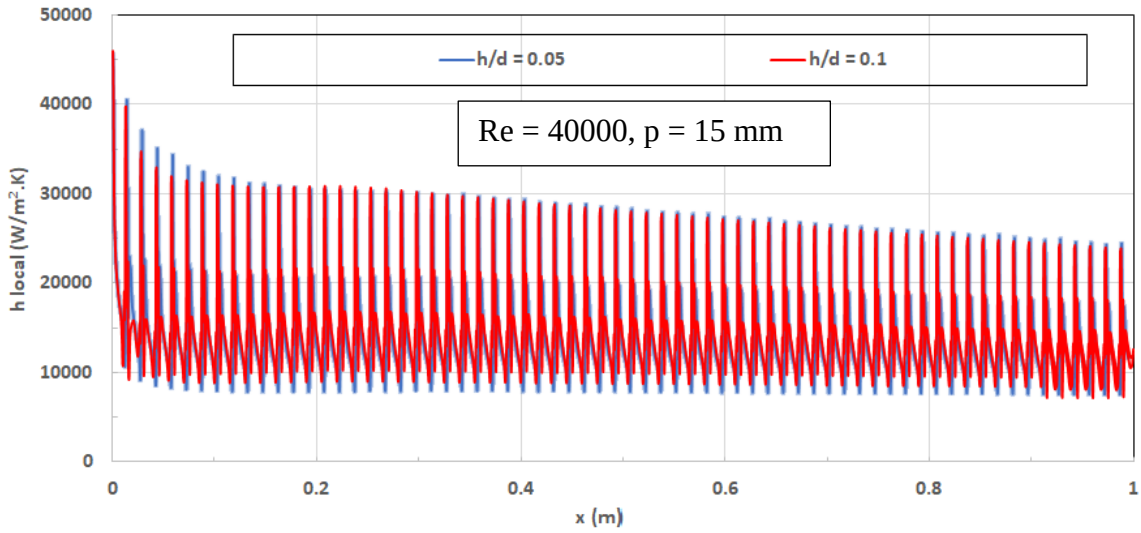

Figure 4.51. Local heat transfer coefficient variations for a semicircle-shaped ribbed tube at different height-to-diameter ratios, P = 15 mm.

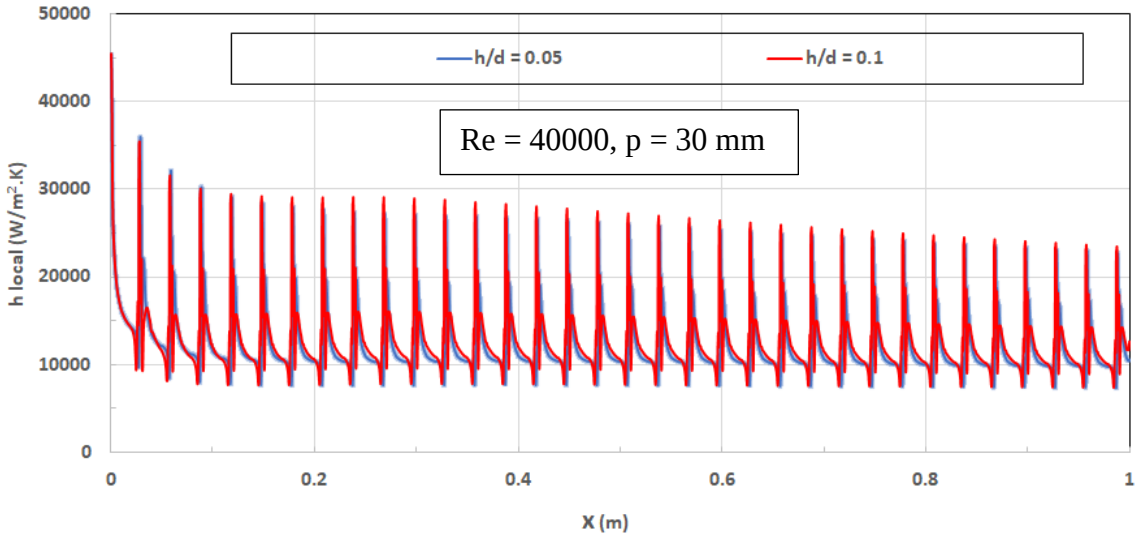

Figure 4.52. Local heat transfer coefficient variations for a semicircle-shaped ribbed tube at different height-to-diameter ratios, P = 30 mm.

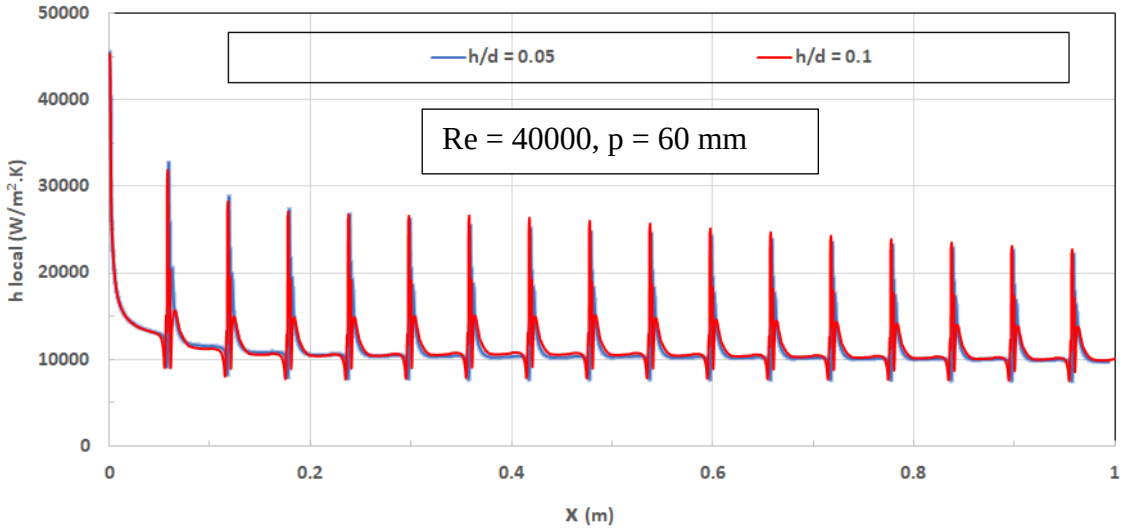

Figure 4.53. Local heat transfer coefficient variations for a semicircle-shaped ribbed tube at different height-to-diameter ratios, P = 60 mm.

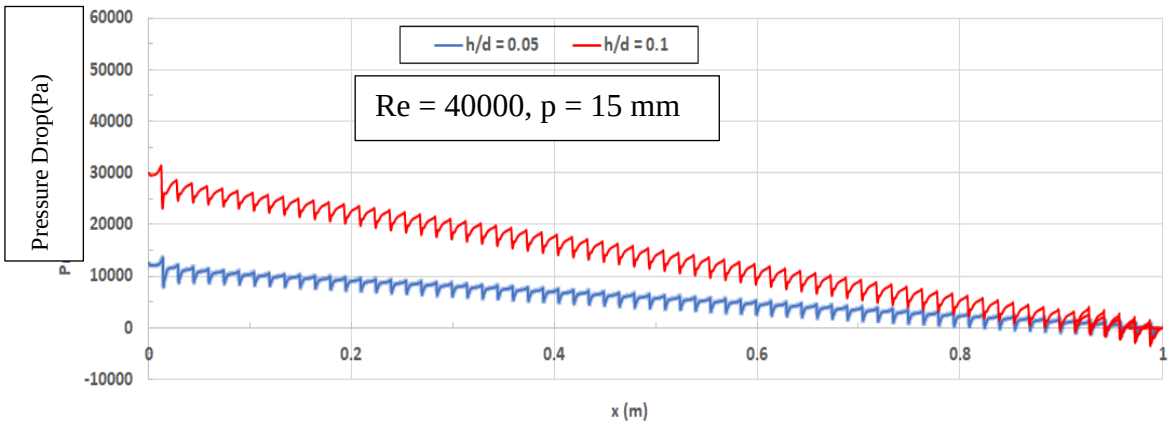

Figure 4.54. Pressure drop variations for a semicircle-shaped ribbed tube at different height-to-diameter ratios, P = 15 mm.

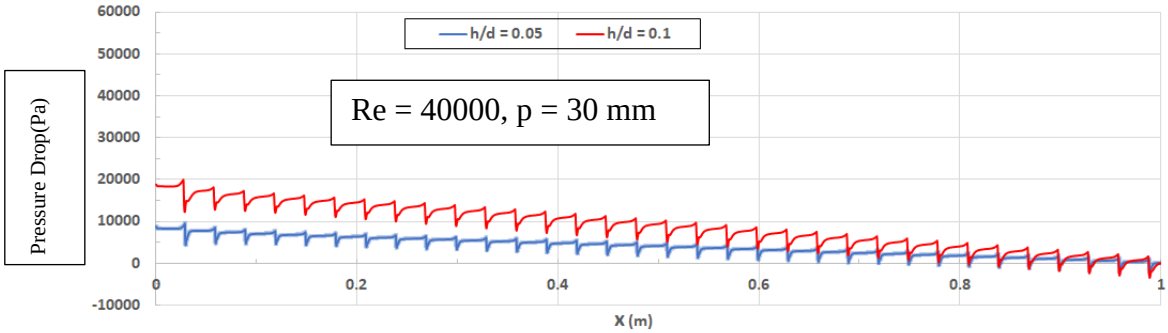

Figure 4.55. Pressure drop variations for a semicircle-shaped ribbed tube at different height-to-diameter ratios, P = 30 mm.

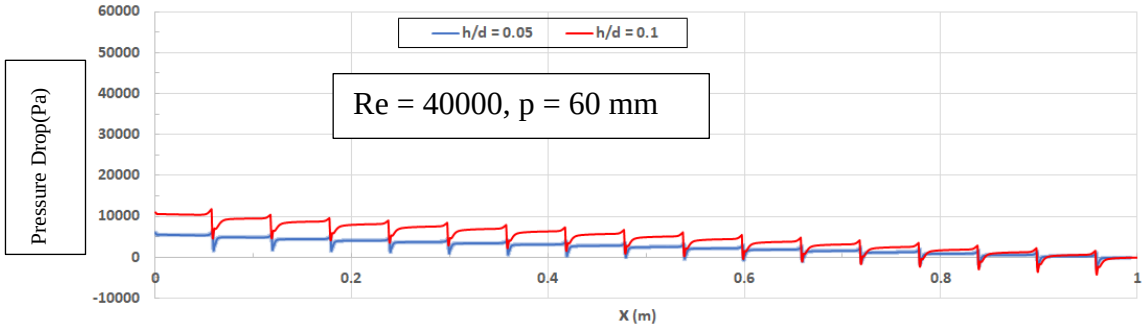

Figure 4.56. Pressure drop variations for a semicircle-shaped ribbed tube at different pipe.

4.5. HEAT TRANSFER AND NANOFLUID FLOW THROUGH A PIPE WITH A HYBRID RIBS CONFIGURATION

The evaluation of flow and thermal effects of ribs configuration is finalized by considering a hybrid ribs arrangement. Figure 4.57 illustrates this configuration, where rectangle, triangle, and semicircle-shaped ribs are used to study thermal and nanofluid flow fields through a ribbed pipe. All nanofluid and geometry specifications that have been determined in the single ribs shapes are again considered in this investigation. The height and width for all rib shapes are 1.5 and 3 mm respectively, and the pitch distance is equal to 15 mm. Four different Reynolds numbers, 10000, 20000, 30000, and 40000, are considered, and the average heat transfer coefficient and pressure drop are calculated. Figures 4.58 and 4.59 compare the results obtained with the corresponding values for single rectangular, triangular, and semi-circular rib shapes. Furthermore, the thermal performance factor defined in equation 22 is also calculated and presented for all rib configurations as illustrated in Figure 4.60.

$$\eta = \frac{(Nu/Nu_o)}{(f/f_o)^{1/3}} \tag{3.22}$$

Where Nu and Nu_o are the average Nusselt number for the ribbed and plain tube, f and f_o are the average friction coefficient for the ribbed and plain tube. Nusselt number and friction coefficient relations have been presented in equations 18 and 20.

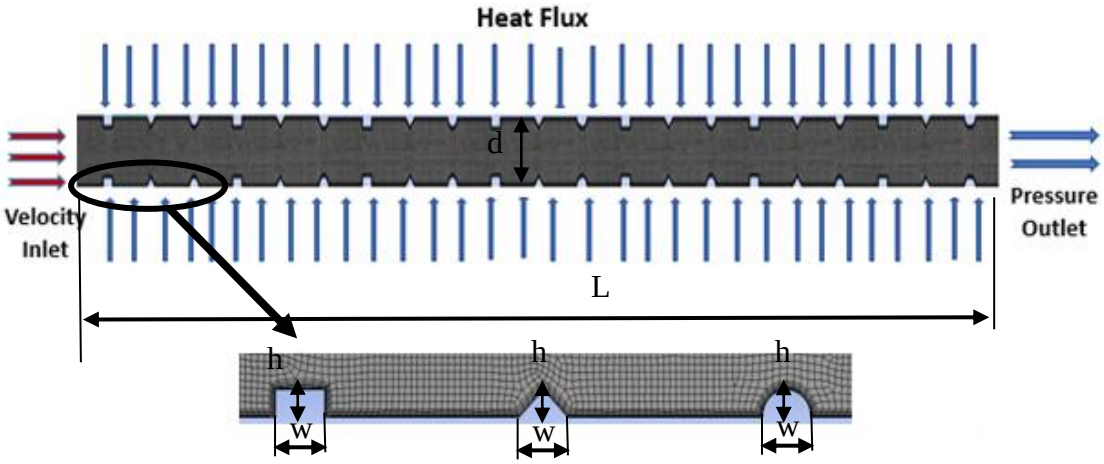

Figure 4.57. studies case geometry and boundary condition: hybrid ribs.

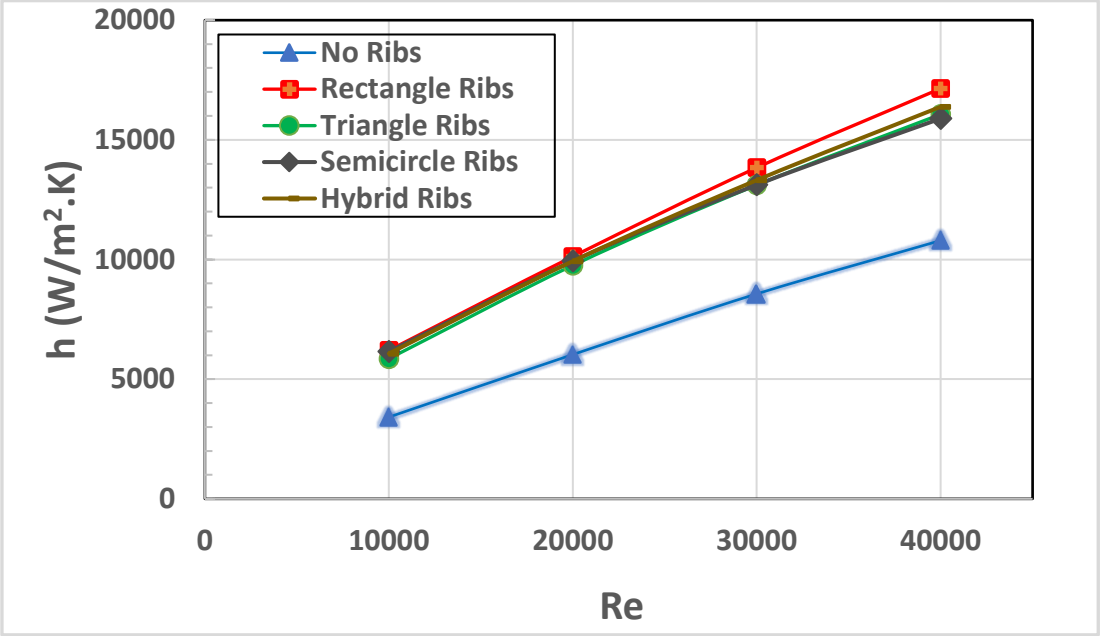

Figure 4.58. Average heat transfer for different rib configurations.

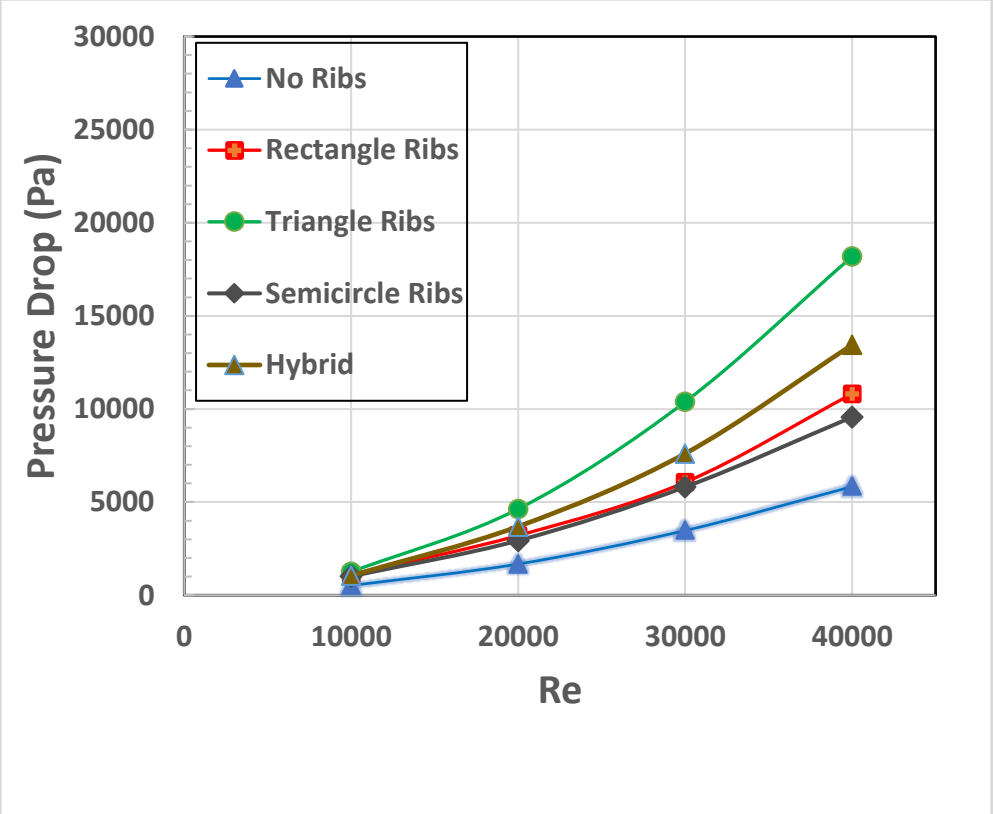

Figure 4.59. Average pressure drops for different rib configurations.

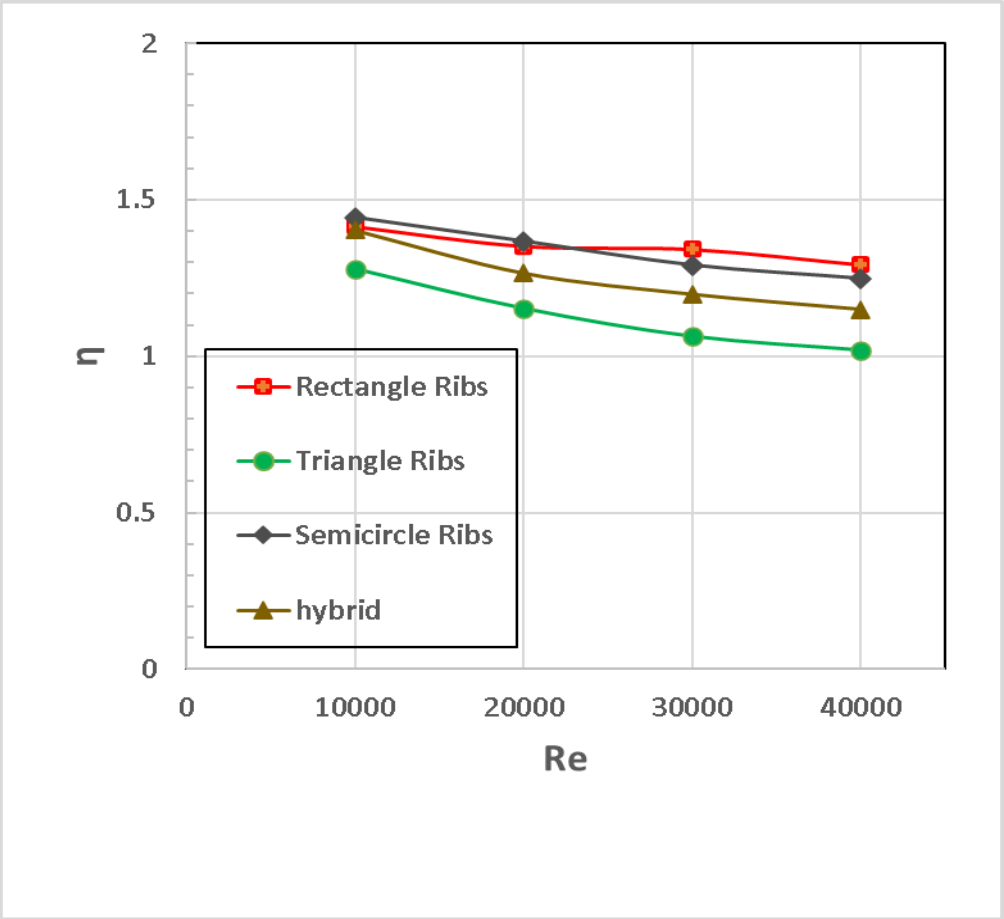

Figure 4.60. Thermal performance factor for different rib configurations.

It can be seen from Figure 4.58 that the average heat transfer coefficient considerably increases by introducing the ribs, regardless of the rib's shape and arrangement, particularly at high Reynolds numbers. However, there is a clear advantage for the rectangle ribs, and then for the hybrid ribs configuration, against the other tested rib shapes, the triangle and semicircle. The average heat transfer coefficient for the rectangle ribs exceeds the value of 17000 W/m^2.K at Reynolds number 40000, and reaches the value of 16400 W/m^2.K for the hybrid ribs arrangement, while it is almost the same for the triangle and semicircle ribs at about 16000 W/m^2.K. The h value for the plain pipe is only about 10000 W/m^2.K at the same Reynolds number value. These results can be attributed to the larger surface areas of the rectangle ribs, as well as to the higher turbulent mixing currents compared to other rib shapes, which enhance the efficiency of heat transfer.

Furthermore, Figure 4.59 shows that the average pressure drop also considerably increases when using ribs with any shape and arrangement. This is particularly true at the high Reynold number value. However, the behaviour in terms of the variation of pressure drop as a function of rib type is different from what has been noticed for average heat transfer coefficient data. The triangle ribs have the highest pressure drop at more than 18000 Pa for Reynolds number 40000, which is almost three times the corresponding value for the plain pipe. The hybrid arrangement also has a relatively high-pressure drop at about 13400 Pa at Reynolds number 40000, then the rectangle ribs at nearly 10800 Pa. The semicircle ribs have the lowest pressure drop among the tested rib arrangements at about 13000 Pa. These behaviours are expected based on the local data reported in the previous sections.

Finally, the results of thermal performance factors for the investigated ribs presented in Figure 4.60 show that the values generally slightly decrease with increasing Reynold number. This tendency is in good agreement with the data reported by Kumar et al. [40], who have used nanofluid particles and ribbed tubes with specifications relatively close to the current investigation but in contrast to the data reported by some researchers, such as Yaningsih et al. [52]. This can be attributed to the fact that the friction factor role is magnified by increasing the Reynolds number compared to that of the Nusselt number at the examined pitch distance and rib height. The conclusion is even further supported by the data presented in Figures 4.58 and 4.59. On the other hand, Figure 4.60 illustrates that the thermal performance factor is higher for the rectangle and semi-circular ribs due to the high Nusselt number values for the first arrangement and the low friction coefficient values for the second one. The triangle ribs have the lowest thermal performance factor values as a result of the relatively enormous pressure drops noticed in this configuration, while the hybrid arrangement data is located in the middle of the presented results.

PART 5

CONCLUSIONS AND RECOMMENDATIONS

Heat transfer enhancement is a very important topic related to a wide range of engineering applications. The heat transfer rates can be increased by applying different techniques, including using ribs of different sizes and shapes. Furthermore, nanofluid technology has been recently widely used in improving cooling processes due to its unique features.

In the current study, heat transfer and nanofluid flow through a channel of circular cross-section, provided with ribs of different shapes and arrangements, are considered using ANSYS FLUENT software. Hybrid nanoparticles of Al_2O_3 and TiO_2, suspended in water with a total volume concentration of 1% (0.5 % each) are used as a working fluid at Reynolds numbers ranging between 10000 and 40000. The dimensions of the pipe are 1000 mm and 15 mm in length and diameter, respectively, and it is subject to a constant heat flux at 5000 W/m^2. The effect of rib shape on the heat and nanofluid flow is investigated by examining rectangle, triangle, and semicircle-shaped ribs in single and hybrid configurations. The effect of rib height and pitch distance on thermal and flow fields is also studied by considering six different designs for each rib shape. The pitch distances considered in the study are p = 15, 30, and 60 mm, and the heights are h = 0.075 and 1.5 mm. According to the findings of this research, the following conclusions can be drawn:

- Using ribs considerably enhances heat transfer rates but, at the same time, significantly increases the pressure losses along the pipe length. Introducing the ribs to the flow increases the interaction surface areas between the fluid and pipe walls and also increases the turbulence mixing. These result in increasing the heat transfer rates and the friction between the fluid and pipe walls.

- The local heat transfer coefficients and pressure drops are directly proportional to Reynolds number values. A noticeable increment in heat transfer coefficient and pressure drops is reported when the Reynolds number is increased from 10000 to 40000.
- The local heat transfer coefficient decreases in the regions directly before and behind the ribs due to the existence of stagnation regions there and reaching its highest value somewhere between the two following ribs as a result of the boundary layer reattachment.
- The areas in front and behind the ribs are characterised by flow-recirculating currents, which significantly increase the local pressure drop.
- The pitch distance has an important impact on both heat transfer coefficient and pressure drop. Decreasing the pitch distance increases the local heat transfer and friction losses due to the high mixing and large friction due to increasing the ribs number.
- The height of the ribs also has a crucial role in the heat transfer and fluid flow data, particularly about the pressure drop values; the effect on the heat transfer coefficient is only noticed at a small pitch distance.
- The shape of the ribs is very important in determining the heat transfer, the pressure losses, and the thermal performance factor. It has been concluded that the rectangle ribs have the highest average heat transfer coefficient with an acceptable friction loss, and as a result, they produce the maximum overall thermal performance among the investigated cases. Also, the semi-circular ribs have a relatively low friction loss due to their circular edges, which has led to a high thermal performance factor, although the average heat transfer coefficient values are not high compared to the other rib arrangements. The triangle ribs have the worthiest thermal performance among the rib shapes considered in the current study because of the very large pressure drops caused by their sharp edges. The hybrid ribs arrangement has not added any special characteristics to the heat and fluid fields, and its results are consistent with the single ribs data.

Based on the results and conclusions of the current study, many points can be suggested to be considered in the forthcoming research. Some of them are:

- It is recommended to conduct further research on the effect of the pitch distance and rib height on the thermal performance factor. The current study has shown these two parameters' noticeable and uneven impact on heat transfer and fluid flow data. Therefore, more investigation is necessary to clearly understand their effects on the overall thermal efficiency of the ribbed geometry.
- Including more nanoparticle types, sizes, and concentrations in the investigations is recommended. This advances our understanding of the effect of nanotechnology on heat and fluid flow.
- It is also recommended to add grooves of different shapes between ribs and investigate the heat transfer and fluid flow behaviour in this case. A grove with optimal depth and width can help control the boundary layer development in the region between ribs, hence increasing the heat transfer efficiency.

REFERECES

1. Saha S. K., Ranjan H., Emani M. S., and Bharti A. K., (2019). Heat Transfer Enhancement in Externally Finned Tubes and Internally Finned Tubes and Annuli. Springer Cham, Springer Nature Switzerland, 175 Pages.

2. S.U.S. Choi, Enhancing Thermal Conductivity of Fluids with Nanoparticles, Developments and Applications of Non-Newtonian Flows, D.A. Siginer and H.P. Wang, eds, FED-vol. 231 / MD-vol. 66 ASME (1995) 99-105.

3. Vira C., Hairuddin A. and Mazlan N., 2022. Promising Use Nanoparticles in the Base Fluid of a System (Preparation, Stability Test and Critical Analysis): A Review. Material Today: Proceedings, Volume 66, Part 5, pp 3135-3139.

4. Hassan, S. O., 2015. Investigation Of Laminar Convective Heat Transfer and Pressure Drop Of SiO_2 Nanofluid In Ducts Of Different Geometries. Master Thesis. University of North Dakota, USA.

5. CDC, The National Institute for Occupational Safety and Health (NIOSH). Nanotechnology. https://www.cdc.gov/niosh/topics/nanotech/defualt.html. 2023.

6. Buzea C., Blandino I. I. P., and Robbie K. Nanomaterials and nanoparticles: Sources and toxicity, Biointerphases vol. 2, issue 4 (2007) pages MR17 - MR172.

7. Gireesha, B. J. and Rudraswamy, N. G., 2014. Chemical reaction on MHD flow and heat transfer of a nanofluid near the stagnation point over a permeable stretching surface with non-uniform heat source/sink. International Journal of Engineering, Science and Technology, Volume 6, pp. 13-25

8. Choi, S. U. S. & Eastman, J. A., 1995. Enhancing Thermal Conductivity of Fluids with Nanoparticles. San Francisco, CA., s.n.

9. Virdi R. L., Chatha S. S., and Singh H., 2016. Potential of Nanofluids as Cutting Fluids – An Evolution. Asian Review of Mechanical Engineering. Vol 5, no1, pp 38-39.

10. Saha G., 2016. Heat transfer performance investigation of nanofluids flow in pipe. PhD thesis. University of Glasgow, UK.

11. Suri S., Ruan G., Winter J. O., and Schmidt C. E., 2013. Microparticles and Nanoparticles. Biomaterials Science. Pp 360-388.

12. W. Rashmi, A.F. Ismail, M. Khalid, Y. Faridah, CFD studies on natural convection heat transfer of Al2O3-water nanofluids, Heat and Mass Transfer 47 (2011) 1301-1310.

13. E. Abu-Nada, Effects of variable viscosity and thermal conductivity of Al2O3-water nanofluid on heat transfer enhancement in natural convection, International Journal of Heat and Fluid Flow 30 (2009) 679-690.

14. Yu, W., France, D. M., Routbort, J. L. and Choi, S. S., 2008. Review and Comparison of Nanofluid Thermal Conductivity and Heat Transfer Enhancements. Heat Transfer Engineering, 29(5), pp. 432-460.

15. Das, S. K., Choi, S. U. S., Yu, W. & Pradeep, T., 2007. Nanofluids: Science and Technology. 1st ed. Wiley-Inter-science, 416 pages.

16. Romano, J. M., Parker, J. C. & Ford, Q. B., 1997. Application Opportunities for Nanoparticles Made from the Condensation of Physical Vapors. Adv. Pm. Part., Volume 130, pp. 12-13.

17. Eastman, J. A., Choi, S. U. S., Li, S., Yu,W., and Thompson, L. J., 2001. Anomalously Increased Effective Thermal Conductivities of Ethylene Glycol-Based Nanofluids Containing Copper Nanoparticles. Applied Physics Letter, 78(6), pp. 718-720.

18. Vallejo J. P., Prado J. I., and Lugo L., 2022. Hybrid or mono nanofluids for convective heat transfer applications. A critical review of experimental research. Applied Thermal Engineering 203, 117926.

19. Sajid M. U. and Ali M. H., 2018. Thermal conductivity of hybrid nanofluids: A critical review. International Journal of Heat and Mass Transfer 126 , 211–234.

20. Xian H. W., Sidik N. A. C., and Saidur R., 2020. Impact of different surfactants and ultrasonication time on the stability and thermophysical properties of hybrid nanofluids. International Communications in Heat and Mass Transfer 110, 104389.

21. Incropera, F.P. and D.P. DeWitt, 2002. Fundamental of Heat and Mass Transfer, 5th ed. New York: John Wiley & Sons.

22. CHO H.; LEE S.; WU S., the Combined Effects of Rib Arrangements and Discrete Ribs on Local Heat Mass Transfer in a Square Duct, ASME Paper No.GT2001–0175.

23. SEYHUN D., 2021 - Effect of rib shape on flow regime and heat transfer, Black Sea Journal of Engineering and Science, 4(4), 201-208.

24. Jiménez, J., 2004. Turbulent flows over rough walls. Annual Review of Fluid Mechanics, 36, 173-196.

25. KESHMIRI A., 2010. Thermal Hydraulic Analysis of Gas-Cooled Reactor Core Flow. Ph.D. Thesis, University of Manchester, UK.

26. Maurer M., Wolfersdorf J. V., and Gritsch M, 2007. An Experimental and Numerical Study of Heat Transfer and Pressure Loss in a Rectangular Channel With V-Shaped Ribs, J. Turbomach. 129(4): 800-808.

27. Manca, O., Nardini, S., and Ricci, D., 2012. A numerical study of nanofluid forced convection in ribbed channels. Applied Thermal Engineering, 37, 280–292.

28. Elwekeel F. N. M., Zheng Q., and Abdala A. M. M., 2015. Numerical Study of Turbulent Flow Through Rib-Roughened Channels with Mist Injection, Volume 5A: Heat Transfer, 5A, 1-10.

29. Togun H., Safaei M. R., Sadri R., Kazi S. N., Badarudin A., Hooman K., and Sadeghinezhad E., 2014. Numerical simulation of laminar to turbulent nanofluid flow and heat transfer over a backward-facing step. Applied Mathematics and Computation. 239, 153-170.

30. Safaei M. R., Togun H., Vafai K., Kazi S. N., and Badarudin A., 2014. Investigation of heat transfer enhancement in a forward-facing contracting channel using FMWCNT nanofluids. Numerical Heat Transfer, Part A: Applications, 66, 1321-1340.

31. Moghadassi A., Ghomi E., and Parvizian F., 2015. A numerical study of water based Al2O3 and Al2O3–Cu hybrid nanofluid effect on forced convective heat transfer. International Journal of Thermal Sciences. 92, 50–57.

32. Suresh S., Venkitaraj K.P., Selvakumar P., and Chandrasekar M., 2011. Effect of Al2O3eCu/ water hybrid nanofluid in heat transfer. Experimental Thermal Fluid Science, 38, 54-60.

33. Togun H., 2016. Laminar CuO–water nano-fluid flow and heat transfer in a backward-facing step with and without obstacle. Applied Nanoscience, 6(3), 371-378.

34. Abdulrazzaq T., Togun H., Safaei M. R., Kazi S. N., et al., 2019. Effect of flow separation of TiO2 nanofluid on heat transfer in the annular space of two concentric cylinders. Thermal science. 321-321.

35. Togun, H., Abu-Mulaweh, H. I., Kazi, S. N., and Badarudin, A., 2016. Numerical simulation of heat transfer and separation Al2O3/nanofluid flow in concentric annular pipe. International Communications in Heat and Mass Transfer, 71, 108–117.

36. Togun H., Kazi S.N., and Badarudin A., 2017. Turbulent heat transfer to separation nanofluid flow in annular concentric pipe. International Journal of Thermal Sciences 117, 14-25.

37. Khdher, A.M., Sidik, N.A., Mamat, R., and Hamzah, W.A., 2015. Experimental and numerical study of thermo-hydraulic performance of circumferentially ribbed tube with Al2O3 nanofluid. International Communications in Heat and Mass Transfer, 69, 34-40.

38. Togun, H., 2017. Turbulent Heat Transfer and Nanofluid Flow in a Pipe with Half Circle Ribs, WSEAS Transactions on Heat and Mass Transfer. 12, 136-143.

39. Togun H., Homod R. Z., Yaseen Z. M., Abed A. M., Dhabab J. M., Ibrahem, R. K., Dhahbi S., Rashidi M. M., Ahmadi G., Yaïci W., and Mahdi, J. M., 2022. Efficient Heat Transfer Augmentation in Channels with Semicircle Ribs and Hybrid Al2O3-Cu/Water Nanofluids. Nanomaterials, 12(15).

40. Al Kumait, A. A. R., Ibrahim, T. K., & Abdullah, M. A., 2019. Experimental and numerical study of forced convection heat transfer in different internally ribbed tubes configuration using TiO2 nanofluid. Heat Transfer - Asian Research, 48(5), 1778–1804.

41. Alrashed A. A. A. A., Akbari O. A., Heydari A., Toghraie D., et al., 2018. The numerical modelling of water/FMWCNT nanofluid flow and heat transfer in a backward-facing contracting channel. Physical B: Condensed Matter, 537, 176-183.

42. Salman S., Abu Talib A. R., Saadon S., and Sultan H. M.T., 2019. Hybrid nanofluid flow and heat transfer over backward and forward steps: A review. Powder Technology, 363, 448–472.

43. Ekiciler, R., and Çetinkaya, M. S., 2021. A comparative heat transfer study between monotype and hybrid nanofluid in a duct with various shapes of ribs. Thermal Science and Engineering Progress, 23. 100913.

44. Ekiciler, R., 2021. Effects of novel hybrid nanofluid (TiO2–Cu/EG) and geometrical parameters of triangular rib mounted in a duct on heat transfer and flow characteristics. Journal of Thermal Analysis and Calorimetry, 143(2), 1371–1387.

45. Kumar V. and Sarkar J., 2022. Numerical Analysis on Hydrothermal Behavior of Various Ribbed Minichannel Heat Sinks with Different Hybrid Nanofluids. Arabian Journal for Science and Engineering, 47, 6209-6221.

46. Togun, H., Hamidatou, S., Mohammed, H. I., Abed, A. M., Hasan, H. A., Homod, R. Z., Al-Fatlawi, A. W., Al-Thamir, M., and Abdulrazzaq T., 2023. Numerical Simulation on Heat Transfer Augmentation by Using Innovative Hybrid Ribs in a Forward-Facing Contracting Channel. Symmetry, 15(3).

47. Versteeg H.K and Malalasekera W, 2007. An Introduction to Computational 67 Fluid Dynamic (The Finite Volume Method). Person Education limited, ed, Essex, England, 503 pages.

48. Ansys Fluent 13 User's Guide., 2013. Ansys Fluent Theory Guide. ANSYS Inc., USA, 15317(November), 724–746.

49. White F.M., I. CORFIELD., 2006. Viscous fluid flow. McGraw-Hill New York, 705 pages.

50. Launder, B.E., and Spalding, D.B., 1972. Lectures in mathematical models of turbulence.

51. Rohsenow, W.M., & Hartnett, J.P. (1998). Handbook of Heat Transfer. McGraw-Hill, New York, 1501 pages.

52. Yaningsig I., Wijayanta A. T., Miyazaki T., and Koyama S., 2018. Thermal Hydraulic Characteristics of Turbulent Single-Phase Flow in an Enhanced Tube Using Louvered Strip Insert without Slant Angles. International Journal of Thermal Science,134, 355-362.

RESUME

His name Wisam Abdulhussein Hasan AL-HUSSEIN he graduated first and elementary education in Dhi Qar city. He completed his high school education in Üsküdar High School. After that, he started the College of Engineering in Al-Rafidain University Department of Refrigeration and Air Conditioning Engineering in 2012. Then, in 2021, he started his assignment as a Research Assistant in Karabük University's Department of Mechanical Engineering. To complete M. Sc. Education